Biology of embryo-derived Kupffer cells

Dilini Radika Soysa

A dissertation

submitted in partial fulfillment of the

requirements for the degree of

Doctor of Philosophy

University of Washington

2019

Reading committee:

Ian N. Crispe (Chair)

Jessica Hamerman

Martin Prlic

Program authorized to offer degree:

Pathobiology

University of Washington

Abstract

Biology of embryo-derived Kupffer cells

Dilini Radika Soysa

Chair of the supervisory committee
Professor Ian N. Crispe
Department of Pathology

Kupffer cells (KCs) are the resident macrophages of the liver, and play a key role in innate immune sensing, and maintaining steady state. KCs are originated from embryonic precursors, or from bone marrow monocytes. In adult unmanipulated mouse liver, at least a subset of KCs are embryo-derived; thus the adult liver KC compartment shows ontogenetic heterogeneity. Liver injury models of pathogenic and sterile inflammation indicate functional heterogeneity of KCs, and they can be pro-inflammatory, anti-inflammatory, immunosuppressive, or reparative. These observations have led to question the relationship between the ontogeny, and the functions in KCs. To date, there are no phenotypic markers to exclusively identify an ontogenetically distinct subset, and this has hampered functional studies of this subset. In this dissertation we explore how the embryo-derived KC subset in the liver respond to irradiation stress and to acute inflammatory stimuli. To this end, we developed a mouse model to specifically label the embryo-derived KCs in the adult liver, and assessed their response to lethal irradiation. We found that the embryo-derived subset resists lethal irradiation and this resistance is mediated through the $p21^{-cip1/WAF1}$ protein. In contrast, the same dose of radiation depleted the bone marrow monocyte-derived KCs. Together, these results indicate that the embryonic origin provide enhanced survival to radiation induced injury. In a lipopolysaccharide-mediated acute inflammation model, the embryo-derived subset responded readily mounting a pro-inflammatory

gene expression pattern. Once the inflammatory stimuli subsided they revert back to the steady state gene expression pattern. These observations indicate that this embryo-derived subset retains plasticity and are able to respond to changing environmental cues.

The research work in this dissertation provides first insights into the underlying biology of embryo-derived KCs. We explored how a embryo-derived KC subset responds to radiation induced sterile damage and to systemic acute inflammation. We demonstrate that in both these models, the embryonic subset possess remarkable ability to resist damage, avoid depletion, respond to changing environment, and reset to steady state.

TABLE OF CONTENTS

LIST OF FIGURES

LIST OF TABLES

Dedication

To my grandfather Hubert,
for his dedication to teaching
and for his love of nature.

Acknowledgements

It has been a long journey with several detours. Along the way many invested their energy, provided guidance, supported in various capacities, stopped by to give me a hand, encouraged me to move on and be who I am. All these people shaped who I am today and are instrumental in me reaching this milestone.

I would like to thank my mentor Nick Crispe for giving me the opportunity to join his lab, and for allowing me to have a project that interests me. Nick encouraged me to think outside the box and gave me the freedom to explore novel research approaches, and enthusiastically supported my research ideas while pointing out drawbacks when needed. Discussions and interactions with Nick during this time allowed me to grow as a scientist. I am specifically thankful to Nick for understanding my life outside lab, and encouraging me to find the right work –life balance. Nick kept a lively atmosphere in the lab and being a part of the Crispe group has been a great joy during my thesis work. From Nick's group, I would like to thank his former graduate student Katie Brempelis, for training me during my rotation, for critical input on my research proposals and for her willingness to talk through my project at all times and for her ongoing friendship; Sebastian Yuen and Sarah Lampert for technical support in my research and their friendship. I would also like to thank the other members of the lab for their input on my project and making it a fun place to work. I would also like to thank our collaborators at the Stanley McKnight lab, especially Jonathan Bean for his insights into RiboTag approach, teaching me RNAseq techniques and analysis, and for his friendship over the years.

I also like to thank my thesis committee Jessica Hamerman, Martin Prlic, Michael Gale and Gwenn Garden for their input and support during the years. I would like to thank Jess and Martin especially for reading my dissertation and following up on my work and future goals through out the years during retreats and symposiums.

A special thanks to my previous mentors and dear friends, Marie-Pierre Hasne, Phil Yates, Jan Boitz, Buddy Ullman and the rest of the Ullman laboratory members from Oregon Health and Science University, for teaching me how to ask research questions in biology, allowing me to design and drive independent projects while I was a research assistant, and encouraging me to apply to graduate school. Ullman lab provided a stepping-stone to graduate school.

During my time in the USA many stepped into support me and made me a part of their family and communities. Among those I would especially like to thank the Edmistons- Blair, Tom, Gena, Lora, Margot, Ken and Susan- for all the holidays, visits, backpacking trips, and their ongoing support and caring for my wellbeing. Many friends supported me through this process. Among those I would like to thank Jessica and the Sokols, Devinka Bamunusingha, Dane and her family, Michael and Katherine, Elie and Andrew Frando for standing by me and helping me getting through many stressful times and making it a fun process altogether. While graduate school through out had its challenges the last push presented many deadlines and the intimidating task of finishing up what you started. I would like to thank David Doucette for being there for me during this last push, checking in constantly, planning breaks from long hours of writing, engaging in lively conversations that kept my mind on task without burning out.

I owe every bit of strength and courage I had to get here to my family and their unconditional love and acceptance of me. My mother, for caring deeply and selflessly, and providing space and freedom to read, write and play, and my father for standing by me and being the wall for me to stand on no matter what life brought up, and my brothers for their deep friendship, understanding and always having my back no matter what.

LIST OF ABBRIVIATIONS

APC = Antigen presenting cell

AST = Aspartate aminotransferase

bmKC=Bone marro-derived kupffer cells

BMT=Bone marrow transplant

Ccl = Chemokine (C-C) motif ligand

Cxcl = C-X-C motif chemokines

D2 = Day two

DAMP = Damage associated molecular patterns

DC=Dendritic cells

emKC=Embryo-derived Kupffer cells

EMP= Erethro myeloid progenitors

FL=fetal liver

HSC = hematopoietic stem cells

IFN = Interferon

IL = Interleukin

IR = Lethal Irradiation

IRF = Interferon regulatory factor

KC = Kupffer cell

LPS = Lipopolysaccharide

LSEC = Liver sinusoidal endothelial cells

MO=Monocytes

MQ=macrophages

NF-kB= Nucler factor kB

NK=natural Killer

NLR=NOD like receptors

PAMP = pathogen associated molecular patterns

PRR = pathogen recognition receptor

ROS=reactive oxegen species

TAM = Tamoxifen

TLR = Toll-like receptors

YS= Yolk Sac

CHAPTER 1: INTRODUTION

An overview of the liver

The liver is the center of metabolic processing in the body. In both humans and mice, the liver processes nutrients, produces proteins, plays a key role in energy homeostasis, and is critical for detoxification. The human liver is located in the right upper quadrant of the abdomen, whereas the mouse liver spans the entire subdiaphragmatic space. While the lobe patterns in mice and human livers are different the basic lobular subunits are conserved in structure and function(1). These hexagonal lobular subunits consist of a centering hepatic vein, radiating hepatocyte beds consisting of 16-20 hepatocytes and portal triads composed of arterioles, venules, bile ductules, and lymphatics(1, 2). The hepatic vein and the portal triad are connected through a microvasculature known as the sinusoids that are lined by a layer of thin walled, fenestrated endothelial cells. These fenestrations allow the exchange of nutrients, macromolecules between the hepatocytes and the blood flow. In the sinusoids the high pressure, well-oxygenated arterial blood mixes completely with the low-pressure, less well-oxygenated, but nutrient-rich, portal venous blood and flow through at a low rate of 5 mmHg or less compared to the pressure gradient 115 mmHg across all other organs(2). The pressure, oxygen and metabolite gradients along the sinusoids result in metabolic zonation. This zonation influences the functions of hepatocytes and the non-parenchymal cells such as immune cells, hepatic stellate cells, endothelial cells along the sinusoids, and their cellular cross talk leading to functional diversity within a lobule (3).

The liver as a lymphoid organ

The liver consists of a unique immune environment (4). Along with nutrients and self-antigens the portal vein blood brings in foreign antigens, whole bacteria and microbial products such as lipopolysaccharide endotoxins (LPS), flagellin, dsRNA, ssRNA, DNA, and lipids. Under normal conditions the portal venous blood contains 1.0 ng/ml LPS(5) and whole bacteria though neither are detectable in the systemic circulation. Thus the liver acts as the second vascular barrier for eliminating bacteria and their products(6). The removal of gut-derived microbial particles and induction of tolerance to harmless foreign antigens are among the key immune functions of the liver. A variety of innate and adaptive

immune cells that are either resident or pass through the liver contribute to maintaining this peripheral tolerance and are crucial for activating immunity in disease settings (4, 7).

The liver contains innate immune cells as well as non-immune cells that act as antigen presenting cells (APCs). The professional APCs are the tissue resident macrophages, known as Kupffer cells (KCs), and the patrolling or resident dendritic cells (DCs). The KCs reside in the sinusoids and present antigens to passing naïve T cells whereas DCs capture intra hepatic antigens, present them *in situ* or enter the lymphatic vessels and travel to the draining lymph nodes to activate naïve T cells(8). Aside from the professional APCs, hepatocytes, liver sinusoidal endothelial cells (LSECs) and hepatic stellate cells have the capacity to present antigens through both MHC class I and II pathways to CD8+ and CD4+ T cells respectively (9, 10). While the APC function of the non-immune cells remains low in steady state, it is ameliorated during immunopathological conditions. This low-level APC function of non-immune cells at steady state may further contributes to the tolerogenic immune environment in the liver(10).

APCs harbor cell surface or intra cellular pathogen recognition receptors (PRR). The cell surface PRRs include Toll-like receptors (TLR) while the intracellular PRRs include nucleotide binding oligomerization domain (NOD)-like receptors (NLR), retinoic acid inducible protein-I (RIG-I)-like receptors (RLR) and various DNA-recognizing receptors, such as cyclic GMP-AMP synthase (cGAS). Together these receptors detect specific pathogen-associated molecular patterns (PAMPs)(11). TLRs recognize bacterial and viral PAMPs such as LPS (by TLR4), lipopeptides (by TLR2-TLR1 and TLR2-TLR6 heterodimers), flagellin (by TLR5), dsRNA (by TLR3), and ssRNA (TLR7). NLRs recognize bacterial cell wall products such as peptidoglycans while RLRs recognize cytosolic viral RNA. The engagement of PAMPs by TLRs activates intracellular signaling cascades that lead to activation of cytosolic transcription factors nuclear factor kappa B (NF-kB) or interferon regulatory factor-3 (IRF3). Nuclear localization of NF-kB and IRF3 activates pro-inflammatory gene expression and type I interferon (IFN) expression respectively. The continuous low-level stimulation of the NF-kB pathway is a specific feature of the liver immune environment (4).

The liver contains a large pool of resident and circulating lymphocytes(12). Among the resident lymphocytes 50% compose of NK and NKT cells(13). Furthermore in the liver CD8+ T cells to CD4+ T cells ratio is higher compared to other tissues (14). Other lymphocytes in the liver include mucosal

associated invariant T cells, innate lymphoid cells, and γδT cells (15). In normal conditions upon interactions with APCs, naïve CD4+ and CD8+ T cells are activated, proliferate, and undergo apoptosis, anergy or differentiate into regulatory T cells and support the maintenance of an immunosuppressive environment(16). Taken together innate and adaptive cells, their crosstalk combined with the unique physiological condition in the liver are important in maintaining the unique immune environment in the liver.

Kupffer cells; the liver resident macrophages

Kupffer cells consist of the largest popualtion of tissue resident macrophages in the adult mammalian liver. KCs are found in the liver microvasculature known as sinusoids, along the endothelial walls with close contact with LSECs(17).

Kupffer cells were first described in1876 by a Latvian embryologist Carl Wilhelm von Kupffer. Using a gold chloride staining method, Kupffer identified star like cells lining the sinusoidal endothelium in various mammal livers and called them “sternzellen” (18, 19). Since then the “sternzellen” were called Kupffer cells. In 1892, Ilya Metchnikoff discovered the “macro and micro” phages (large and small eaters) in tissues and introduced the idea of a “macrophage system” through the body (20). In 1924, Aschoff built further on the “macrophage system” idea and proposed the reticulo-endothelial system (RES), a cell system composed of reticulum cells, reticuloendothelia (phagocytic endothelia), and histiocytes (macrophages) in the liver (21). In the RES the KCs were thought to originate from the endothelial cells. In 1974, using perfusion and cytochemistry analysis of rat liver Wisse distinguished KCs from the endothelial cells and identified them as tissue resident macrophages in the liver sinusoids (22). In 1969, using radiation induced depletion and radiolabeled thymidine-[3H] incorporation studies on origin and kinetics of peritoneal macrophages, Van Furth and Cohn proposed the idea of the “Mononuclear phagocyte system” (MPS)(23). According to this proposal the mononuclear phagocyte system consisted of rapidly dividing bone marrow pro-monocytes that give rise to blood monocytes, which then entered the tissues, and differentiated into tissue macrophages upon radiation injury. This view was widely accepted in the field and the KCs were considered to be a part of the mononuclear phagocyte system and the idea of RES was disregarded.

Kupffer cells play a key role in maintaining liver homeostasis and accomplishing immunity. KCs are equipped with a large number of cell surface scavenger receptors that bind multiple ligands and promote the removal of non-self or altered self targets through opsonized or non-opsonized mechanisms. These abundantly expressed scavenger receptors on KCs include macrophage receptor with collagenous structure (*Marco*), *CD163, CD68, CD36,* complement receptor of the immunoglobulin superfamily (*CRIg* or *Vsig4*), mannose receptor c-type 1 (*Mrc1*), Macrophage scavenger receptor 1 (*Msr1*), and C-type lectin domain family 4-f (*Clec4f*). Along with splenic red pulp macrophages, KCs play an important role in the clearance of senescent red blood cells and hemoglobin metabolism using CD163(24). KCs also express a high level of activating Fc receptors for IgG (FcγR1(CD64), FcγR2 (CD32)) that are involved in antibody-dependent opsonized particle uptake and thus are important in immune complex clearance.

During stress conditions KCs demonstrate distinct immune functions by altering their gene expression to produce large amount of cytokines, chemokines, and in some settings, tissue matrix. The stress response of KCs is initiated through the recognition of PAMPs of extracellular or intracellular pathogens – bacteria, virus, fungi- or by damage-associated molecular patterns (DAMPs) that serves as signals of liver injury. DAMPs or PAMPs signaling alters the response of KCs in a context dependent manner leading to pro-inflammatory, anti-inflammatory, reparative or immunosuppressive states(25, 26). This initial response results in a cascade of immune mechanisms that either contributes to restoring the liver back to steady state or prolonging the resolution of inflammation and leading to a chronic state of disease.

In adult mice, immune cells are replaced by the differentiation of their respective precursors generated through hematopoiesis. However the mature tissue resident macrophages possess a unique ability to self-renew, without loss of function, a quality that was previously restricted to stem cells (27, 28). This self-renewing ability of KCs was first demonstrated by Bouwens et.al in 1984. The authors reported that upon zymosan stimulation KCs underwent self-renewal, which was distinct from the infiltrating monocyte differentiation. This study disputed the MPS paradigm which stated that macrophages are originated from monocytes (29). Today, self-renewal is widely accepted as the method of propagation for long-lived tissue resident macrophages. While the triggers and the molecular mechanisms of how a fully

mature functional macrophage self-renew is poorly understood, the current studies do not rule out longevity as another means of long life span in KCs.

Kupffer cell heterogeneity

Heterogeneity of KCs is demonstrated with respect to the phenotype, origin and function (30-32). This has translated to the idea that distinct KC subsets may exist in the liver. If subsets exist, do they relate in terms of phenotype, function and ontogeny, if so how, and do they represent true subsets or just states of a continuum, are research questions that need deeper explorations.

Phenotypic heterogeneity

In mice, the traditional view considers all tissue resident macrophages in the unmanipulated liver as KCs. Early studies used cytochemical analysis based on location and cell shape to identify KCs (21). Since the identification of F4/80 (also known as *Emr-1* or *Adgre1*), as a pan tissue resident macrophage marker(33), KCs are identified as F4/80^{hi} cells in both *in situ* histological and isolated cell suspension analysis of the liver tissues.

In the recent years fluorescence-activated cell sorting (FACS) analysis of KCs in fate mapping models(34, 35) has indicated the presences of a distinct macrophage population in the unmanipulated mouse liver with a F4/80^{lo} CD11b^{hi} phenotype, termed “liver macrophages”. While this identification of the F4/80^{lo} liver macrophage population in unmanipulated mice is recent, the existence of this population was widely reported during acute inflammation conditions of the liver. During stress conditions Ly6C^{hi} monocytes infiltrate the liver and differentiate into Ly6C^{lo} monocytes, which in turn upregulate F4/80 and Cx3cr1 giving rise to an intermediary phenotype between macrophages and monocytes (36, 37). These intermediary cells can further upregulate F4/80 to become F4/80$^{lo/hi}$ KCs or Cx3cr1 to become DCs (37). Currently, the fate of this infiltrating monocyte-derived macrophage population, i.e whether they are a transient population or integrate into the resident KC compartment post resolution, is unclear. Further validations are needed to confirm whether the F4/80^{lo} population is a bona fide macrophage population that co-exists with KCs in unmanipulated mice.

Immunophenotypic analysis using mass cytometry indicated the existence of two KC subsets based on the presence or the absence of CD11c on F4/80^{+}CD11b^{+}Ly6C^{lo}MHC Class II^{hi} KCs in

unmanipulated mice (37). Using fluorescence reporter expression, and phenotypic analysis, Sierro et. al reported the presence of a distinct subset of macrophages in the liver capsular region. In contrast to $F4/80^{+}CD11b^{+}TIMD4^{+}$ KCs, these capsular macrophages did not express TIMD4 but expressed a high level of CX3CR1(38). How these subsets identify with the traditionally known $F4/80^{hi}$ KCs and whether these studies reveal distinct subsets of KCs within the KC compartment are currently unclear.

FACS sorted $F4/80^{hi}$ KCs and the $F4/80^{lo}$ liver macrophages have distinct transcriptomes further supporting that they are distinct subsets (34, 39). Single cell RNAseq analysis of liver cells also indicated the presence of two subsets. In this study the authors identified the *Clec4f*, *Clec1b* and *Marco* expressing subset as KCs and the *Clec4e* and *Clec4d* expressing subset as the liver macrophages (40). Whether these genes show a distinction at the protein level and how they relate to the $F4/80^{-lo}$ vs $^{-hi}$ subsets is still unclear.

Taken together, the studies thus far suggest that KCs are phenotypically heterogeneous but how non-traditional markers such as TIMD4, CX3CR1, CD11C and MARCO correlate with the $F4/80^{hi}$ resident KCs is yet to be determined. MARCO and TIMD4 expression are not limited to KCs while CX3CR1 and CD11C can be DC or monocyte markers. Thus it raises the question of cellular contaminations during the cell isolation processes. Lynch et. al. demonstrate how different cell isolation protocols effect the efficiency of KC isolation and how KCs can be contaminated with tightly adhering liver endothelial cells (41). Therefore robust, independent validation is key to establishing phenotypic heterogeneity in KCs.

Ontogenetic heterogeneity

In 1978, Van Furth and colleagues used radiolabeled thymidine incorporation and bone marrow chimeras to show that circulating monocytes become KCs over time (42). Depletion of circulating monocytes using hydrocortisone prevented labeling of KCs while the mean turnover of KCs was reported as 21 days. Parabiosis studies conducted by Wacker et. al. in 1986 further confirmed that the circulating monocytes give rise to KCs (43). Based on these observations and other studies that demonstrated similar monocytic origin, KCs were considered to solely originate from bone marrow precursors. While this view of monocytic origin of KCs was widely accepted, the evidence that monocytopenic humans, as well as Ccr2 knock out ($Ccr2^{-/-}$) mice that lack circulating monocytes, contained normal levels of KCs among

other tissue resident macrophages, indicated that blood monocytes may not be the sole precursor of tissue macrophages. Furthermore, KCs first appeared in the fetal liver at ED10, before bone marrow hematopoiesis is established, indicating non-bone marrow precursors exist and can give rise to KCs (21).

With the advent of new tools to study tissue resident macrophage kinetics and cell fate *in vivo,* the view of the mononuclear phagocyte system has changed drastically. Multiple fate mapping studies have demonstrated that in mice, the fetal liver is seeded by embryonic precursors that differentiate into KCs and that these KCs live long into adult hood through self-renewal. Embryonic stage Cx3cr1 driven fate mapping and intravital microscopy revealed that the Yolk sac (YS) Cx3cr1-marked precursors seed developing fetal liver up to ED12 and give rise to KCs that maintain into adulthood (34, 44, 45). Fate mapping studies that distinguish F4/80^{hi} CD11b^{lo} KCs versus F4/80^{lo} CD11b^{hi} liver macrophages in the adults showed that they originate from YS-derived precursors versus hematopoietic stem cells(HSC)-derived fetal monocytes respectively indicating precursor based heterogeneity of adult KCs (34, 35, 46). Other fate mapping strategies, including early *Csf1r, Tie2*, or *Kit* promoter driven inducible Cre systems have further confirmed the embryonic origin of adult KCs(35, 46-48). While it is clear that the embryonic precursors give rise to adult KCs, the types of precursors- YS-derived Pre-macrophages, YS-derived erythro myeloid progenitors (EMPs), HSC-derived from Aorto-gonado mesonephros(AGM), fetal monocytes-derived from EMPs or HSCs- and the timing of embryonic seeding is yet to be defined. Another noteworthy aspect is that none of these embryonic stage fate-mapping models indicate complete labeling of adult KC compartment, while brain microglia labeling is near complete in all models suggesting that it may not be just an artifact of the fate mapping strategies. This raises the possibility that yet unknown precursors or waves of seeding contribute to the adult KC compartment.

Fate mapping, adoptive transfer and parabiosis experiments in adult stages provide some insight into the ontogenetic nature of the post-birth KC compartment. Using adoptive transfer of adult monocytes into neonates, Scott. et. al. showed that the donor monocytes readily seeded the developing liver to become long-lived self-renewing KCs while they did not seed the microglia compartment (49). This study suggests that the liver KC compartment remains open post-birth and circulating bone marrow-derived monocytes seed, differentiate and integrate into the KC compartment. Fate mapping and phenotypic

studies done on the adult mice showed that the capsular region macrophages in the liver are constantly replaced by monocyte-derived macrophages, further suggesting that KC compartment remains partially open in the adult mice in a location-based manner. In contrast to these studies, parabiosis experiments demonstrated that KC in the adult mice were maintained without a major contribution of bone marrow-derived monocytes(38). Furthermore adult stage Cx3cr1 driven fate mapping marked circulating monocytes but they did not contribute to the KC compartment at steady state (50-52). Thus, the extent of openness of the KC compartment post-birth remains unclear.

Taken together, the evidence thus far reveals that in unmanipulated mouse liver, a subset of KCs are embryo-derived, while another subset is derived from post birth bone marrow monocytes. Further experiments are needed to determine whether it is just the aforementioned subsets or more ontogenetically distinct subsets exits.

Functional heterogeneity

Functional heterogeneity of KCs is described with respect to their localization and stress response, in terms of their ability to migrate, turnover or expand locally, and perform distinct immune functions.

While KCs are found throughout the liver their density and phenotype vary based on the location. In rat liver, the density of KCs increases from peri-venous to peri-portal regions. Cytochemical analysis in mouse liver indicated that the peri-central regions are sparsely populated while the peri-portal regions show a dense KC population. Furthermore the peri-portal KCs are larger in size compared to the peri-venous KCs (37, 53). KCs residing closer to the peri-portal region are more phagocytic and show a higher activity of lysozyme enzymes compared to the KC closer to the peri-venous region(53). A recent study indicates that phagocytosis imprints heterogeneity in macrophages making them more anti-inflammatory(54). Taken together it is possible that the peri-venous versus peri-portal location impacts the phagocytic functions, which in turn imprints immune functional heterogeneity in the KCs. Hepatic capsular macrophages, that are phenotypically different from KCs, engage in immune-surveillance, act as gatekeepers, and recruit neutrophils to prevent bacterial dissemination from peritoneal cavity (38).

Ablation of these macrophages reduced neutrophil recruitment and increased intrahepatic bacterial burden. This study further indicates functional heterogeneity based on location for KCs.

In vivo studies using intravital microscopy showed that the KCs do not migrate towards the site of a wound in a model of localized thermal injury while peritoneal macrophages migrated through the mesothelium and swarm the injury site (55). *In situ* immunofluorescence analysis in radiation chimeric mice showed that in a CD8+ T cell activation model only the bone marrow-derived KCs migrated towards the inflammatory foci (56). Collectively these studies indicate that the resident KCs remain sessile during injury.

Intracellular FACS analysis of the cell proliferating marker Ki67 revealed less than 1% detection in the KC population indicating that at the steady state only very few cells self-renew (57). Under stress conditions, however, these dynamics alter drastically. An acetaminophen-induced hepatic injury model indicated that resident KCs reduced upon injury, however they increased during resolution phase through self-renewal (57, 58). In this model, the recruited monocyte-derived liver macrophages and the resident KCs showed distinct pro-restorative properties with respect to the level of scavenger receptor and matrix metalloprotease expression (57). In a *Listeria monocytogenes* infection model resident KCs were shown to undergo rapid necroptotic death, mounting a pro-inflammatory immune response that lead to the recruitment of monocyte-derived macrophages. These recruited macrophages were polarized to an anti-inflammatory state by basophil mediated IL4 production and they replaced the resident KCs (59). In contrast, in a helminth infection model, KCs underwent rapid proliferation to a higher density in a IL4 dependent manner to induce a Th2 response, without relying on recruited monocyte-derived macrophages (60). Using a *Kit* promoter driven inducible fate mapping to label embryo-derived KCs, Lai et. al. showed in a model of blood stage malaria the resident embryo-derived KCs are transiently lost before the onset of peak parasitemia. In this model monocyte-derived KCs replenished the empty niche, rather than the embryo-derived KC self-renewal (61). These studies indicate that the resident KCs are both eliminated and replaced by monocyte-derived macrophages or they expand through self-renewal in a context dependent manner.

Pathogenic or sterile liver injury models demonstrate that the KCs can be pro-inflammatory, anti-inflammatory, immunosuppressive or reparative. KC activation towards a pro-inflammatory phenotype

results in release of pro-inflammatory cytokines such as IL1, TNF or chemokines such as CCL2, CXCL2- that attract monocytes or neutrophils and NKT cells that produce IFNγ and TNFa to further perpetuate the acute inflammatory response (62). KC activation towards an anti-inflammatory state is triggered by IL4, IL33, and IL13 interleukins which upregulate anti-inflammatory gene expression such as *Il10* and *Arg,* and increase phagocytosis (63). In liver transplants, graft-derived KCs upregulate Fas-ligand (*FasL*) and induce apoptosis in host-derived T cells through the engagement of the Fas receptor (64). Depletion of KCs in experimental rodent transplants had resulted in graft rejection, indicating the critical role of KC driven immunosuppression in transplant tolerance. During injury resolution phase KCs acquire a pro-restorative state, secrete matrix metalloproteinase (*Mmp8, Mmp12*) and support wound healing(25). KCs also contribute to the pathophysiology of certain metabolic diseases. KC depletion has shown resistance to metabolic diseases such as diet induced hepatic steatosis and insulin resistance indicating their pathological role (65).

These studies indicate the functional heterogeneity in KCs and present the fundamental question, "what dictates this functional heterogeneity?". Is it the unique environment based on the location? Is it solely the origin of the KCs? Is it a combination of both origin and the environment? These will be fascinating questions for the future.

Ontogeny versus function

Apart from steady state immune surveillance and metabolic regulations, KCs perform diverse immune functions during stress conditions. Whether these distinct immune functions are performed by subsets of KCs with distinct origins, or independent of the origin, all KCs are able to perform these diverse functions is paramount in understanding the biology of KCs.

While embryo-derived KCs and bone marrow monocyte-derived KCs can coexist in the liver, phenotypic markers to identify each subset are still lacking. Recent fate mapping studies indicated that the adult F4/80^{hi} versus F4/80^{lo} subsets reflect YS versus fetal monocyte-derived KC subsets respectively. However, post-birth monocyte-derived KCs also show F4/80^{lo} phenotype. This may suggest that F4/80^{lo} phenotype is monocyte-derived KC specific, while it does not distinguish between the fetal versus adult monocyte origin.

Steady state immunophenotyping indicates that F4/80 can express at a low level on monocytes that are in intermediary transition stages to become liver macrophages or dendritic cells (37). Furthermore, in mice eosinophils also express low levels of F4/80 (39). During stress conditions, use of F4/80 expression as an ontogenetic marker becomes even more problematic since infiltrating monocytes upregulate F4/80 during differentiation to macrophages. While TIMD4 is used to distinguish embryo-derived KCs from infiltrating monocyte-derived macrophages in inflammatory settings, it is expressed on all resident KCs in unmanipulated liver. However irradiation studies and KC depletion studies using chemicals indicate that over time monocyte-derived KCs can acquire TIMD4 expression, suggesting that despite of the origin all long-lived self-renewing KCs can express TIMD4 (66).

Attempts to understand origins versus functions were mostly performed on radiation chimeric mice where donor versus host KCs can be identified using the allotype differences. These experiments provide insights into the functions of recruited monocyte-derived KCs post irradiation versus resident KCs. However they do not parse out the embryo- versus bone marrow monocyte-derived KC functions within the resident population. Thus understanding the origin versus functions aspect requires incorporation of fate mapping to accurately label and track long-lived embryo-derived KC subset.

Kupffer cell plasticity

Plasticity, the ability to polarize to distinct functional states, is considered a hallmark of macrophages (67-69). This quality is widely demonstrated in *in vitro* stimulation studies, where different stimuli (TLR4 ligands) and cytokines (M-CSF, IFNγ, IL4, IL13) produce functionally opposing, thus polarized, macrophages. Specifically, IFNγ and TLR4 ligands polarized macrophages toward M1-classically activated- phenotype, while IL-4 and IL-13 polarized them toward M2- alternatively activated-phenotype(70). M2 state is further subdivided to M2a, M2b and M2c states based on distinct input signals. Classically activated macrophages perform pro-inflammatory roles, whereas alternatively activated macrophages perform anti-inflammatory and reparative roles. A transcriptome analysis of human macrophages stimulated with diverse ligands indicated that they polarize into diverse functional states, thus suggesting that the functional states can also exist in a continuum (71).

Kupffer cells show distinct immune functions in various stress models, and in some, these functions are reported as M1 or M2 skewed. An alcoholic liver disease model indicated M1 polarization, whereas schistosoma infection and fibrosis models indicated M2 polarization for KCs(72, 73). In other studies, the observed KC functions did not align with the cytokine profiles indicated for in vitro M1 or M2 classifications. This suggests that the M1/M2 paradigm is not straightforward in *in vivo* settings, and that the functional states may exist in a continuum (69). Taken together, the existence of diverse immune functions in response to inflammation in KCs suggests plasticity of these cells. However, the evidence supporting macrophage heterogeneity suggests the existence of functionally distinct macrophage subsets. Thus the concept of KC heterogeneity limits drawing firm conclusions about their plasticity.

Environment versus function

Resident macrophages in distinct tissues show tissue specific transcriptomes(39, 74). These distinct transcriptomes are shaped by primary macrophage specific transcription factors such as Pu.1 and Zeb2, and combined with tissue specific cytokines such as Tgfb for Microglia (75, 76). In the peritoneum, retinoic acid induces *Gata6* expression that turns on a tissue specific signature in peritoneal macrophages (77). In addition to their tissue specific functions, resident macrophages constantly probe their environment for danger signals, thus in vivo resident macrophages can assume various functional states depending on their exposure to various environmental changes, even at steady state. The presence of ontogenetically distinct KC subsets at steady state further complicates understanding the environmental influence in shaping the functions. Thus, in order to parse out how environment dictates resident macrophage function it is important to consider macrophages of similar origin.

DISSERTATION AIMS

To date studies indicate that Kupffer cells are heterogeneous in terms of their origin and function, however it is unclear whether the distinct origins of KCs influence their functions. While *in vitro* studies indicate that the environmental cues can dictate distinct functional states in macrophages underscoring their plasticity, the plasticity of resident macrophages remains poorly understood. In this dissertation we aim to elucidate the role of origin and the role of the environment in shaping KC responses. Here we will use a fate-mapping model to specifically label an embryo-derived long-lived KC subset. First, we will describe their steady state dynamics and response to radiation induced stress. Next, we will investigate their response to acute inflammation and resolution and will compare it to a long-lived cardiac macrophage subset with a similar origin. In chapter 2 we will describe the materials and methods used in chapter 3 and 4. Chapter 3 focuses on the response of embryo-derived versus bone marrow monocyte-derived KC subsets to radiation-induced injury. Chapter 4 describes the response of embryo-derived KCs to lipopolysaccharide induced acute inflammation and resolution and compares this response to embryo-derived long-lived cardiac macrophages. Chapter 5 integrates the findings from chapter 3 and 4 to further our understanding of biology of embryo-derived KCs.

CHAPTER 2: MATERIALS AND METHODS

This chapter provides materials and methods used for chapters 3 and 4.

Mice

Wild type CD45.1 and CD45.2 mice, RiboTag (Stock No: 011029) and Cx3cr1-eyfp-CreER (Stock No: 021160) mice were purchased from The Jackson Laboratory (Bar Harbor, ME). Emr1Cre (+/+) breeders were a gift from Dr. Klaus Pfeffer (Heinrich Heine University, Düsseldorf, Germany) and used to breed experimental mice in-house at the University of Washington (Seattle, WA). All mouse experiments described in this study were performed under Institutional Animal Care and Use Committee approval (University of Washington, protocols #4308-01). They were housed in a specific pathogen free environment, provided with ad libitum food and water unless otherwise noted, and monitored daily.

Cell isolation and RibolP sample collection

Mice were anesthetized with Avertin. For the liver, two thirds of the right posterior lobe cut off, for histology a piece was put into 4% para-formaldehyde in PBS and for Ribo IP several punches were collected using a 2.0mm uni-core (Harris Uni-core, Redding, CA) and immediately placed in an ethanol slurry and stored at -80°C until processing. Hearts were first perfused with 10 ml of PBS, and the tissue was harvested for Ribo IP using 2.0mm uni-core. Liver non-parenchymal cell isolation was performed as described by Mohar. et. al. (78).

Flow cytometry

Non-parenchymal cells (10^6) were first treated with 1:50 Fc block (BioLegend, TruStain FcX™anti-mouse CD16/32) for 10 min at 4°C followed by staining with the appropriate antibodies for surface antigens at 4°C in the dark for 30 min. Intracellular staining was performed on surface antigen stained cells using Cytofix/Cytoperm™ (BD Biosciences, Franklin, NJ) according to the manufacturer's protocol. Stained cells were analyzed using fluorescence-activated cell sorting (FACS) on a LSRII (BD Biosciences, Franklin, NJ) and FlowJo software version 10.5.0 (FlowJo, LLC, Ashland, OR). List of antibodies used in the Table 1.

Generation of bone marrow chimeras

Adult mice were lethally irradiated with a single dose of 10 Gy using a Gammacell 40 Exactor (Best Theratronics, Ontario, Canada) and were reconstituted immediately by retro-orbital infusion of 5-7x10^6 bone marrow cells. Mice were left for 8 or13 weeks before blood, bone marrow and liver were assessed for chimerism. In experiments to determine radiation-induced responses within 24 hours, mice were not reconstituted with a bone marrow transplant. In all experiments control mice that did not receive irradiation received a bone marrow transplant retro-orbitally except at 24 hr experiments.

Tamoxifen inductions

Post natal mice of up to 2 days old were oral gavaged with a single dose of 1mg Tamoxifen (T5648, Sigma) dissolved in corn oil in a total of 50ul using a 24G-1" Straight 1.25mm ball stainless gavage needle (Braintree Scientific Inc. MA). 1 week old mice were orally gavaged with 1mg of Tamoxifen dissolved in 100ul and 6 weeks old mice were oral gavaged with 2.5mg Tamoxifen dissolved in 200ul corn oil.

RiboTag immunoprecipitation and RNA isolation

Frozen liver punches were processed, polysome immunoprecipitation was performed and mRNA was isolated as described by Senz et. al.(79).

Kupffer cell depletion

Clodronate or the control liposomes (Standard Macrophage Depletion Kit - Clodrosome® + Encapsome®) SKU# CLD-8901, Encapsula Nanoscience, Brentwood, TN) were injected intraperitoneally to 3 weeks old male mice at a dose of 5mg/20g body weight in total of 300ul to deplete Kupffer cells.

Immunofluorescence Imaging

Liver pieces were fixed in 4% para-fromaldehyde in PBS for 12 hours then transferred to 30% D-glucose and incubated overnight at 4°C. Samples were OCT-embedded and cryo-sectioned mounted on

Superfrost glass slides (Thermo fihser). Sections were blocked at room temperature for 1 hr with blocking buffer (0.02% Triton-X100 (Thermo fisher), 2% BSA (Sigma), and 5% Donkey serum (Jackson Immuno research, West Grove, PA)), incubated overnight with primary antibodies, Rabbit anti-HA clone SG77 (# 71-5500, Thermofosher) at 1:100, Rat anti-mouse F4/80 clone BM8 (#123101, BioLegend) at 1:100 dilution in blocking buffer. Sections were washed with 0.02% Tween in PBS and incubated with secondary antibodies, donkey anti-rabbit Alexa Fluor 680, and donkey anti-Rat Alexa Fluor 594 (Thermo fisher) diluted at 1:100 and 1:250 respectively in blocking buffer for 1 hr at room temperature. Sections were mounted using DAPI-Fluoromount-G (SouthernBiotech, Birmingham, AL) media and imaged. All images were taken on a Leica TCS SP8 X (Leica Microsystems, Buffolo Grove, IL) confocal microscopy using 40X objective. Microscopy was performed at the W.M. Keck microscopy center at University of Washington, Seattle.

Gene expression analysis

Complementary DNA was generated using the QuantiTect Reverse Transcription Kit (Qiagen), preamplified using BIO-X-ACT Short Mix (Bioline USA Inc., Taunton, MA) and the TaqMan assays of interest (Thermo Fisher Scientific). Microfluidic quantitative RT-PCR was performed on a BioMark HD microfluidics system (Fluidigm, South San Francisco, CA). The Fluidigm Gene Expression software was used to calculate Ct thresholds and Excel used to calculate relative expression levels and fold change value. Gene expression was normalized to *Gapdh* and *Hprt*.

Measurement of liver enzymes

Levels of Aspartate Aminotransferase (AST) were quantified from serum. Blood collected from the portal vein was allowed to clot over night at 4 C, centrifuged at 6000 rpm for 10 min, and the supernatant collected. When necessary, the supernatant was clarified for an additional 4 min at 6000 rpm. AST levels were quantified using the Aspartate Aminotransferase (AST/SGOT)-SL Kit (Sekisui Diagnostics LLC).

Lipopolysaccharide administration

Male mice, aged 8-10 weeks were intra-peritoneally administered with 2mg/Kg LPS dissolved in sterile PBS. Controls received same volume of PBS. Mice were euthanized at 4 Hrs or 2 weeks post administration with avertin anesthesia, portal vein blood collected for serum analysis, heart and liver tissues harvested for RiboIP.

RNAseq library preparation and analysis

cDNA libraries were constructed using NuGEN Trio RNA-Seq (Catalog # 0507)(NuGEN, San Carlos, CA) and 2-10 ng of total RNA. Libraries were quantified with NEBNext Library Quant Kit for Illumina (Catalog # E7630, New England BioLabs, Ipswich, MA) before sequencing them on a NextSeq500 (Illumina, San Diego, CA) using NextSeq500 High-Output v2 75 cycles consumables (FC-404-2005)(Illumina). Libraries were sequenced 75 cycles using single ended reads with 8 additional reads for barcodes. Sequencing reads were converted from BCL to FASTQ format and demultiplexed using Bcl2fastq2 software. The first 5 base calls were then trimmed and low quality reads filtered out using FASTX-Toolkit. Reads were then aligned to GRCm38/mm10 UCSC mouse genome using TopHat2 . Differential expression was determined using Cuffdiff from Cufflinks using a false discovery rate (FDR) < 0.05 and requiring a 2 fold difference in means. Data were visualized using R version 3.4.4 “Someone to Lean On” within RStudio utilizing tidyr, dplyr, and ggplot2.

Statistical analysis

Graphs present data from 3 or more independent experiments. Exact numbers and repetitions are noted in the figure legends. All groups were assumed to be normally distributed with similar variance between groups. No randomization or blinding of the investigator was performed. Groups were compared with Unpaired t test with Welch's correction or one-way ANOVA with Turkey post-hoc analysis. Multiple-gene expression comparisons were performed using Multiple t-test followed by Holm-sidak post hoc analysis. Significant p-values are represented by asterisks at the following levels: *, $P \leq 0.05$; **, $P \leq 0.01$; ***, $P \leq 0.001$; and ****, $P \leq 0.0001$; while ns = not significant ($P > 0.05$). All statistical analysis was performed in either GraphPad Prism 7 (La Jolla, CA) or Microsoft Excel (Microsoft, Redmond, WA).

CHAPTER 3: THE RELATIONSHIP BETWEEN KUPFFER CELL ONTOGENY AND RADIOSENSITIVITY

Abstract

Kupffer cells (KCs) are pivotal innate immune sensors in the liver. When exposed to lethal irradiation a subset of "sessile" KCs survives, while others are replaced by bone marrow monocyte-derived KCs (bm-KCs). Here we focused on the identity of the radioresistant KC subset and the mechanism of resistance. Using a lineage-tracing model we show that embryo-derived, Cx3cr1-marked, long-lived KCs resist irradiation, and resemble the sessile subset in terms of gene expression while bm-KCs do not survive irradiation. Using gene expression, we analyzed the immediate response of bm-KCs and Cx3cr1-marked KCs to irradiation. While both subsets upregulated the *Cdkn1a* gene, encoding p21-$^{cip1/WAF1}$, Cx3cr1-marked KCs showed a greater increase in response to irradiation. This elevated *Cdkn1a* expression provided an increased survival potential to the Cx3cr1-marked KCs. Synthesizing these data, we argue that long-lived sessile KCs are radioresistant because they upregulate p21-$^{cip1/WAF1}$ expression and undergo reversible cell cycle arrest.

Introduction

Kupffer cells (KCs) the liver resident macrophages are located in the liver vascular channels known as sinusoids. As important innate immune sensors KCs are among the first responders to liver stress and may either stimulate or suppress immunity. At steady state, KCs support liver homeostasis by scavenging bacteria in the portal blood flow, engulfing aging red blood cells and regulating iron metabolism (63).

In contrast to lymphocytes, monocytes, and dendritic cells, tissue resident macrophages in brain (microglia) and epidermis (Langerhans cells) are highly radioresistant (80-82). However in the liver only a subset of KCs resists lethal irradiation while the other subset is replaced by donor bone marrow monocyte-derived KCs (bm-KCs) (56, 83). This radio resistant KC subset is long-lived and they do not take part in the inflammatory recruitment process and thus termed sessile KCs (56, 84). Gene expression analysis and epigenetic chromatin modification studies have confirmed that while the bm-KC become

broadly similar to the sessile KC post recovery, the two subsets do not become identical to each oher (74, 83). While the sessile KC subset is identified post irradiation, the identity of this subset in unmanipulated mice and why only a subset of KCs resists irradiation is not yet understood.

Kupffer cells traditionally comprise all of the fully mature macrophages in the steady-state liver, identified by F4/80 staining in the mouse (85). A developing consensus asserts the view that KCs are a single population of long-lived cells that are seeded from embryonic precursors, and that any other macrophages found in the liver are transients, better-termed “liver macrophages”. In favor of this view, several lineage-tracing models have concluded that all liver-resident macrophages are embryo-derived (35, 46-48, 50, 52). In this view, yolk sac (YS) erythro myeloid progenitors (EMPs) and fetal liver monocytes give rise to the long-lived liver resident macrophages in the adult liver. Several studies further distinguished the F4/80^{-hi} Cd11b^{-lo} subset as YS-derived KC and the F4/80^{-lo} CD11b^{-hi} subset as liver macrophages (34, 35).

In contrast, some evidence favors the concept that long-lived KCs are themselves heterogeneous, with a subset coming from blood monocytes. In adoptive transfer experiments into neonates, blood monocytes could integrate into the KC niche in the postnatal developmental period, indicating that the liver macrophage compartment remains open at least up until the postnatal period (49). Another study identified resident Cx3Cr1^{-hi} F4/80+ sub-capsular macrophages that are continuously replenished by blood monocytes in the steady state liver further supporting the presence of bm-KCs in the normal adult liver (38). Single cell transcriptome analysis reports two distinct KC clusters based on gene expression-*Marco, Clec4f, Clec1b* versus *Clec4e, Clec4d* subsets (40). However the relationship of these two clusters to ontogeny or to the issue of KCs versus liver macrophages remains unclear.

While the relationship between subsets elucidated in fate mapping, phenotype, and gene expression studies are yet to be resolved, a strong case can be made that the liver contains at least two subsets of macrophages –YS EMP-derived versus monocyte-derived cells. In this study we explored the identity of the sessile KC subset in relation to ontogeny- YS versus monocyte origin- and potential mechanisms of radioresistance. In addition to traditional fluorescence-based cell sorting (FACS) methods

we used an *in situ* gene expression analysis method based on RiboTag reporter mice, that is independent of cell isolation, to specifically analyze the translatome and thereby to study gene expression (79, 86).

Here we show that RiboTag approach combined with inducible or non-inducible Cre Recombinase systems allow fate mapping and gene expression analysis of KCs. Using translatome analysis we show that the bm-KCs start to resemble sessile KCs over time in chimeric mice but remain transcriptionally distinct. An inducible fate mapping strategy combined with RiboTag allowed consistent labeling of an embryo-derived, postnatally Cx3cr1-marked KC subset that also resisted irradiation. Using gene expression analysis we showed that these embryo-derived, Cx3cr1-marked radio resistant KCs are identical to sessile KCs. In contrast the bm-KC subset was sensitive to irradiation. Gene expression analysis immediately following lethal irradiation indicated increased upregulation of *Cdkn1a* in the Cx3cr1-marked KC subset, compared to bm-KCs and this elevated expression allowed increased survival capacity to the Cx3cr1-marked subset.

Thus using a combination of fate mapping, irradiation chimeras, KC depletion and a RiboTag based translatome analysis we identified the radioresistant sessile KC subset as embryo-derived postnatally Cx3cr1-marked F4/80^{-hi} KC subset, and show that the survival of this subset is dependent on the elevated expression of the *Cdkn1a* gene and therefore likely its gene product, p21-$^{cip1/WAF1}$.

Results

RiboTag reporter mice allow *in situ* gene expression analysis of Kupffer cells.

Current knowledge of gene expression in KCs is based on the analysis of isolated cells. Such cell isolation is performed on a single cell suspension using FACS methods where KCs are identified as a F4/80^{-hi} and CD11b+ subset within the CD45+ leukocyte population. While there is no universally accepted protocol to generate a single cell suspension, all methods described so far include at least a 30 min enzymatic digestion to disintegrate the tissue. A recent study demonstrate the loss of KCs based on the techniques used and show that the purity of isolated KCs is dependent on careful selection of surface markers to exclude contaminating endothelial cells (41). In radiation chimeras, Klein et al were only able to isolate donor bm-KC in a liver cell suspension, while subsequently Beattie et al isolated both sessile

and bm-KC subsets using perfusion techniques, emphasizing the difficulty of basing the analysis of KCs exclusively on cells isolated using tissue dissociation (56, 83).

We adopted a strategy first described by Sanz et al in neurons to bypass the cell isolation problem and analyze gene expression by cell specific activation of the RiboTag reporter (Figure 3-1) (79). RiboTag mice contain a modified ribosomal protein- RPL22- that encodes a 3' hemaglutinin (HA) epitope tag. In the presence of Cre recombinase, the modified exon-linked HA tag is activated irreversibly, and this generate a modified RPL22-HA protein containing ribosomes in a cell specific manner. These modified ribosomes form polysome with actively translating mRNA in the cells and immunoprecipitation (Ribo IP) of the polysomes enriches for the cell specific translatome (Figure 3-1A). Ribo IP is performed on a total liver lysate that is generated within minutes (in our hands, around 3 minutes) of organ harvest minimizing any effects on gene expression due to prolong exposure of cells to enzymatic treatments or incubations. Furthermore RiboTag allows *in situ* identification of the labeled cell population though immunofluorescence.

To validate the RiboTag approach in KCs we first used Emr1Cre, a tissue resident macrophage specific Cre driver that uses the promoter from the F4/80 antigen gene (87). We generated *Emr1Cre*$^{+/-}$ *::RiboTag*$^{+/-}$ mice, performed Ribo IP and analyzed gene expression using qRT-PCR for 140 genes (Figure 3-1B and Figure 3-8). Tissue resident macrophage genes identified by the Immgen consortium(39) *Emr1, MerTK, CD64* showed over 10 fold enrichment while KC specific gene *Clec4f(74)* and phagocytosis gene *Marco* showed over 50 fold enrichment. Phagocytosis genes-*Vsig4, Mcr1* and iron metabolism related genes *CD163, Hmox-1* were also strongly enriched mirroring the known KC functions at steady state. Analysis of hepatocytes genes *Alb, Hamp1, Cyp2f2* and sinusoidal endothelial cells genes *Tie2, Lyve1* indicated a 10 fold or more de-enrichment while hepatic stellate cell transcript abundance was low in both input and Ribo IP fractions. Other myeloid cell genes such as *Siglecf, Ccr2, Ly6c, DEC205* showed up to 2 fold enrichment, de-enrichment or remained unchanged relative to total liver RNA. Furthermore immunofluorescence staining using anti-HA and anti-F4/80 antibody on cryo-preserved sections revealed RiboTag stained KCs *in situ* (Figure 3-1C). Due to the auto fluorescence of liver tissue we were unable to quantify the HA-labeling *in situ* and thus used an intra cellular FACS based approach to calculate the recombination efficiency.

We isolated KCs as previously described by Mohar et. al.(78), stained for phenotypic markers and performed intra cellular staining for RiboTag using anti-HA antibody prior to FACS analysis. Kupffer cells were gated as CD45+, CD11b+, Tie2-, Ly6G-, Siglecf-, F4/80^{hi} cells in the Live single cell population (Figure 3-2). In *Emr1Cre+/-::RiboTag+/-* mice 82% of KCs were labeled with RiboTag while no other cell subset showed labeling (Figure 3-1D). The exclusive labeling of the F4/80^{hi} cells further confirms the high specificity of Emr1Cre in activating reporters in KCs as previously reported (88). Since Emr1 is a pan tissue resident macrophage marker we also analyzed gene expression in cardiac and brain tissue using Ribo IP in *Emr1Cre+/-::RiboTag+/-* mice. We found that both microglia and cardiac macrophages show enrichment of tissue macrophage genes (Figure 3-1E). A recent study describes the translatome analysis in microglia using RiboTag approach (86). We further extend the use of the RiboTag approach to KCs.

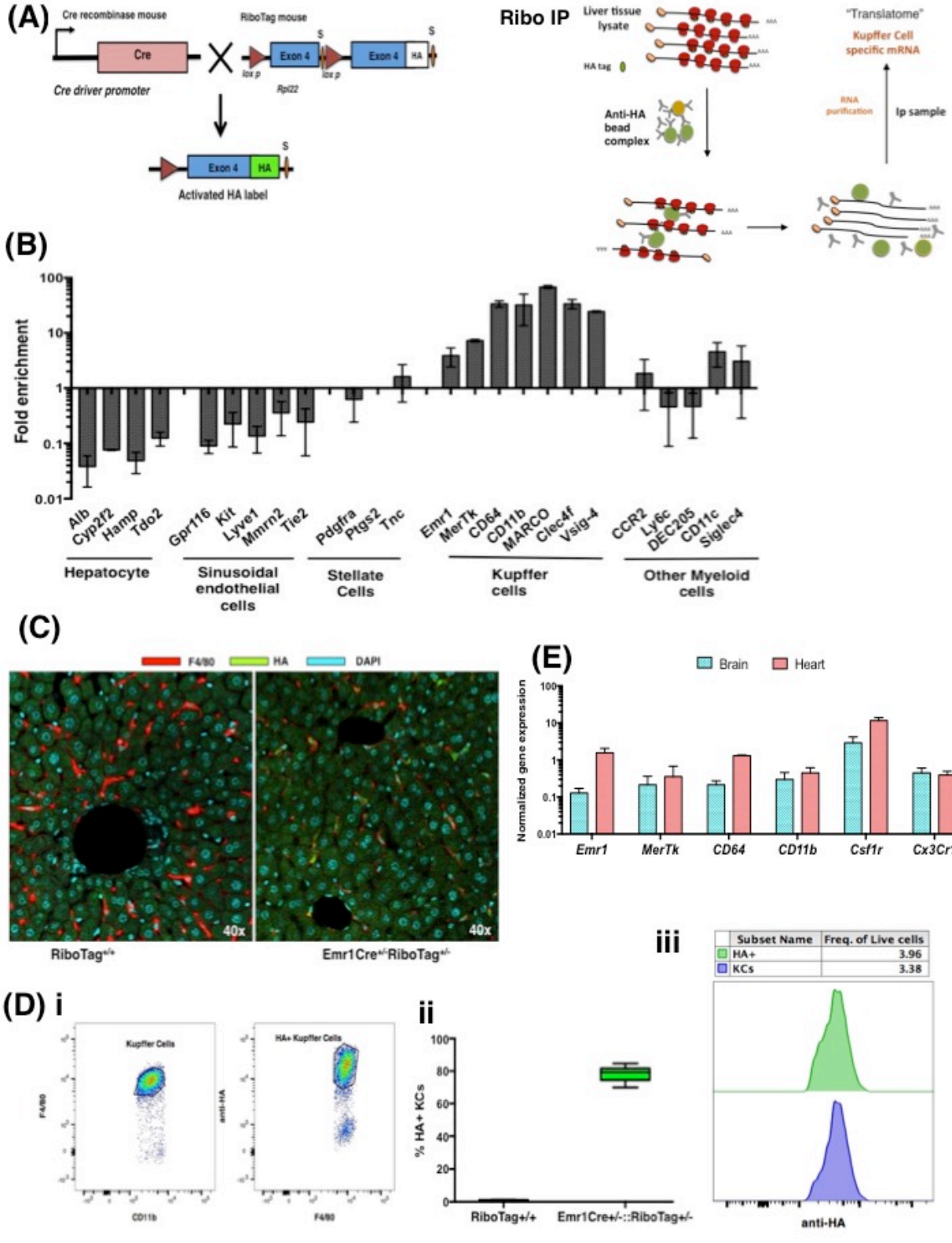
(A)
Cre recombinase mouse
RiboTag mouse
Cre
Exon 4
Exon 4
HA
lox p
lox p
Rpl22
Cre driver promoter
Exon 4
HA
Activated HA label
Ribo IP
Liver tissue lysate
HA tag
Anti-HA bead complex
"Translatome"
Kupffer Cell specific mRNA
RNA purification
Ip sample
(B)
Fold enrichment
100
10
1
0.1
0.01
Alb
Cyp2f2
Hamp
Tdo2
Gpr116
Kit
Lyve1
Mmrn2
Tie2
Pdgfra
Ptgs2
Tnc
Emr1
MerTk
CD64
CD11b
MARCO
Clec4f
Vsig-4
CCR2
Ly6c
DEC205
CD11c
Siglec4
Hepatocyte
Sinusoidal endothelial cells
Stellate Cells
Kupffer cells
Other Myeloid cells
(C)
F4/80
HA
DAPI
40x
40x
RiboTag+/+
Emr1Cre+/-RiboTag+/-
(E)
Brain
Heart
Normalized gene expression
100
10
1
0.1
0.01
Emr1
MerTk
CD64
CD11b
Csf1r
Cx3Cr1
(D) i
Kupffer Cells
HA+ Kupffer Cells
F4/80
CD11b
anti-HA
F4/80
ii
% HA+ KCs
100
80
60
40
20
0
RiboTag+/+
Emr1Cre+/-::RiboTag+/-
iii
Subset Name
Freq. of Live cells
HA+
3.96
KCs
3.38
anti-HA

Figure 3-1. Emr1Cre driven RiboTag reporter allows translatome analysis and in situ identification of KCs. (A)Diagram illustrates the RiboTag reporter activation by Cre recombinase and the enrichment of cell specific mRNA in polysome immunoprecipitation (RiboIP). (B)Fold enrichment (IP/Input) of KC-associated genes in Emr1Cre+/-::RiboTag+/- mice compared to other liver cells. (C)Immunofluorescence images demonstrating the expression of HA antigen-RiboTag- (Green) on F4/80 (Red)-marked KCs in liver sections from RiboTag+/+(left) and Emr1Cre+/-::RiboTag+/-(right) mice. Nuclei:Cyan (40Xmagnification). (D)Intracellular FACS analysis showing; the proportion of HA-labeled KCs(i), the recombination efficiency of Emr1Cre driver in KCs(ii), the percent HA-labeled cells(green) and the percent KCs(Purple) in the live cell population(iii). (E)Gene expression analysis of tissue resident macrophages in brain and heart of Emr1Cre+/-::RiboTag+/- using RiboIP. Data represent 3 independent experiments with n=4 mice/group. B,E:bars represent the mean±S.D.

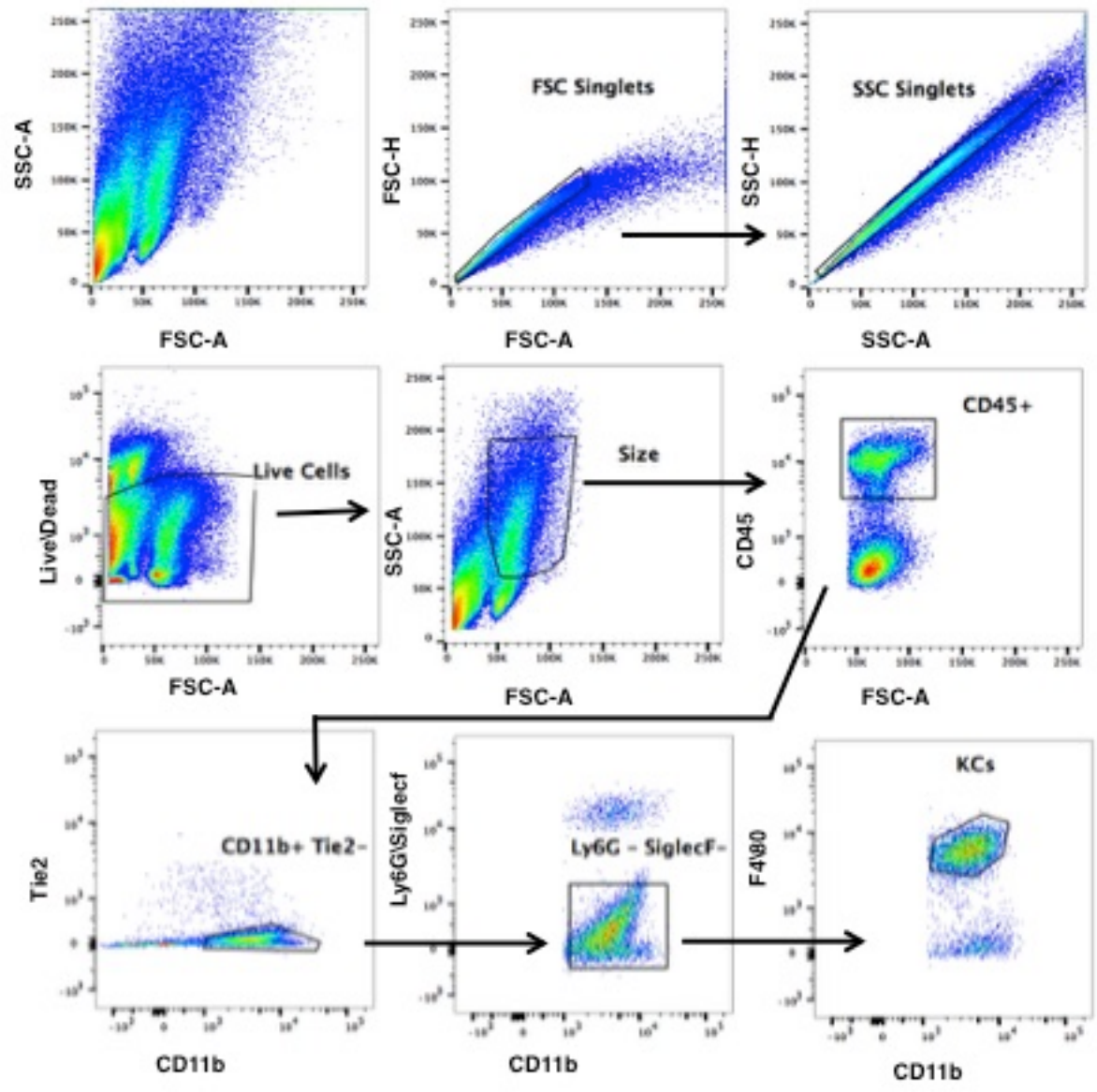

Figure 3-2. Gating strategy for Kupffer cells. Representative FACS plots showing gating strategy to identify KCs from a single cell non-parenchymal cell suspension isolated from the liver.

Gene expression in sessile Kupffer cells versus bm-KCs

A recent study reports a comparison of transcriptome in sessile vs bm-KCs 8 weeks post irradiation where the KCs were isolated using FACS sorting (83). In this study the LysM-Cre transgene was used to activate a GFP reporter in KCs of either the host or the donor origin. We set out to compare the gene expression of the two subsets using the RiboTag approach where only the translatome is analyzed. We generated irradiation bone marrow chimeras of two types. In one CD45.1 WT bone marrow was transplanted to lethally irradiated CD45.2+ Emr1Cre+/-::RiboTag+/- mice and in the other Emr1Cre+/-::RiboTag+/- bone marrow was transplanted into lethally irradiated CD45.1+ WT mice (Figure 3-3). In these chimeras, the Emr1Cre and RiboTag transgenes were localized to either the sessile KCs or the bm-KCs. Immunofluorescence image of cryo-preserved liver tissue indicated the host versus donor derived KC subsets 8 weeks post irradiation (Figure 3-3B).

First we compared the expression of 94 genes in the two subsets 8 weeks post-lethal irradiation (Figure 3-3C and Figure 3-4). Translatome analysis indicated that characteristic tissue macrophage genes *Emr1, MerTK, CD64* and phagocytosis related genes *Clec4f, Vsig4, Msr1* were expressed to a similar level in both subsets. Among the differentially expressed genes, sessile KCs showed a significantly higher expression of phagocytosis related gene *Marco*, apoptotic cell engulfment related gene *Timd4*, c-lectin family scavenger receptor *Colec12*, ion homeostasis related gene *Hmox1* and cyclin dependent cell cycle inhibitor *Cdkn1a*. The bm-KCs showed a significantly higher expression of MHC Class II genes *H2-Ab1*, and *H2-Aa* while the MHC Class I gene *H2-K1* remained similar in the both subsets. We further confirmed the protein level upregulation of TIMD4 and MHC Class II molecules (IA/IE) on the respective subsets (Figure 3-3D). While these data are consistent with previous findings on differentially expressed genes in sessile KCs vs bm-KCs (83), we did not find the hemoglobin scavenger receptor-*CD163*- and erythropoietin receptor-*Epor*- to be different between the two subsets. Possible explanations for these discrepancies are the differences between dissociation and FACS-sorting versus *in situ* mRNA capture, and the differences between transcriptome versus translatome analysis. A recent study clearly documents the differences in gene expression in microglia in a side-by-side analysis of sorted cell transcriptome versus Ribo IP translatome (86). Overall we confirmed the previous

observations(74, 83) that sessile KCs and bm-KCs show similar expression in many macrophage genes, but were not identical.

Since in a bone marrow chimera experiment only the sessile subset was exposed to 10Gy irradiation, it is plausible that differentially expressed genes in the sessile subset were due to the radiation, rather than to a subset distinction. To test this we compared the gene expression of non-irradiated control mice, which received a bone marrow transplant to sessile KC subset post 8 weeks irradiation. Among the upregulated genes in the sessile subset, *Marco* and *Cdkn1a* showed an irradiation induced upregulation that persisted up to 8 weeks (Figure 3-3E). Next we wanted to see whether the differential gene expression between sessile vs bm-KCs balanced out over time. Klein et al indicate the continued existence of two subsets of KCs in irradiation chimera mice up to 13 weeks but the gene expression of each subset has not been analyzed so far. We analyzed the gene expression in sessile KC vs bm-KC subset 13 weeks post irradiation. While the level of *Timd4, Colec12, Hmox1, Cdkn1a, H2-Ab1, H2-Aa* expression became comparable by 13 weeks, *Marco* expression remained 40 fold higher in sessile KCs compared to the bm-KC subset (Figure 3-3F). Collectively our results along with previous findings indicate that tissue environment is not the sole driver of gene expression in KCs.

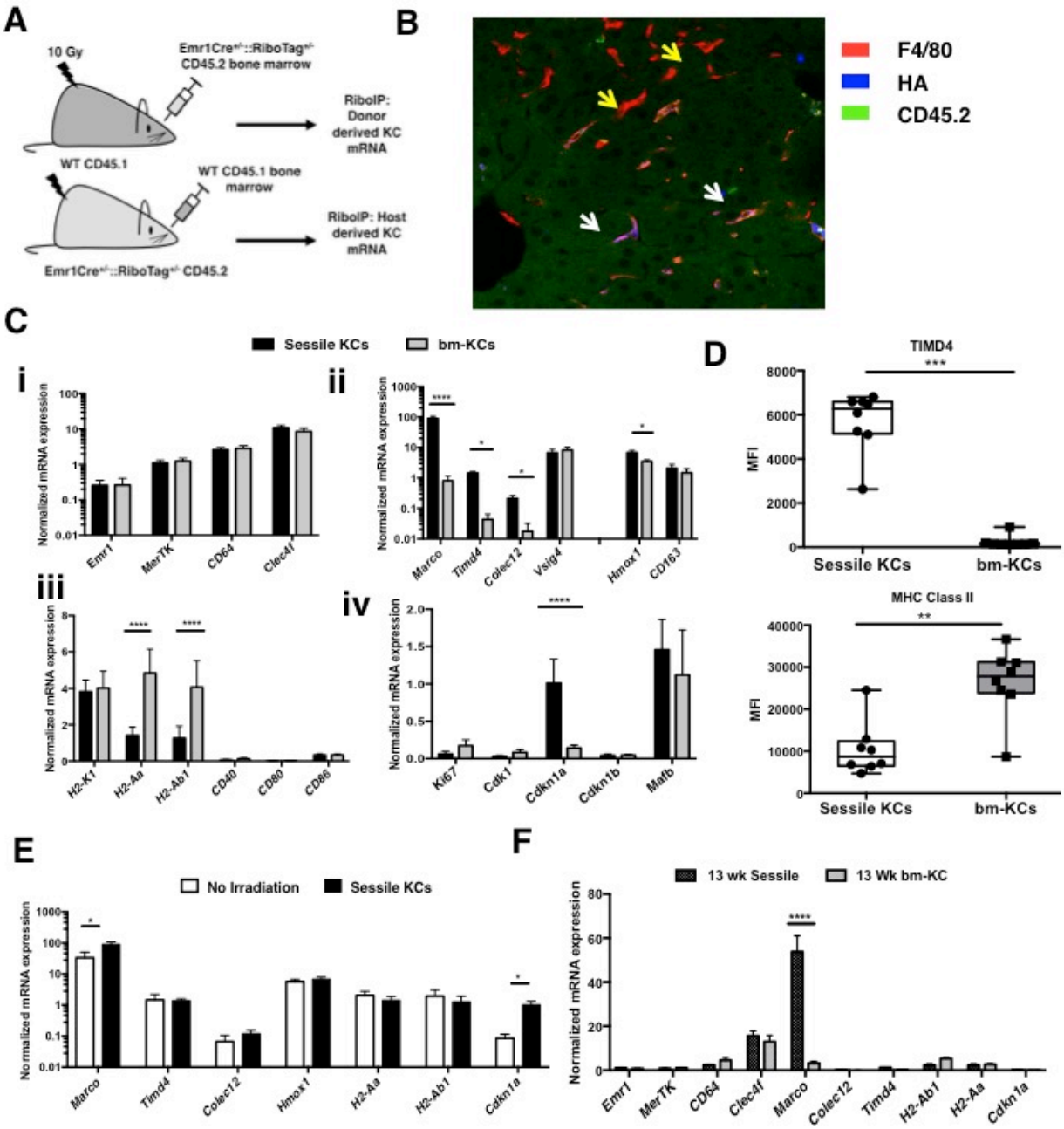
A
10 Gy
Emr1Cre+/-::RiboTag+/- CD45.2 bone marrow
RiboIP: Donor derived KC mRNA
WT CD45.1
WT CD45.1 bone marrow
RiboIP: Host derived KC mRNA
Emr1Cre+/-::RiboTag+/- CD45.2
B
F4/80
HA
CD45.2
C
Sessile KCs
bm-KCs
i
ii
iii
iv
Normalized mRNA expression
Emr1
MerTK
CD64
Clec4f
Marco
Timd4
Colec12
Vsig4
Hmox1
CD163
H2-K1
H2-Aa
H2-Ab1
CD40
CD80
CD86
Ki67
Cdk1
Cdkn1a
Cdkn1b
Mafb
D
TIMD4
MFI
Sessile KCs
bm-KCs
MHC Class II
E
No Irradiation
Sessile KCs
F
13 wk Sessile
13 Wk bm-KC

Figure 3-3. Gene expression analysis of radioresistant sessile KCs and bm-KCs. (A)Diagram illustrates the generation of radiation chimeras between wild type and Emr1Cre+/-::RiboTag+/- mice. (B)Immunofluorescence image demonstrating the sessile (white arrows) and bm-KCs (yellow arrows) in a radiation chimera where sessile KCs express RiboTag(blue) and CD45.2(green). (C)Gene expression analysis of sessile versus bm-KCs at 8 weeks post-irradiation of KC-associated genes(i), phagocytosis and ion metabolism-associated genes(ii), antigen presentation-associated genes(iii) and cell cycle-associated genes(iv). (D)FACS analysis of surface TIMD4 and MHC class II protein levels in sessile versus bm-KCs (E)Radiation-induced gene expression differences in sessile KCs compared to non-irradiated mice at 8 weeks post-irradiation. (F)Gene expression differences at 13-weeks post irradiation between the sessile and the bm-KCs. Data represent at least 3 independent experiments with n=4 mice/group. D:indicates Median Fluorescence Intensity (MFI). C,E,F:indicate the mean±S.D.*P≤0.05,**P≤0.01,***P≤0.001(Mann-Whitney test with P-values adjusted for multiple comparisons using Holm-Bonferroni method)

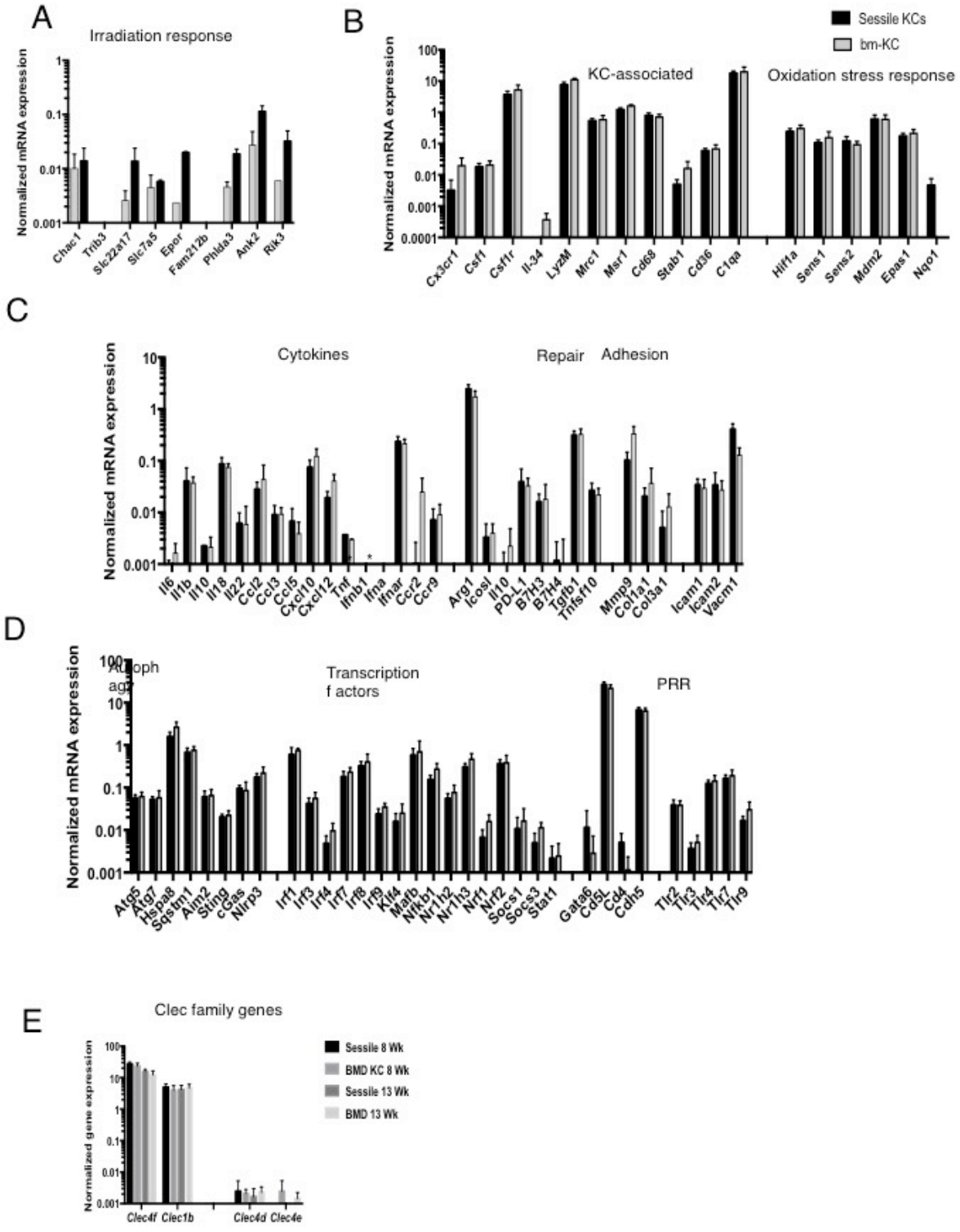
A
Irradiation response
Normalized mRNA expression
Chac1
Trib3
Slc22a17
Slc7a5
Eper
Fam212b
Phlda3
Ank2
Rik3
B
Sessile KCs
bm-KC
KC-associated
Oxidation stress response
Normalized mRNA expression
Cx3cr1
Csf1
Csf1r
Il34
LyzM
Mrc1
Msr1
Cd68
Stab1
Cd36
C1qa
Hif1a
Sens1
Sens2
Mdm2
Epas1
Nqo1
C
Cytokines
Repair
Adhesion
Normalized mRNA expression
Il6
Il1b
Il10
Il18
Il22
Ccl2
Ccl3
Ccl5
Cxcl10
Cxcl12
Tnf
Ifnb1
Ifna
Ifnar
Ccr2
Ccr9
Arg1
Icosl
Il10
PD-L1
B7H3
B7H4
Tgfb1
Tnfsf10
Mmp9
Col1a1
Col3a1
Icam1
Icam2
Vacm1
D
Transcription
f actors
PRR
Normalized mRNA expression
Atg5
Atg7
Hspa8
Sqstm1
Aim2
Sting
cGas
Nlrp3
Irf1
Irf3
Irf4
Irf7
Irf8
Irf9
Klf4
Mafb
Nfkb1
Nr1h2
Nr1h3
Nrf1
Nrf2
Socs1
Socs3
Stat1
Gata6
Cd5L
Cd4
Cdh5
Tlr2
Tlr3
Tlr4
Tlr7
Tlr9
E
Clec family genes
Normalized gene expression
Sessile 8 Wk
BMD KC 8 Wk
Sessile 13 Wk
BMD 13 Wk
Clec4f
Clec1b
Clec4d
Clec4e

Figure 3-4. Gene expression analysis of sessile and bm-KCs in radiation chimera mice. Gene expression analysis **(A-D)** 8 weeks and **(E)** 13 weeks post-irradiation. Either the Emr1Cre$^{+/-}$::RiboTag$^{+/-}$ or WT CD45.1 adult mice were exposed to 10Gy irradiation and administered a congenic bone marrow transplant. Ribo IP isolated either host or donor KC subset RNA. Gene expression was determined using RT-PCR and normalized to *Gapdh* and *Hprt.* Data represent 3 independent experiments with n=3 mice per group. Bars indicate the mean ± S.D n.d: no detects, bm-KC: bone marrow monocyte derived KCs: Sessile: radioresistant host derived KCs

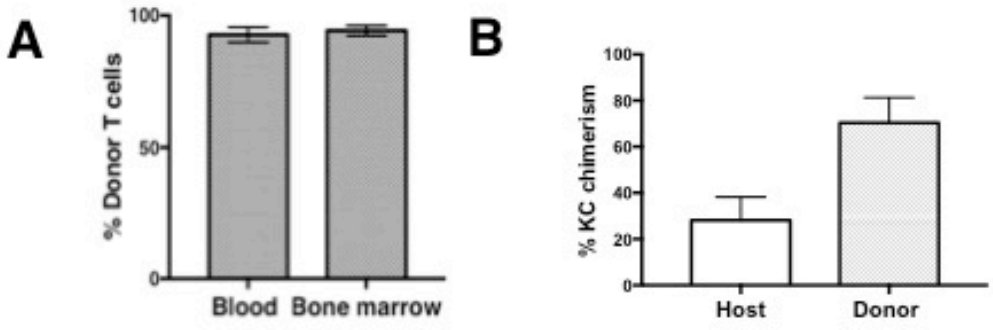

Figure 3-5. Chimerism post lethal irradiation.
(A-B) FACS analysis of percent donor T cells in portal vein blood, Bone marrow (A), percent donor versus host Kupffer cells (B) in mice 8 weeks post lethal irradiation (10Gy) and a bone marrow transplant. Data represent 3 independent experiments with n=4 mice per group. Bars indicate the mean ± S.D

Cx3cr1-based lineage-tracing labels embryo-derived, long-lived Kupffer cells in the adult liver

While it is clear that a subset of KCs resist irradiation the origin of this sessile subset in non-irradiated liver remains unclear. First we set to label the embryo-derived KCs in adult mice using a fate mapping approach.

We devised a RiboTag reporter and inducible Cre recombinase based strategy to label embryo-derived KCs immediately after birth. Fracktalkine receptor (Cx3cr1) driven Tamoxifen inducible Cre -Cx3Cr1CreER- is used in tissue macrophage lineage tracing (34, 50, 51). Developmental studies in embryo indicate that Cx3cr1 is expressed in yolk sac precursors that give rise to tissue macrophages and maintain expression on microglia and a subset of cardiac macrophages all the way into adulthood (34, 51, 52, 89, 90). However in KCs, Cx3cr1 ceases expression after the early postnatal period (34, 50). Furthermore Cx3cr1 is also expressed on a subset of dendritic cells and monocytes, thus a constitutive Cx3cr1-Cre driver would not have been truly cell type-specific. Therefore to evaluate the extent of Cx3cr1 expression in KCs and monocytes post birth we analyzed 2-days old postnatal liver using intra cellular FACS. In postnatal liver only 43% KCs expressed CX3CR1 while monocytes did not show expression (Figure 3-6B and Figure 3-7). This indicates by day 2 at least 43% of embryo-derived KCs continue to express Cx3cr1 while it is possible that some has already ceased expression. Furthermore there was no Cx3cr1 expression on monocytes suggesting that Cx3cr1+ monocyte-derived macrophages were not seeding the liver within the first 2 days. Thus the first 2 days after birth provides a window to label embryo-derived KCs using the Tamoxifen inducible Cx3Cr1-eyfp-CreER model. We bred Cx3Cr1-eyfp-CreER$^{+/+}$ mice with RiboTag$^{+/+}$ mice and the offspring were Tamoxifen-induced within the first two days of birth (Figure 3-6A). When the mice were 8 weeks old we analyzed the liver tissue by immunofluorescence and showed that only a subset of KCs were labeled with RiboTag, while others clearly showed no labeling (Figure 3-6C). Intra cellular FACS analysis indicated that 37% of the total KCs in the adult mice are RiboTag-labeled hence are Cx3cr1-marked, representing the embryo-derived KC subset (Figure 3-6D).

In contrast to KCs, microglia constitutively express Cx3cr1 thus we analyzed the percent RiboTag labeling of microglia in adult mice post day 2 Tamoxifen induction and found it to be 80% (Figure 3-6D). This indicates the labeling efficiency of Cx3cr1-eyfp-CreER promoter is about 80%. Furthermore

intracellular FACS revealed that monocytes or dendritic cells in the adult liver do not carry RiboTag labeling, indicating that any cell that may get labeled in the early postnatal period are turned over by 8 weeks (Figure 3-6D). We also induced labeling at 1 week and 6 weeks after birth, analyzed at 10 weeks of age and found that the labeling has significantly reduced to 2% and <1% respectively (Fig 3f). This further supports the previous observations that the Cx3cr1 expression ceases on embryo-derived KCs early on and the Cx3cr1 fate-mapping strategy can be only used to label embryo-derived KCs within the first days of birth.

To determine the turn over of Cx3cr1-marked KCs in the liver, we conducted a time course analysis for percent HA+ KCs among the total KCs on postnatal day 2 induced mice at 2, 3, 10-weeks and 4, 6, 9, 12-months post induction. Interestingly the Cx3cr1-marked KCs survived at least 12 months and maintained their 37% frequency among total KCs up to 9 months before declining to 22% by 12 months (Figure 3-6E) making a strong case for their stability over time. This observation is consistent with a previous report that postnatal labeled KCs survived up to 9 months (34) while our labeling strategy indicated a third of the KCs surviving, compared to the previously reported 7%.

Next we examined the gene expression of the Cx3cr1-marked KCs using the Ribo IP approach and showed that consensus tissue macrophage genes (*Emr1,MerTK, CD64*) and KC related genes (*Marco, Clec4f*) were highly enriched while hepatocyte, sinusoidal endothelial cells, hepatic stellate cells and other myeloid markers are either de-enriched or show no change (Figure 3-6F and Figure 3-8). We also performed immunofluorescence to detect embryo-derived KCs *in situ* and showed that only a subset of KCs carried the HA label (Figure 3-6C). Taken together these data show that Cx3cr1-eyfp-CreER combined with RiboTag fate mapping allows both labeling and gene expression analysis of Cx3cr1-marked, embryo-derived KCs following postnatal Tamoxifen induction.

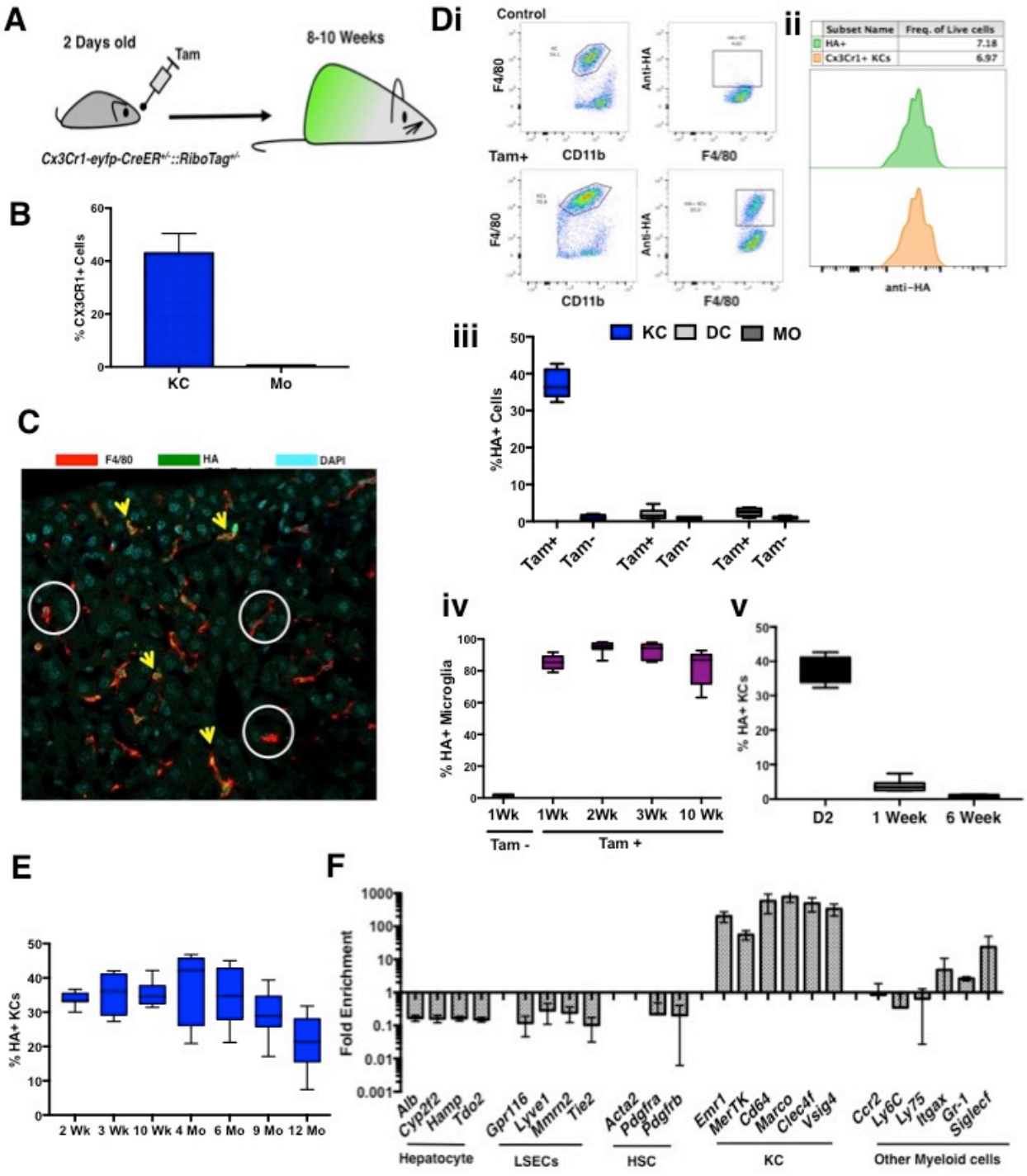
A
2 Days old
Tam
8-10 Weeks
Cx3Cr1-eyfp-CreER+/-::RiboTag+/-
B
% CX3CR1+ Cells
KC
Mo
C
F4/80
HA
DAPI
Di
Control
Tam+
F4/80
CD11b
Anti-HA
ii
Subset Name
Freq. of Live cells
HA+
7.18
Cx3Cr1+ KCs
6.97
anti-HA
iii
KC
DC
MO
%HA+ Cells
Tam+
Tam-
iv
% HA+ Microglia
1Wk
2Wk
3Wk
10 Wk
Tam -
Tam +
v
% HA+ KCs
D2
1 Week
6 Week
E
% HA+ KCs
2 Wk
3 Wk
10 Wk
4 Mo
6 Mo
9 Mo
12 Mo
F
Fold Enrichment
Alb
Cyp2f2
Hamp
Tdo2
Gpr116
Lyve1
Mmrn2
Tie2
Acta2
Pdgfra
Pdgfrb
Emr1
MerTK
Cd64
Marco
Clec4f
Vsig4
Ccr2
Ly6C
Ly75
Itgax
Gr-1
Siglecf
Hepatocyte
LSECs
HSC
KC
Other Myeloid cells

Figure 3-6. Cx3cr1-based fate mapping labels embryo-derived long-lived KCs in the adult liver. (A)Diagram illustrates the irreversible labeling of KCs within the first 2-days of birth in Cx3cr1-eyfp-CreER+/-::RiboTag+/- mice following Tamoxifen administration. (B)Percent cells expressing CX3CR1 in KCs and monocytes in 2-days old mice determined by FACS. (C)Immunofluorescence image of adult mouse liver, post D2-Tamoxifen induction, indicating the presence of F4/80+ KCs(red) and HA antigen(green). Yellow arrows: postnatally Cx3cr1-marked KCs, White circles: non-labeled KCs. (D)Intracellular FACS analysis of; adult mice post day-2 Tamoxifen induction compared to the control showing the RiboTag-labeled KCs (i), the percent HA-labeled and Cx3cr1-marked KCs in the live cells(ii), the percent HA-labeling in liver KCs, dendritic cells(DC) and monocytes(MO)(iii), percent HA-labeled microglia following day2 induction(iv), percent HA-labeled KCs in 10 weeks old mice following Tamoxifen induction at 2-days, 1-week or 6-weeks(v). (E)Following 2-days Tamoxifen induction, Cx3cr1-labeled KC turnover up to 12 months analyzed using FACS. (F)Fold enrichment of KC-associated genes. Data represents >3 independent experiments with n>5 mice/group. B,F:bars indicate the mean±S.D.

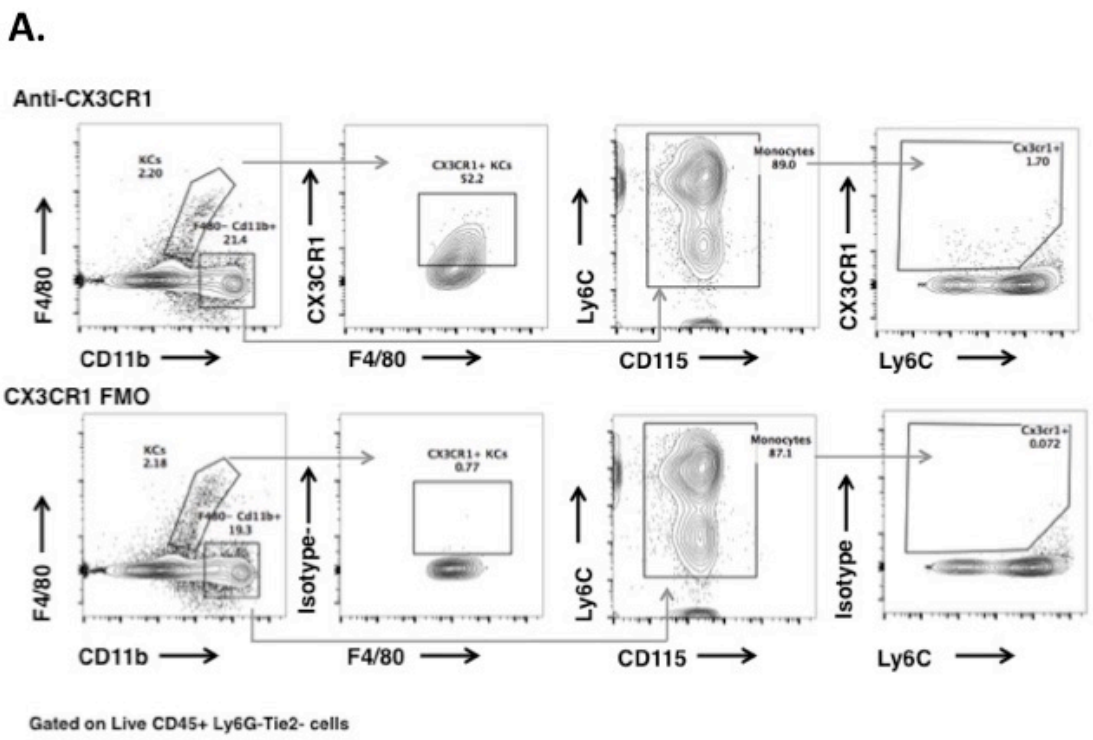

Figure 3-7. Gating strategy indicating the CX3CR1 expression of Kupffer cells and monocytes in 2-days old mice. Day2 old mice livers were isolated, minced and digested in Collagenase IV containing RPMI media, stained and FACS analyzed. Panels indicate the CX3CR1 expression on Kupffer cells and Monocytes compared to FMOs (bottom panel). Data represent 3 independent experiments with n=3 neonates per group

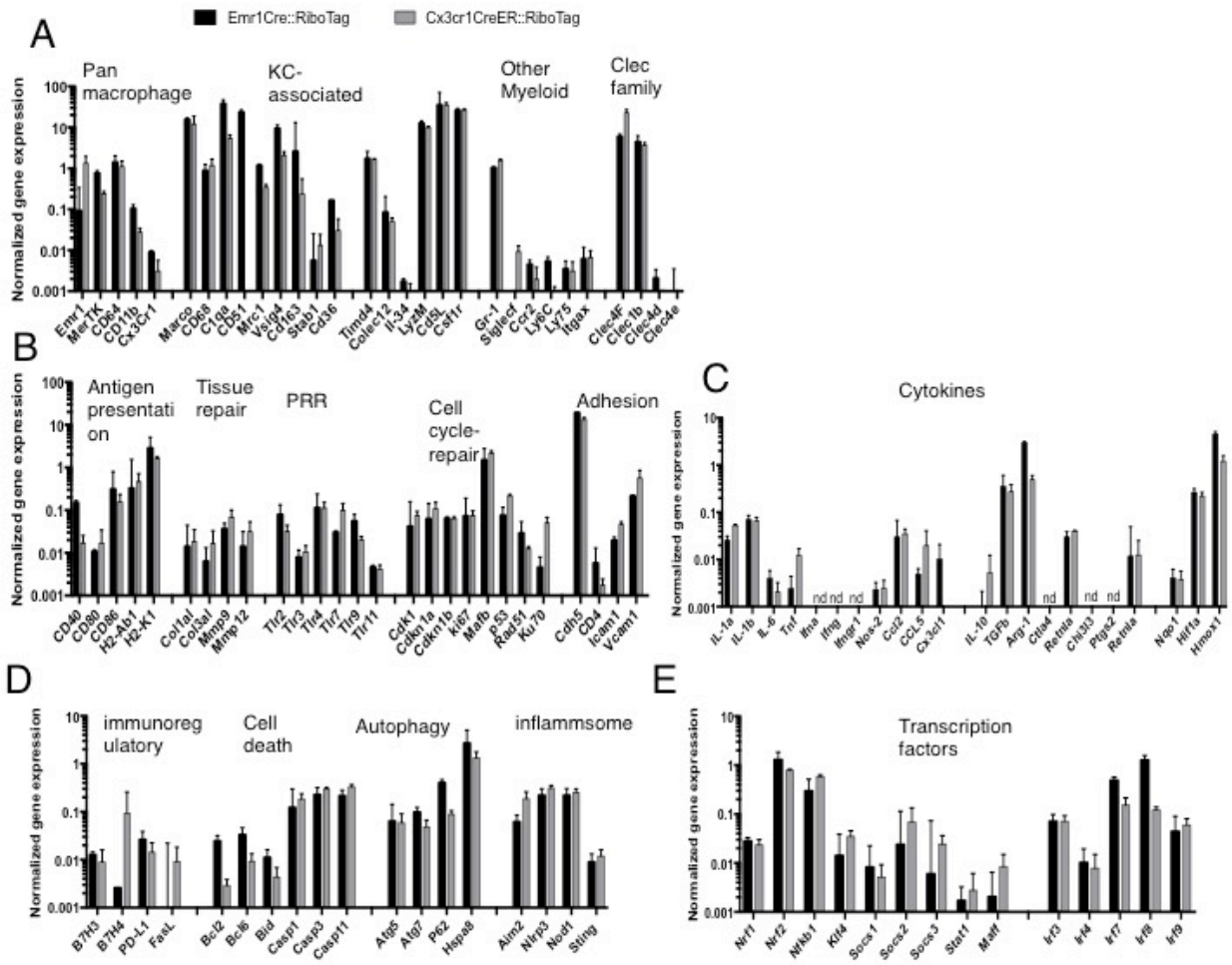

Figure 3-8. Gene expression analysis of Kupffer cells using RiboTag approach. (A-E) Gene expression from total KCs (Emr1Cre$^{+/-}$::RiboTag$^{+/-}$ mice) and the embryo-derived long-lived KC subset (Cx3cr1CreER$^{+/-}$::RiboTag$^{+/-}$ mice) was assessed in un-manipulated 10 week old adult male mice. Gene expression was measured using mRNA isolated from immunoprecipitation of RiboTag bearing polysomes. All genes are normalized to *Gapdh* and *Hprt* genes. Data represent 3 independent experiments with n=3 mice per group. Bars indicate the mean ± S.D

Embryo-derived Cx3cr1-marked KCs resist irradiation and express sessile KC genes.

Next we wanted to determine whether the Cx3cr1-marked KCs resist lethal irradiation. We generated irradiation chimeras in cx3cr1-marked KC bearing Cx3Cr1-eyfp-CreER+/-::RiboTag+/- mice (Figure 3-9). Eight weeks post irradiation immunofluorescence analysis of cryo-preserve sections clearly indicated the HA-label bearing Cx3cr1-marked KCs that persisted irradiation (Figure 3-9C).

Intracellular FACS analysis indicated that 19% of the host derived KCs in the irradiated group and 26% of the KCs in the non-irradiated control group were composed of Cx3cr1-marked KCs (Figure 3-9D). These results indicate that Cx3cr1-marked, embryo-derived KCs are relatively radio resistant. Furthermore there is a subset of non-labeled host derived KCs that also resisted irradiation. The current fate mapping strategy does not allow the identification of this subset while it is possible that this represents embryo-derived KCs that did not label due to ceased Cx3cr1 expression. Next we compared the gene expression of Cx3cr1-marked radioresistant KC subset to the sessile KC subset and found that at gene expression level, the two subsets resemble each other (Figure 3-9E). The genes that show elevated expressions in the sessile subset (*Marco, Timd4, Colec12, Cdkn1a*) compared to bm-KC subset were equally elevated in the radioresistant Cx3cr1-marked KCs. These observations demonstrate that the sessile KCs consist of Cx3cr1-marked, embryo-derived, long-lived KCs.

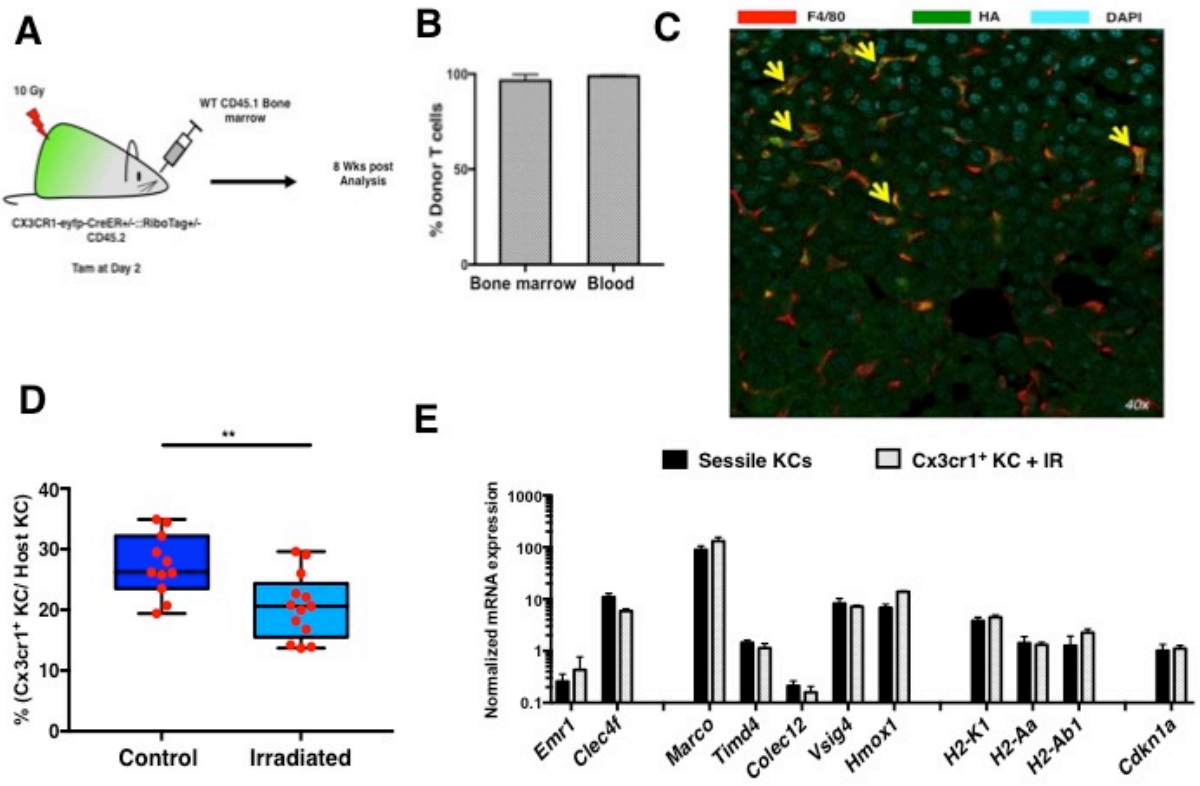

Figure 3-9. Embryo-derived Cx3cr1-marked KCs survive lethal irradiation and express sessile KC genes. (A)Diagram illustrates the generation of the irradiation chimera in adult mice with Cx3cr1-marked KCs. (B)Percent donor Tcell chimerism 8 weeks post-irradiation and bone marrow transplant. (C)Immunofluorescence image demonstrating the radioresistant Cx3cr1-marked embryo-derived KCs(yellow arrows) in the chimeric liver 8 weeks post-irradiation. Red:F4/80, Green:HA antigen, Cyan:Nucleus. (D)FACS analysis of the percent Cx3cr1-marked KCs among the total host KCs in irradiated mice compared to non-irradiated controls 8 weeks after irradiation. (E)Gene expression comparison between sessile KCs and embryo-derived Cx3cr1+KCs 8 weeks post-irradiation. Data represent>3 independent experiments with n=3mice/group. B,E:bars indicate the mean±S.D. Red dots:individual mice.**P≤0.01,Mann-Whitney test, IR:10Gy Irradiation Cx3cr1+:Day2 Tamoxifen induced Cx3cr1-marked KCs.

Bone marrow monocyte derived Kupffer cells are sensitive to lethal irradiation.

So far our results suggest that a subset of Cx3cr1-marked embryo-derived KCs both resist irradiation and resemble sessile KCs in gene expression. While this observation links the sessile KCs to embryo origin we cannot rule out the possibility that the long-lived bm-KCs also resist irradiation. Using a diphtheria toxin based depletion strategy to deplete and repopulate KC compartment with monocyte-derived KCs Scott et al indicate that repopulated KCs are long-lived through self-renewal and closely resemble the resident KCs (49). Thus it is possible that bm-KCs also able to resist irradiation and be a part of the sessile subset. Thus we next explored whether the bm-KCs also resist irradiation.

Clodronate liposomes are widely used to deplete liver phagocytes, and while the depletion is not restricted to KCs it is effective in depleting >98% of KCs (91). Clodronate depletion kinetics indicate that immediately after administration all F4/80^{-hi} KCs are depleted and over time blood monocytes differentiate into F4/80+ macrophages that will slowly morph into F4/80^{-hi} KCs (37). To generate a KC compartment that was solely derived from bone marrow monocytes and that also harbors the RiboTag reporter, we performed Clodronate depletion in 3 weeks old *Emr1Cre+/-::RiboTag+/-* mice (Figure 3-10A). First we performed a time course analysis to assess the repopulation kinetics of F4/80^{-hi} KCs (Figure 3-10B and Figure 3-11). FACS analysis for F4/80^{-hi} KCs 2 days after Clodronate treatment indicated total ablation of this population while 6 weeks post treatment the F4/80^{-hi} population was reestablished to the levels of the control liposome treated group. To exclude the possibility that any remaining resident KCs may clonally expand during emergency repopulation and contribute to the bm-KC compartment, we administered Clodronate into Cx3cr1-marked KC bearing mice at 3 weeks and analyzed at 6 weeks post treatment. Intracellular FACS analysis indicated that Cx3cr1-marked KCs were completely ablated in the Clodronate group, while there was no effect in the control liposome treated group (Figure 3-10C). This confirmed that following Clodronate treatment the repopulation of KCs only occurs from monocyte differentiation, and not from clonal expansion of long-lived resident or sessile KCs.

While at 6 weeks post Clodronate treatment the F4/80^{-hi} KC population is re-established, we wanted to verify that the cells resembled fully differentiated KCs in their gene expression. We found that

both Clodronate and control liposome groups show similar level of expression in a panel of 46 genes, which included consensus tissue macrophage genes (*Emr1, CD64, MerTK*), KC-associated genes (*Clec4f, Vsig4, C1q, Marco*) and genes encoding antigen presenting molecules (*H2-Aa, H2-Ab1*) (Fig. 4d). In contrast to previous findings that show *Timd4* and *Colec12* genes are restricted to embryo-derived KC (49) our data show that these genes are equally expressed in both un-depleted and repopulated KCs. While our gene expression analysis was performed 6 weeks post repopulation, previous analysis were done by 4 weeks of repopulation (49). Thus these data suggest that over time bm-KCs become more like the KCs that they replaced.

Collectively these data indicate 6 weeks post Clodronate treatment, repopulated bm-KCs have largely approximated to the original KCs at the gene expression level. To explore the radio sensitivity of these bm-KCs we lethally irradiated either Clodronate or control liposome-treated Emr1Cre+/-::RiboTag+/- mice post 6 weeks and reconstituted with WT CD45.1 bone marrow (Figure 3-10E). Eight weeks post transplant we analyzed the donor vs host chimerism in blood and liver KCs (Figure 3-10E) Clodronate-treated mice had significantly lower number of host KCs (<5%) compared to control liposome-treated mice (~25%) suggesting that bm-KCs are sensitive to lethal irradiation. These data clearly indicate that bm-KCs do not contribute significantly to the radioresistant sessile KC subset.

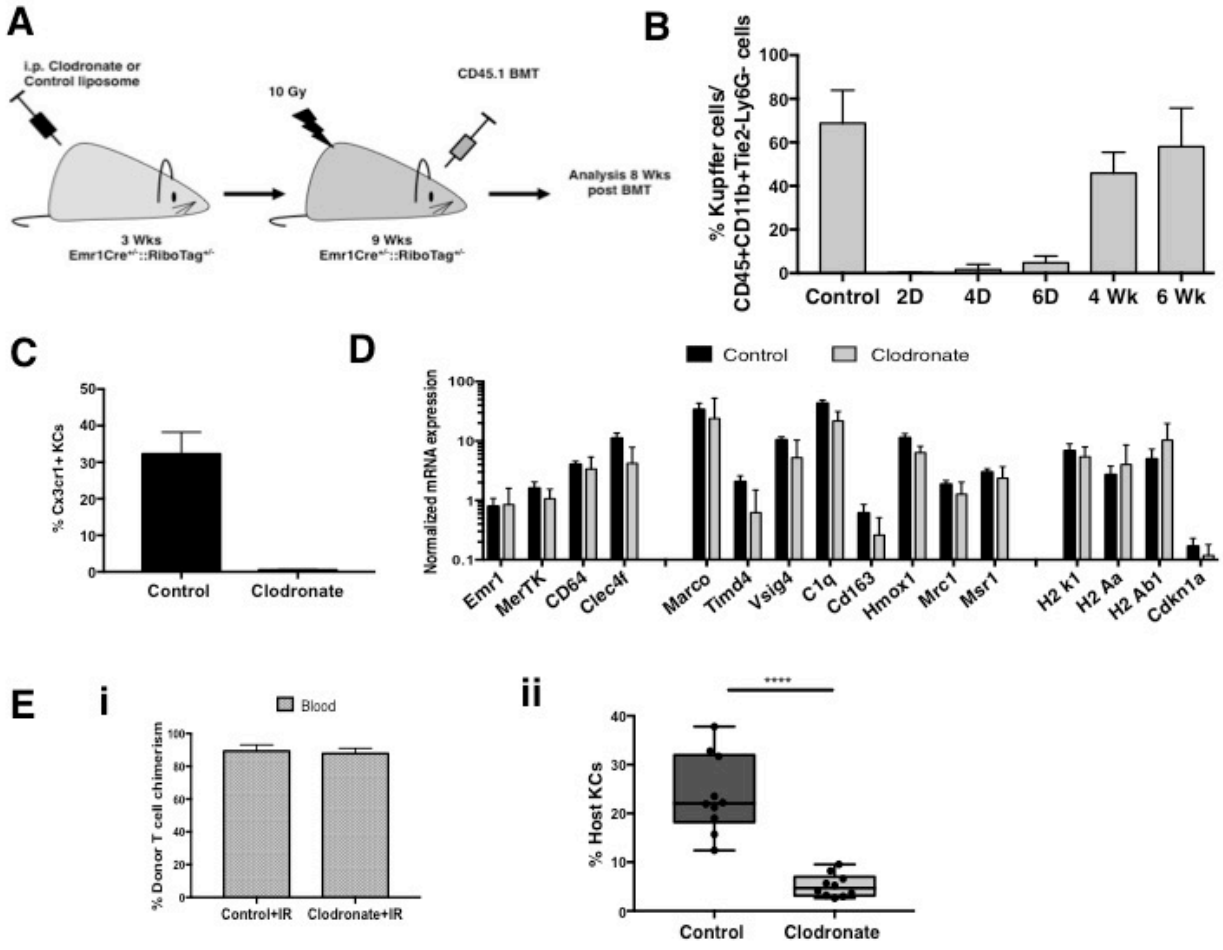

Figure 3-10. bm-KCs are sensitive to irradiation.
(A)Diagram illustrates the Clodronate depletion of resident KCs and radiation chimera generation in Emr1Cre+/-::RiboTag+/- mice. Control mice received liposomes without Clodronate. (B-C)FACS analysis of depletion-repopulation kinetics of resident KCs (B), and embryo-derived Cx3cr1-marked (Cx3cr1+) KCs(C) following Clodronate treatment compared to controls. (D)Gene expression analysis of KC-associated genes in control and Clodronate-treated mice 6 weeks post-administration. (E)Percent donor Tcell chimerism(i) and percent host KCs in control and Clodronate treated mice 8-weeks post-irradiation, determined by FACS(ii). Data represent 3 independent experiments with n>3 mice/group. B-E:bars indicate the mean±S.D. Dots:individual mice.****P≤0.0001, Mann-Whitney test, IR:10Gy Irradiation, D:days, Wk:Weeks.

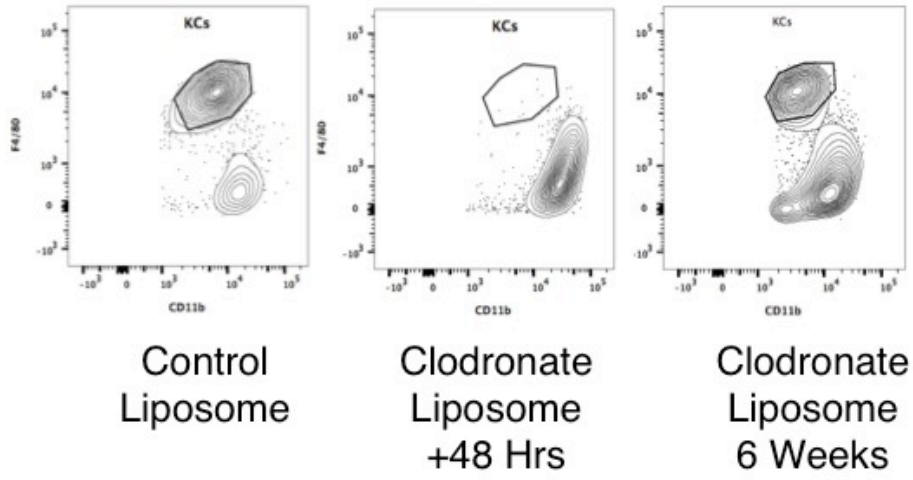

Figure 3-11. Representative FACS plots indicating the Kupffer cell depletion using Clodronate liposome. KCs are gated as Cd45+, Tie2-, Ly6G-, Siglecf-,CD11b+,F4/80+ subset in the live single cells non-parenchymal cell suspension. Clodronate or the control liposomes are given to 3 week old Emr1Cre$^{+/-}$::RiboTag$^{+/-}$ mice and the livers were harvested at the indicated time point for analysis. Data represent 3 independent experiments with n=3 mice per group

Immediate response of Cx3cr1-marked, long-lived sessile KCs and bm-KCs to radiation injury

So far our data indicate that bm-KCs do not resist irradiation while a subset of Cx3cr1-marked, embryo-derived KCs resist irradiation and resemble sessile subset in their gene expression. Next we set to explore the mechanisms that confer this unique radio-resistance in Cx3cr1-marked sessile KC subset. A recent study indicates that embryo-derived Langerhans cells resist irradiation through a CDKN1A mediated pathway while bone marrow-derived dermal dendritic cells undergo apoptotic death upon irradiation (92). This could suggest that an embryonic origin confers radio-resistance on multiple myeloid lineages. Thus we next explored the responses of the two KC subsets to irradiation following 24 hours.

First we assessed irradiation-induced damage in Cx3cr1-marked, embryo-derived KCs vs repopulated bm-KCs after Clodronate treatment. Using intracellular staining and FACS we detected phosphorylated histone variant H2AX protein, which is a marker of DNA double strand breakage (93) at 24 hours after lethal irradiation. The two KC subsets both showed similar (>2 fold) upregulation of the gamma-H2AX protein, indicating that both subsets were equally susceptible to X-irradiation induced double strand breaks (Figure 3-12A).

Next we compared the expression of genes in the two subsets 24 hrs post irradiation. We analyzed gene expression in 92 genes that were previously implicated in the radiation response, inflammation, macrophage functions and in cell death versus survival (94-96). Both subsets showed a significant upregulation of p53 dependent radiation-induced genes *Phlda3, Mdm2, Sens2* and *Cdkn1a* while anti oxidant responsive gene *Nrf2* was also elevated (Figure 3-12B,C and Figure 3-13). Cell cycle progression genes *Cdk1* and *Ki67* were down regulated in both groups indicating cell cycle arrest while *Cdkn1b* (encoding $p27^{kip}$) remained unchanged (Figure 3-12B and Figure 3-14). Interestingly the *Cdkn1a* up-regulation in Cx3cr1-marked KCs were 2.5 times higher than in bm-KCs (Figure 3-12B). We further confirmed the elevated expression of $p21^{cip\text{-}1/WAF1}$ protein in Cx3cr1-marked KCs using intracellular staining and FACS analysis (Figure 3-12D).

We hypothesized that the increased upregulation of *Cdkn1a* provides a survival advantage to the embryo derived KCs. To check this hypothesis we generated radiation chimeras in *Cdkn1a* -/- mice and WT mice. Eight weeks post lethal irradiation and congenic bone marrow transfer, we analyzed for the abundance of sessile KCs in each group of chimeras (Figure 3-12E). This experiment revealed that

Cdkn1a-/- group had two third less sessile KCs compared to the control group. Overall these experiments confirmed that elevated upregulation of the *Cdkn1a* gene and its protein product, $p21^{cip1/WAF1}$, in Cx3cr1-marked KCs results in improved survival of radiation-induced damage.

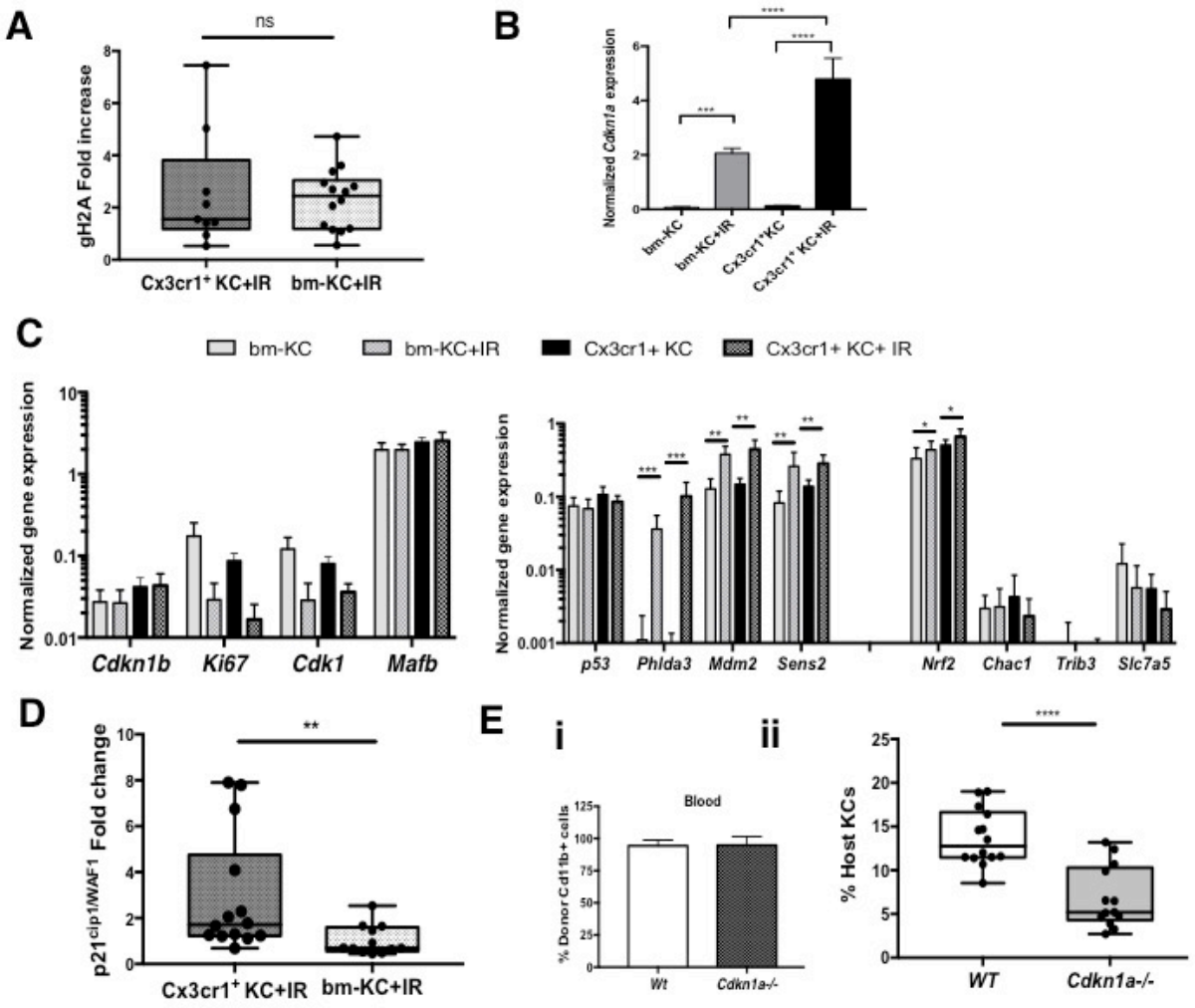

Figure 3-12. Immediate response of Cx3cr1-marked sessile KCs and bm-KCs to irradiation. (A)Comparison of γ-H2AX protein fold change compared to non-irradiated controls 24 hours post-irradiation in bm-KC versus Cx3cr1-marked KCs using FACS analysis. (B-C)Gene expression analysis of cell cycle associated- and radiation-induced genes. (D)Cell cycle inhibitor p21Cip1/WAF1 protein fold change compared to non-irradiated control mice determined by FACS. (E)Donor CD11b+ chimerism in blood(i), and percent host-derived KCs(ii) determined using FACS 8-weeks post irradiation. Data represent at least 3 independent experiments with n>3 mice/group. C,Ei:bars indicate the mean±S.D. Dots:individual mice.**P≤0.01,****P≤0.0001.A,B,D,Eii:Mann-Whitney test with P-values adjusted for multiple comparisons using Holm-Bonferroni method. IR:10Gy Irradiation, Cx3cr1+KC:Day2 Tamoxifen induced Cx3cr1-marked KC.

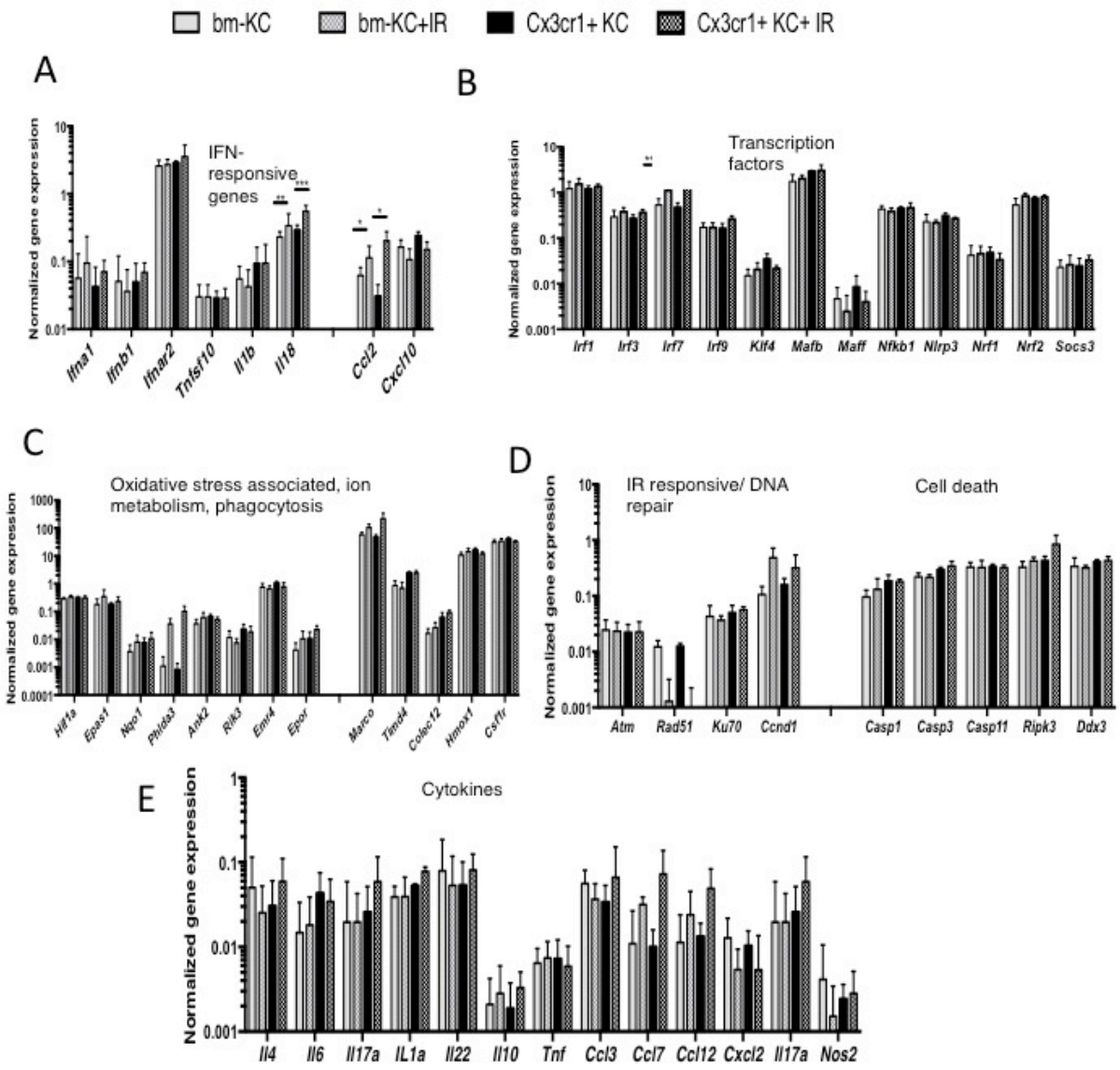

Figure 3-13. Immediate response of bm-Kupffer cells and Cx3cr1-marked Kupffer cells to 10Gy irradiation. **(A-E)** Gene expression was analyzed 24 hour post-irradiation on either the mice bearing bm-KCs or the neonatally-Cx3cr1-marked long lived KCs, and compared to control non-irradiated mice. Gene expression was normalized to *Gapdh* and *Hprt.* Data represent 3 independent experiments with n=3 or more mice per group. Bars indicate the mean ± S.D bm-KC: repopulated monocyte derived KCs following Clodronate depletion, Cx3cr1+: neonataly labeled KCs, IR: 10Gy irradiation

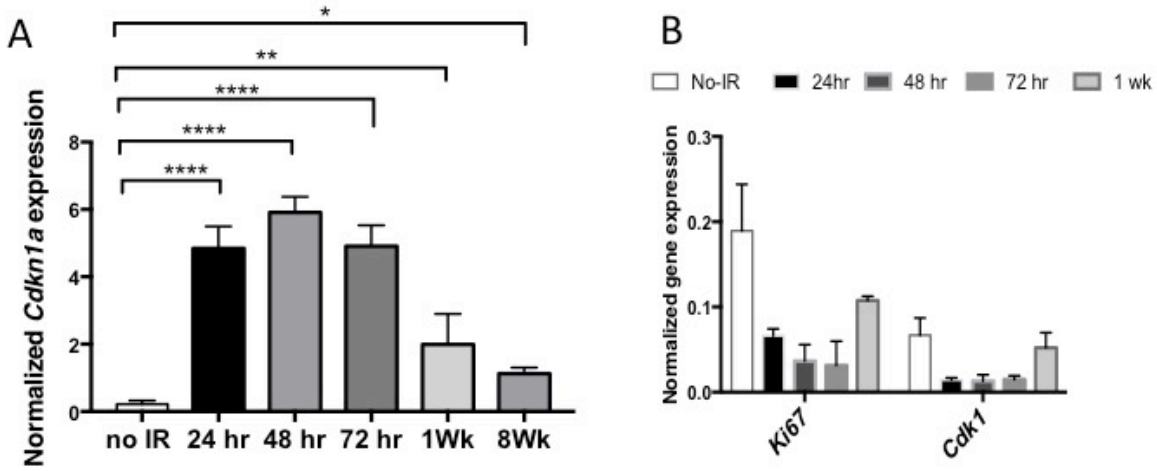

Figure 3-14. Kinetics of cell cycle related gene expression following irradiation. Emr1Cre::RiboTag mice were exposed to 10Gy irradiation and the gene expression was analyzed at 24, 48, 72, 96 hours and 1 week post irradiation compared to the non-irradiated controls for cell cycle inhibitor *Cdkn1a* **(A)** and cell cycle progression genes *Ki67* and *Cdk1* **(B)** Gene expression was normalized to *Gapdh* and *Hprt.* Data represent 3 independent experiments with n=3 or more mice per group. Bars indicate the mean ± S.D Significance is indicated by * and determined by Kruskal-Wallis test ** $P \leq 0.01$ **** $P \leq 0.0001$.

Discussion

Heterogeneity of KCs is evident both at the steady state and under stress conditions (63). At steady state, multiple fate mapping studies, phenotypic studies, single cell RNA sequencing analyses and irradiation-repopulation studies indicate the presence of two subsets of KCs, but the relationships and functions of each of these subsets remain unclear. In this study we investigated the identity and the radioresistance mechanism of the long-recognized radioresistant sessile KCs (56). Using fate mapping, KC depletion and radiation chimeras we identified the sessile KCs as the postnatally Cx3cr1-marked, embryo-derived subset while bm-KCs were eliminated by lethal irradiation. In contrast to bm-KCs, the Cx3cr1-marked subset showed a greater increase in *Cdkn1a* gene and $p21^{cip1/WAF1}$ protein following irradiation. In a *Cdkn1a* null background the sessile KCs significantly lost the ability to survive irradiation indicating that the enhanced upregulation of this cyclin-dependent kinase inhibitor provided greater survival potential to the Cx3cr1-marked subset.

Fate mapping studies indicate that the KCs with Cx3cr1 expression in postnatal stage are derived from embryonic precursors (50) specifically YS EMP (34). Our postnatal labeling strategy consistently labeled at least a subset (~37%) of this YS-derived KCs based on the continued Cx3cr1 expression. Using irradiation experiments and gene expression analysis, we clearly demonstrate that the sessile subset is congruent with the YS-derived KC subset. In contrast, bm-KCs are sensitive and do not survive irradiation. While YS-derived KCs are products of EMPs, the bm-KCs are products of hematopoietic stem cells (HSC)-derived monocytes. This suggests that the KCs that originated from HSCs are predisposed to radiation-induced death while radioresistance is a feature of YS EMP-derived KCs. In contrast to a recent report that concluded YS-derived KCs are partially ablated in response to irradiation (83), we argue that the radiosensitive subset is the HSC-derived KCs in unmanipulated mice. In fact some fate-mapping studies indicate that KCs are derived from embryonic HSC (48), while analysis of post natal liver indicate the possibility of bone marrow monocyte-derived KCs integrating into the KC niche (49). While our study does not directly identify these early HSC-derived long-lived KCs, radiation experiments strongly suggest the existence of a YS-derived and a HSC-derived KC subset. In support of this line of thinking microglia that are solely derived from YS EMPs are also radioresistant.

The greater upregulation of the gene encoding cyclin-dependent kinase inhibitor p21-$^{cip1/WAF1}$ in Cx3cr1-marked KCs, compared to bm-KCs, readily explains the greater survival of this subset. The p21-$^{cip1/WAF1}$ protein is a p53-induced molecule, that exerts G1-cell cycle arrest in the context of radiation damage, which may lead to cellular senescence or apoptosis (97, 98). However p21-$^{cip1/WAF1}$ expression may also be regulated by p53-independent mechanisms, and in this context it is involved in promoting cell survival (94, 99). The p21-$^{cip1/WAF1}$ protein is recruited to DNA double strand breaks induced by radiation, and initiates a major double strand break repair mechanism through the non-homologues end joining pathway (100). Furthermore p21-$^{cip1/WAF1}$ regulates anti-oxidative response by directly interacting with *Nrf2* (101). An extensive body of research exists on the p21-$^{cip1/WAF1}$ protein's pro-survival roles on human cancer cells (99). Cytoplasmic accumulation of p21-$^{cip1/WAF1}$ has shown to resist Fas mediated apoptosis (102) and prostaglandin A2 mediated apoptosis (103). In our study the upregulation of p21-$^{cip1/WAF1}$ in both subsets within 24 hours of irradiation conforms to the well-known p53 dependent radiation response. However, it is possible that the 2.5 times higher level of *Cdkn1a* gene expression in the Cx3cr1-marked subset compared to bm-KCs is due to p53 independent pathways, and this elevation confers radio-resistance on the Cx3cr1-marked subset. While *Cdkn1a* expression decreased by 1-week post irradiation in Cx3Cr1-marked KCs, it remains significantly high in the sessile subset compared to non-irradiated controls for at least 8 weeks post irradiation, further suggesting a pro-survival role for p21-$^{cip1/WAF1}$ in this subset.

Gene expression analysis indicated that the macrophage-associated collagenous receptor *Marco* expression remained 40-fold higher out to at least 13 weeks in sessile subset compared to bm-KCs. Interestingly, when resident KCs were completely depleted, the repopulating bm-KCs show similar level of *Marco* expression to the resident KCs. These observations suggest that the bm-KCs may assume distinct transcriptional patterns during repopulation of a completely vs a partially empty niche, indicating plasticity. This may also indicate the possible existence of two distinct niches where one is occupied by the sessile KCs and the other by bm-KCs. Furthermore single cell RNAseq analysis indicate two subsets of KCs based on *Marco* expression in mice (40) suggesting that *Marco* may distinguish the two subsets in un-manipulated mice.

Our studies offer an enriched picture of KC heterogeneity. If KCs are defined as long-lived resident liver macrophages, they consist of a minimum of two subsets, distinguished by their ontogeny, gene expression and radio-sensitivity. The inputs that determine their gene expression include the progenitor cells from which they arise, the time during development when they colonize the liver, and potentially also the micro-anatomic niche that they occupy. It is interesting that Clodronate depletion creates short-lived gaps in the sinusoidal layer, suggesting that a subset of KCs is integrated into the endothelium (104). Based on the restoration of *Marco* gene expression in bm-KCs post-Clodronate, we suggest a model on which YS-derived KCs occupy these intra-endothelial niches early in ontogeny, which directs their distinctive gene expression including high *Marco* expression. In emergency repopulation after irradiation, these niches remain occupied by YS-derived sessile KCs; but after total KC depletion, the niches are occupied by bm-KCs, which adopt some of the properties of the former occupants.

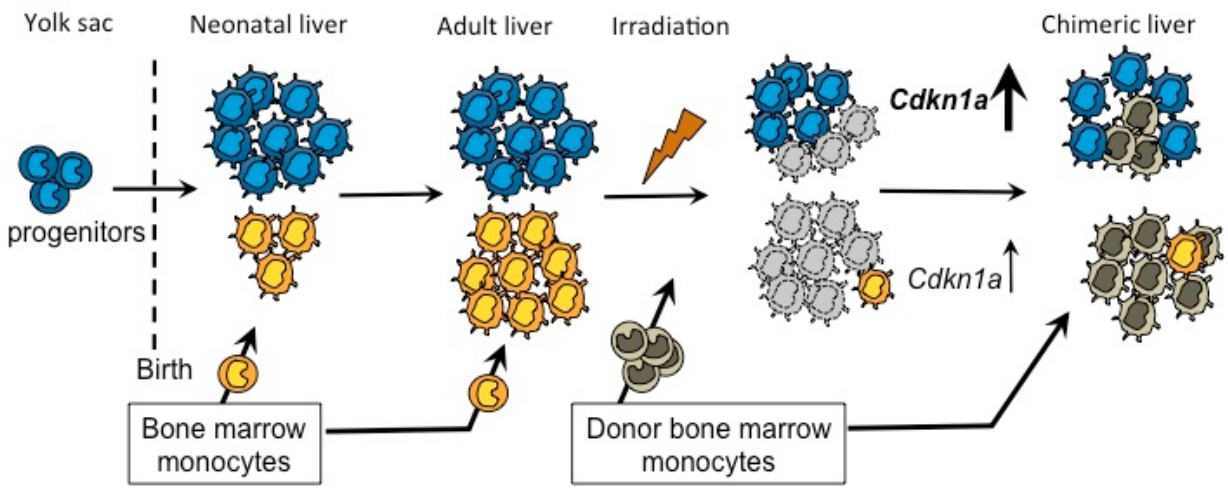

Figure 3-15: Graphical abstract

CHAPTER 4: RESPONSE OF EMBRYO-DERIVED HEPATIC AND CARDIAC MACROPHAGES TO ACUTE INFLAMMATION AND RESOLUTION

Abstract

Hepatic and cardiac macrophages are important innate immune sensors that play a key role in maintaining tissue homeostasis. Fate mapping and parabiosis studies indicate that a subset of these macrophages is embryo-derived and live into adulthood. While functions of these embryo-derived macrophages are studied in organ specific inflammation models, their response to common inflammatory stimuli has not been reported. Here we adopted an LPS model of acute systemic inflammation to study the response of embryo-derived liver and cardiac macrophages to acute inflammation and followed them into their resolution phase. Our data indicate that while the long-lived embryo-derived macrophages in the liver and the heart show tissue specific gene expression, they are readily polarized to a pro-inflammatory state in response to acute inflammation. Interestingly this polarization was completely reversed to the steady state post resolution, indicating plasticity despite their tissue specificity.

Introduction

Tissue resident macrophages of the liver and the heart are important innate immune sensors that are also essential for maintaining homoeostasis. While hepatic macrophages are located in the sinusoids closely interacting with the blood borne matter, cardiac macrophages are dispersed among the cardiomyocytes away from the vasculature. During steady state, both macrophages are involved in scavenger function and lipid metabolism.

In adult mice, both the liver and the heart contain a resident macrophage compartment constituting ontogenetically distinct macrophages. Recent fate mapping studies have shown that both in the liver and the heart a subset of resident macrophages originate from fetal precursors, seed the developing tissues before birth and continue to long live into the adult hood (35, 46, 51, 52, 105). After birth, bone marrow monocytes can migrate into the tissues, differentiate into macrophages, and integrate into the resident population in a context dependent manner. The neonatal liver and heart are both open to monocyte-derived macrophage seeding (49, 51, 106) and these macrophages can also self-renew into

adulthood. During stress, recruited monocytes can integrate into the macrophage compartment and perform resident macrophage functions (83, 107).

Since the identification of the embryo-derived macrophage subset, their steady state dynamics and the functions during stress within the tissue has been reported. Using a fate mapping strategy Molawi et. al showed that bone marrow monocyte-derived macrophages replaced the embryonic subset over time, while in liver the embryonic subset maintained at least up to an year(51, 66). In a model of blood stage malaria infection, embryo-derived liver macrophages diminished and were replaced by monocyte-derived macrophages, whereas during a helminth infection, embryo-derived liver macrophages expanded through self-renewal(61). In the neonatal heart, during cardiomyocyte injury the embryo-derived macrophage subset expanded and supported repair, whereas ablation of this subset limited cardiac infarct healing in the adult mice(106, 107). These studies indicate that within a tissue the embryo-derived subset respond to stress in a context dependent manner. Whether those responses are hardwired into these macrophages or whether they possess the ability to polarize towards a functional state based on the environment signals are not yet understood.

In vitro stimulation studies indicate that macrophages polarize towards diverse functional states in response to diverse external stimuli, thus indicating plasticity(68, 108). While plasticity is considered a hallmark of macrophages, it is not clearly demonstrated in *in vivo* settings for the tissue resident macrophages. In a CCl_4 induced fibrosis model, recruited $Ly6C^{lo}$ monocyte-derived liver macrophages showed a pro-inflammatory phenotype, but morphed into a reparative phenotype over the course of resolution(109). This study indicates that the monocyte-derived macrophages are able to polarize into distinct functions based on the environment. However, this is not demonstrated for macrophages of embryonic origin in the liver. The existence of diverse immune functions such as pro-inflammatory and anti-inflammatory in response to inflammation in tissue resident macrophages may suggest plasticity, but the inability to distinguish between subsets of distinct origins within the resident population has limited drawing any firm conclusions on plasticity. Thus we sought to understand how these long-lived macrophages with a similar origin in distinct tissues respond to a common inflammatory stimulus.

Here we report the embryo-derived hepatic and cardiac macrophage subsets response to lipopolysaccharide (LPS) induced acute inflammation and resolution. We used inducible Cx3cr1-driven

RiboTag reporter expression system to label the embryo-derived long-lived hepatic and cardiac macrophage subsets in the adult. Using translatome analysis we show that the two subsets have unique gene expression during steady state. In response to LPS-induced inflammation both subsets mounted a common response as well as tissue specific responses. Furthermore, both subsets maintained their tissue specific identity during the acute inflammation. Once the acute inflammation was resolved, both subsets reverted back to the pre-acute inflammation gene expression, however the cardiac subset was slower to recover. Our data provide the first insight into how long-lived macrophages of embryo-origin respond to acute inflammation and resolution in distinct tissues.

RESULTS

RiboTag reporter activation in total and embryo-derived cardiac macrophages

Macrophage specific gene expression is traditionally analyzed in cells isolated using FACS method. Cardiac macrophages express the pan tissue resident macrophage marker F4/80 and are traditionally FACS isolated using F4/80+ CD11b+ population among the CD45+ Autofluoresence+ leukocytes(52). Here we adopted the RiboTag approach first described by Sanz et. al. to label and analyze gene expression in cardiac macrophages. Chapter 3 describes the use of RiboTag approach in the liver macrophages. Briefly in RiboTag approach, the RiboTag reporter is activated using Cre mediated recombination of a modified ribosomal gene- *Rpl22*- that has a hemagglutinin (HA) epitope tag. Once the HA-tag is activated, the HA-labeled polysomes and the bound actively translating mRNA can be immunoprecipitated (RiboIP) to isolate mRNA for gene expression analysis.

We first used F4/80 (*Emr1*) driven Cre to activate the RiboTag reporter in total cardiac macrophages. In adult mice we gated cardiac macrophages as CD45+, Autofluoresence+, CD11b+, Ly6G-, CD11C-, F4/80+ subset in the single live cells. We also included the recently recognized pan tissue resident macrophage gene *CD64* to further verify the macrophage identity(39)(Figure 4-1A). Non-inducible Emr1Cre driven labeling indicated ~70% labeling of the total cardiac macrophages. In the same mice, brains and liver indicated ~60 % and ~80% labeling (Figure 4-1C). Thus the Emr1Cre driven

RiboTag gene recombination efficiency is variable among the tissues. The variability in labeling could be due to low levels of F4/80 expression or haploinsufficiency in a subset of macrophages.

The fracktalkine receptor *Cx3cr1* is expressed on early YS-derived macrophages that seed the developing tissues(34, 45). In the adult *Cx3cr1* is expressed on Ly6C^{lo} monocytes, dendritic cells and in some tissue macrophages including microglia and peritoneal macrophages. Fate mapping studies have previously used *Cx3cr1*-driven tamoxifen inducible Cre to label embryo-derived cardiac macrophages in adult mice(51, 52). These studies have used Tamoxifen before or after birth to induce fluorescence reporter activation in cardiac macrophages. Here we administered Tamoxifen to 2 days old neonates to activate RiboTag reporter in *Cx3cr1* expressing embryo-derived cardiac macrophages. During this day-2 window a subset of liver macrophages that were embryo-derived also get labeled (Chapter 3).

Intracellular FACS analysis of 8-10 weeks old adult hearts revealed HA labeling in 45% of the total cardiac macrophages, indicating the day 2 labeled long-lived, Cx3cr1-marked embryo-derived cardiac macrophage subset (Figure 4-1B,D). In liver 37% of macrophages were Cx3cr1-marked (Chapter 3). Thus in both liver and heart at least a third of the macrophages are embryo derived and long-lived into adulthood.

Phenotypic heterogeneity within the cardiac macrophage population is reported based on the cell surface CX3CR1, MHC Class II, TIMD4 and CCR2 expression(51, 52, 107, 110). Among those, the TIMD4^{+} expressing subset is identified as the long-lived resident cardiac macrophage population while the CCR2^{+} subset has a monocytic origin and is continuously replenished by bone marrow-monocyte derived macrophages(107). We first analyzed neonatal and adult mouse hearts for CX3CR1 expressing cardiac macrophages (Figure 4-2A). The neonates and the adults showed ~90% and 80% CX3CR1 expression respectively confirming the previous reports(51), that vast majority of the cardiac macrophages show CX3CR1 expression. Within the total cardiac macrophage population in the adult, only a subset expressed MHC class II, CCR2 and TIMD4 as previously reported (Figure 4-2B,C). Next we analyzed the HA-labeled long-lived subset for CX3CR1, MHC class II, CCR2 and TIMD4 expression (Figure 4-2D). Most embryo-derived long-lived cardiac macrophages expressed CX3CR1, while ~80% expressed MHC class II. TIMD4 expression was limited to ~22%, while CCR2 expression was observed on ~8% of the long-lived subset. Our results indicate that the embryo-derived long-lived subset is

phenotypically heterogeneous in terms of expression of the above-analyzed surface markers, while none of them are exclusive to the embryo-derived population.

A.

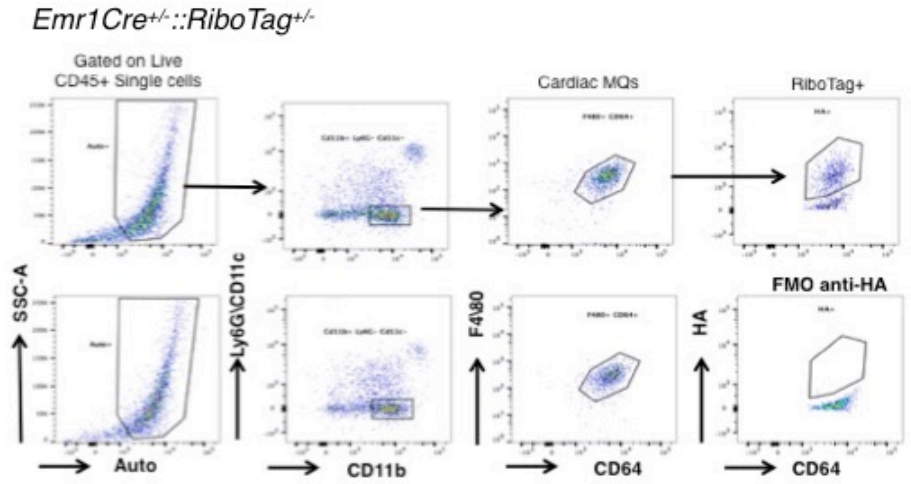
Emr1Cre+/-::RiboTag+/-
Gated on Live
CD45+ Single cells
Cardiac MQs
RiboTag+
SSC-A
Auto
Ly6G\CD11c
CD11b
F4\80
CD64
FMO anti-HA
HA
CD64

B.

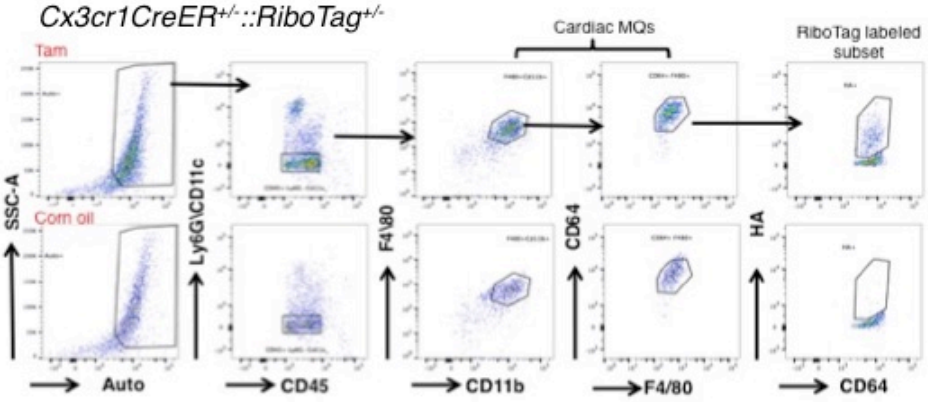
Cx3cr1CreER+/-::RiboTag+/-
Tam
Corn oil
Cardiac MQs
RiboTag labeled subset
SSC-A
Auto
Ly6G\CD11c
CD45
F4\80
CD11b
CD64
F4/80
HA
CD64

C.

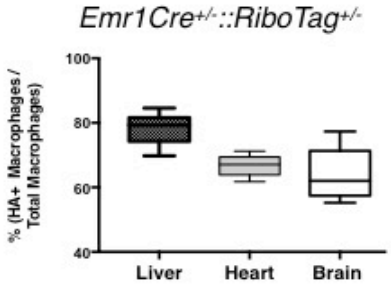
Emr1Cre+/-::RiboTag+/-
% (HA+ Macrophages / Total Macrophages)
100
80
60
40
Liver
Heart
Brain

D.

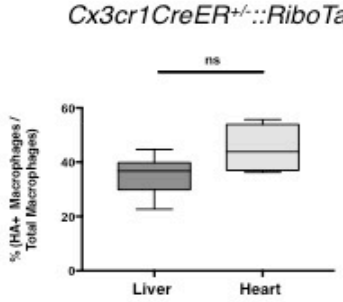
Cx3cr1CreER+/-::RiboTag+/-
ns
% (HA+ Macrophages / Total Macrophages)
60
40
20
0
Liver
Heart

E.

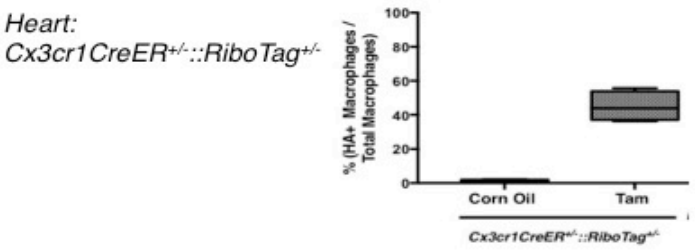
Heart:
Cx3cr1CreER+/-::RiboTag+/-
% (HA+ Macrophages / Total Macrophages)
100
80
60
40
20
0
Corn Oil
Tam
Cx3cr1CreER+/-::RiboTag+/-

Figure 4-1: **RiboTag reporter activation in total and embryo-derived tissue resident macrophages.** Representative FACS plots showing the gating strategy for total cardiac macrophages and HA-labeled subset in (A) *Emr1Cre*$^{+/-}$*::RiboTag*$^{+/-}$ and (B) *Cx3cr1CreER*$^{+/-}$*::RiboTag*$^{+/-}$ mice. (C) Recombination efficiency in RiboTag activation in brain, liver and heart macrophages in *Emr1Cre*$^{+/-}$*::RiboTag*$^{+/-}$ mice and (D) in liver and heart macrophages of *Cx3cr1CreER*$^{+/-}$*::RiboTag*$^{+/-}$ mice. (E) Percent HA-labeled cardiac macrophages post day 2 tamoxifen induction in adult mice compared to corn oil control. A-E: HA-labeling quantified using intracellular FACS analysis. All animals are 8-10 weeks old male mice. All data represent n=3 independent experiments with 3 or more mice per group.

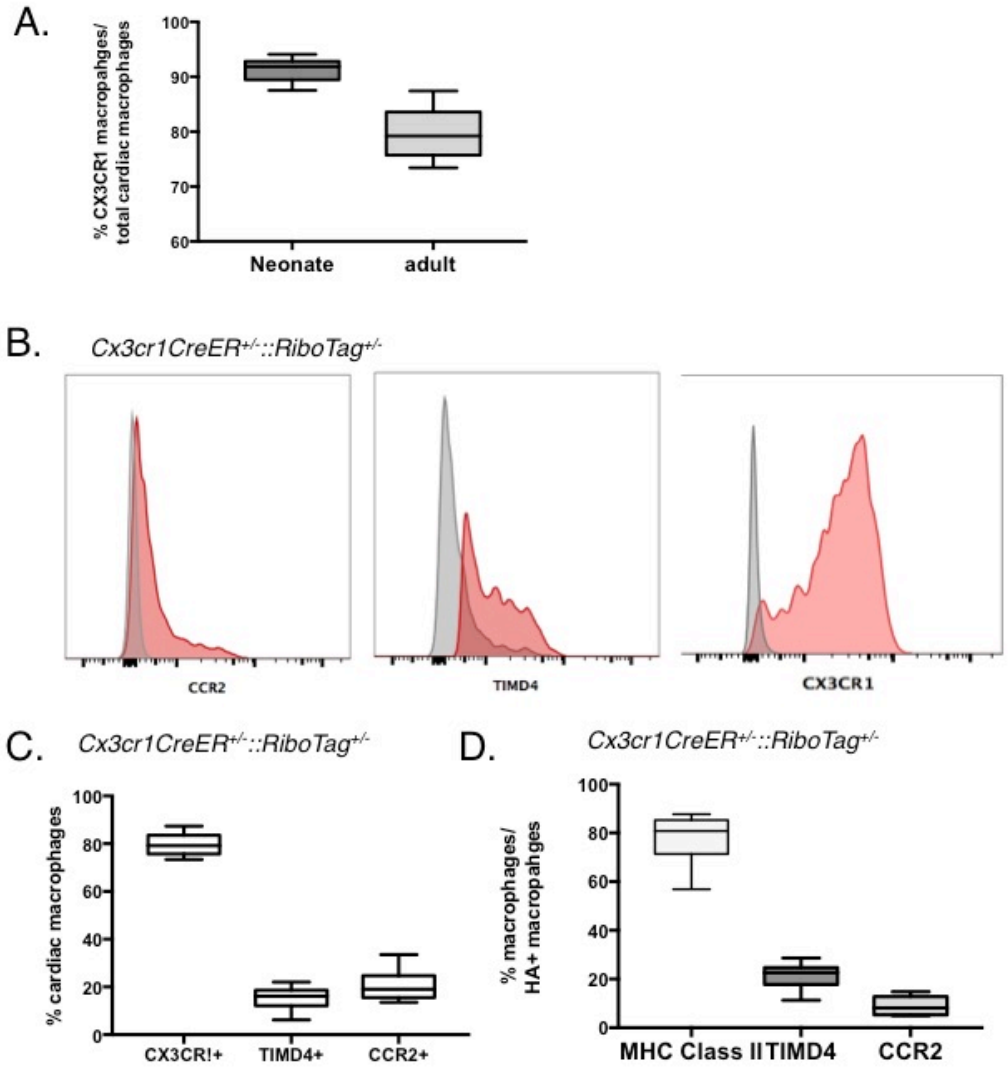

Figure 4-2: Phenotypic diversity of cardiac macrophages. (A) FACS analysis of C-X3-C Motif Chemokine Receptor-1 (CX3CR1) expression on day 3 old neonates and 8 weeks old adult wild type mice. (B) Representative histograms illustrating the surface expression of CX3CR1, CCR2 and TIMD4 on total cardiac macrophages in *Cx3cr1CreER*$^{+/-}$*::RiboTag*$^{+/-}$ mice. Percent macrophages expressing CX3CR1, CCR2 and TIMD4 (C) within the total cardiac macrophages and (D) within the HA-labeled embryo-derived long-lived cardiac subset in *Cx3cr1CreER*$^{+/-}$*::RiboTag*$^{+/-}$ mice. A-D: Data represent n=3 independent experiments with 3 or more mice per group.

Steady state gene expression analysis of the liver versus heart macrophages

Resident macrophages are essential for maintaining steady state in their respective tissues(63, 110). Next we sought to analyze the steady state gene expression of total hepatic versus cardiac macrophages. RiboTag reporter allows *in situ* gene expression analysis bypassing the FACS based cell-sorting strategy. We isolated macrophage specific mRNA using RiboIP in *Emr1Cre*$^{+/-}$*::RiboTag*$^{+/-}$ mice and performed qRT-PCR (Figure 4-3 A-F). Both tissues indicated enrichment for the pan tissue resident macrophage markers *Emr1, Mertk, CD64* and myeloid marker *CD11b* while the normalized expression levels were different among the tissues. *Cx3cr1* was only expressed in the cardiac macrophages as previously described. Phagocytosis genes *Marco, Clec4f, CD51* and *Vsig4* all had 10 folds or higher expression in hepatic macrophages compared to the cardiac macrophages while repair associated genes *Col1a1, Col3a1* and *Mmp9* were significantly elevated in the cardiac macrophages. These differences parallel known steady state functions such as exceptional phagocytic nature of liver macrophages and the reparative roles of cardiac macrophages(63, 110).

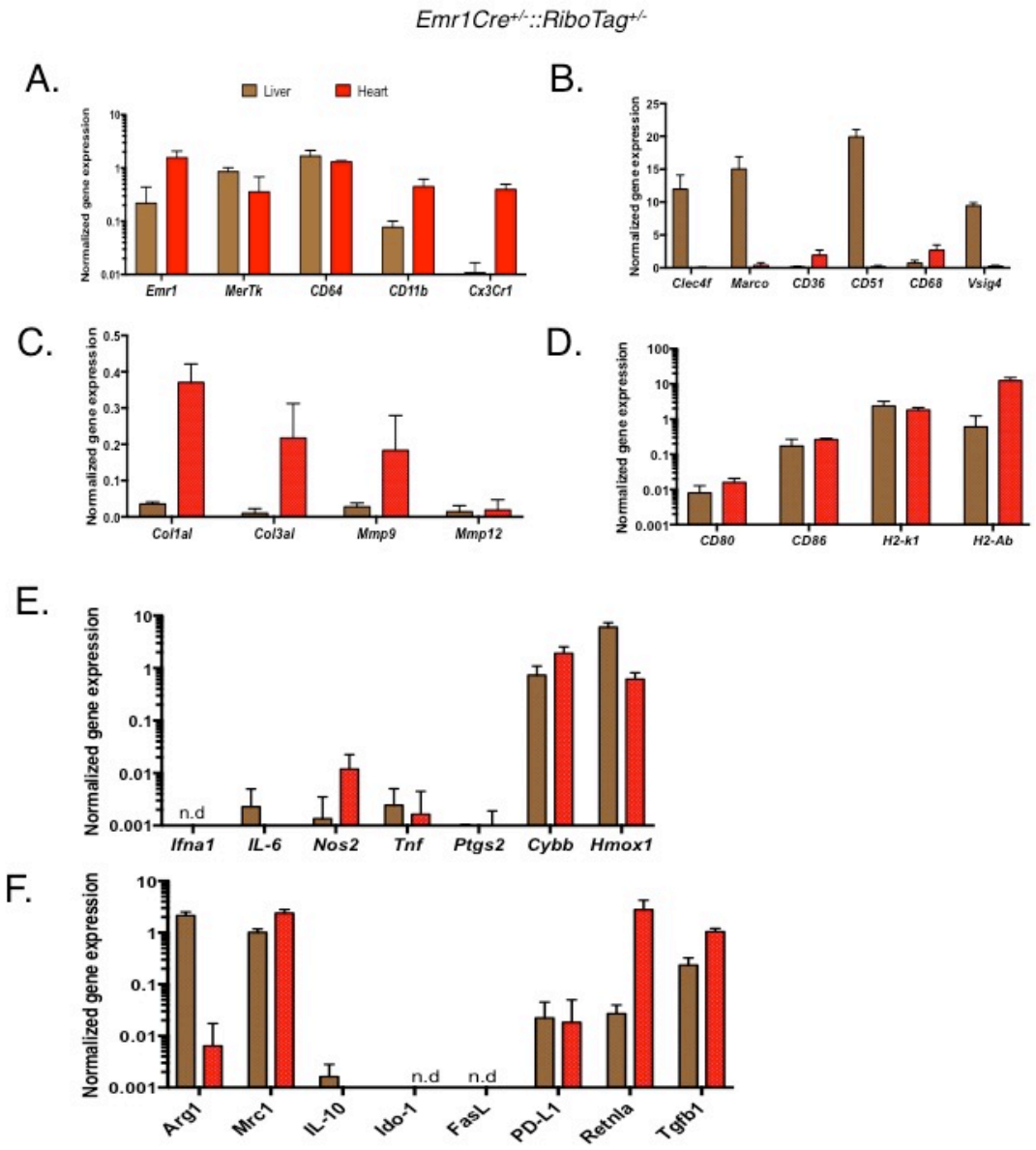

Figure 4-3: Steady state gene expression analysis of total cardiac versus hepatic macrophages. Gene expression analysis of *Emr1Cre*$^{+/-}$*::RiboTag*$^{+/-}$ mice liver and heart macrophages for (A) Tissue resident macrophage (B) phagocytosis associated (C) Repair associated (D) Antigen presentation associated (E) Inflammation associated and (F) immunosuppressive genes. In all graphs gene expression is normalized to the mean of *Gapdh* and *Hprt.* Each group indicate n=6 mice. Bar graphs indicate mean± SD.

Steady state gene expression analysis of the embryo-derived long-lived subset to the total macrophages within the liver versus the heart

In both liver and heart tissues more than one third of the macrophages are embryo-derived and long lived into adulthood (Figure 4-1 and Chapter 3). Next we sought to understand whether the embryo-derived subset follow the same gene expression as the total macrophages within each tissue. We compared the gene expression of the embryo-derived subset in the *Cx3cr1CreER*$^{+/-}$*::RiboTag*$^{+/-}$ model to the total macrophage gene expression in the *Emr1Cre*$^{+/-}$*::RiboTag*$^{+/-}$ model (Figure 4-4). In the heart, total macrophages showed a higher expression level for phagocytosis genes such as *CD68, CD36, Vsig4, Mrc1,* while the embryo-derived subset showed an elevated expression of repair-associated genes such as *Col1a1* and *Col3a1* (Figure 4-4A-D). While these differences were not significant they do point towards possible functional heterogeneity within the cardiac macrophages with distinct origins. However in the liver, the embryo-derived subset tracked the total macrophage at the gene expression to a similar extent (Figure 4-4E and F).

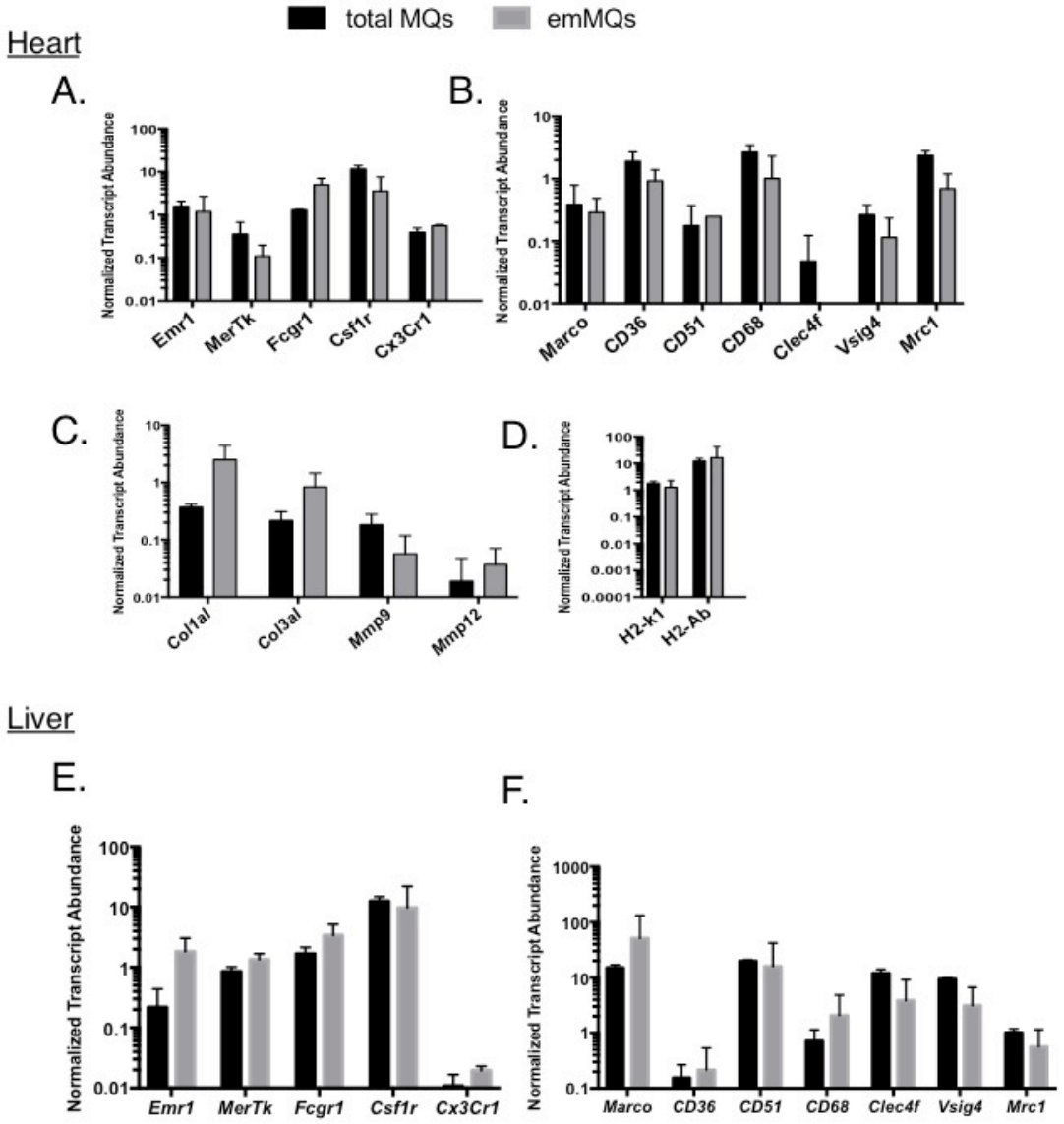

Figure 4-4: Steady state gene expression analysis of embryo-derived subset to the total macrophages within liver and heart. (A-F)Gene expression comparison of the embryo-derived subset (emMQs) in day 2 tamoxifen induced *Cx3cr1CreER*$^{+/-}$*::RiboTag*$^{+/-}$ mice to total macrophages (Total MQs) in *Emr1Cre*$^{+/-}$*::RiboTag*$^{+/-}$ mice analyzed using qRT-PCR. (A) Tissue resident macrophage genes (B) phagocytosis associated genes (C) Repair (D) antigen presentation associated genes in heart tissue. (E) Tissue resident macrophage genes (F) phagocytosis associated genes in liver tissue. In all graphs gene expression is normalized to the mean of *Gapdh* and *Hprt.* Each group indicate n=6 mice. Bar graphs indicate mean± SD.

Steady state gene expression analysis of the embryo-derived long-lived macrophage subsets within the liver and the heart

Cx3cr1 expressing YS-precursors seed developing tissues in the embryo and once seeded acquire tissue specific gene expression through transcriptional changes(45). In our fate-mapping model the *Cx3cr1*-marked hepatic versus cardiac macrophage subset represent these long-lived embryo-derived macrophages in each tissue. We hypothesized that despite the common origin; the embryo-derived subset will show a gene expression pattern specific to the tissue they reside at steady state. We compared the translatomes of embryo-derived long-lived hepatic versus cardiac macrophage subsets using RNAseq analysis (Figure 4-5). A heat map of the two subsets showed unique gene expression patterns despite their similar origin (Figure 4-5A). Pathway analysis indicated that the cardiac subset is enriched for genes important for muscle development and extra cellular matrix organization while the liver subset indicated pathway enrichment for complement and coagulation cascades and lipid metabolism (Figure 4-5B). While a previous study indicated that *Egfr* and *Lifr* gens are specific to cardiac macrophages(111) our analysis of the embryo-derived subset only indicated elevated expression of *Lifr* while *Egfr* was elevated in the liver subset. The previously identified liver specific gene(74) *Clec4f* was more highly expressed as expected in the liver subset (Figure 4-5C).

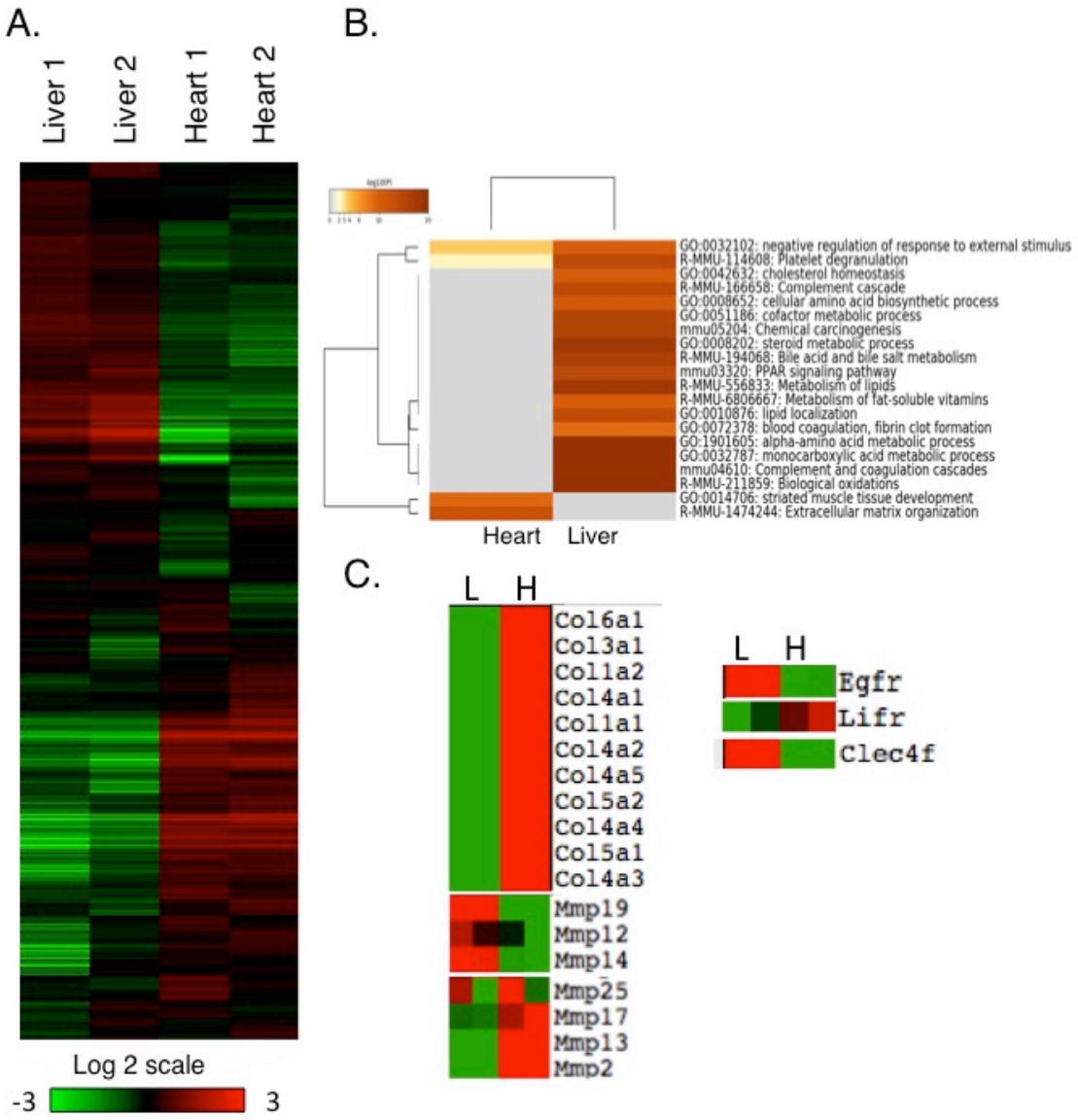

Figure 4-5: Steady state translatome analysis of embryo-derived macrophage subset in liver and heart. (A) Heat map of all genes expressed in liver versus heart embryo-derived macrophages at steady state. (B) Pathway analysis for of steady state gene expression in liver and heart and (C) selected block of differentially expressed genes in liver versus heart embryo-derived macrophages at steady state. RNAseq analysis was performed in n=2 mice. Heat map generated using Cluster 3.0 and the Pathway analysis was done using www.metascape.org.

Embryo-derived macrophage subsets response to acute inflammation and their recovery in the heart and the liver

Steady state gene expression comparison showed that despite the common origin embryo-derived macrophage subsets perform functions that are unique to liver and heart. Next we sought to find out how they respond to acute inflammation in a LPS induced inflammation model. LPS administration initiates TLR4 signaling, which involves mitogen activated protein kinases (MAPK) and nuclear factor kappa B (NF-κB) in different pathway branches and ultimately induces inflammatory cytokine and chemokine expression, macrophage migration and phagocytosis. First we administered a sub-lethal dose of LPS to wild type mice and analyzed the serum Aspartate Aminotransferase (AST) levels, a marker of liver and heart damage, from 15 min to 2 weeks at various intervals (Figure 4-6A). Compared to the control group, in the treatment group AST levels peaked at 24 hours and subsided to baseline by 1 week. At 2 weeks the AST levels remained at baseline. Furthermore we observed the animals for septic shock symptoms and all animals started showing visible lethargy by 4 hours and they developed hypothermia by 12 hours. These symptoms were lost by 48 hours. Based on the time course and the symptoms presented we picked 4 hours as the early time point to analyze the gene expression, while 2 weeks post LPS was used as the post acute inflammation. Next we performed the LPS induction on *Cx3cr1CreER*$^{+/-}$*::RiboTag*$^{+/-}$ mice that were tamoxifen induced at day 2 to label the long-lived embryo-derived macrophages (Figure 4-6B). We harvested tissues from PBS control and at 4 hours and 2 weeks post LPS, performed Ribo IP to isolate subset specific mRNA and analyzed the translatome using RNAseq.

Translatome analysis revealed that as early as 4 hours, the global gene expression in the embryo-derived subsets in both tissues changed drastically from steady state demonstrating their ability to respond to LPS induced environmental changes (Figure 4-7 and 9). We identified 1531 and 1837 genes respectively in the liver and the heart subsets that were significantly upregulated by 2-fold or more by 4 hours with another 1071 and 524 significantly downregulated 2-fold or more (visualized using volcano plots in Figure 4-7A). Among the significantly upregulated genes in response to LPS, 862 were common to both subsets while among the down regulated genes 246 were common to both subsets

(Figure 4-7B). Pathway analysis identified GO terms such as inflammatory response, NF-kB signaling, cytokine production and response to interferon beta among the upregulated pathways, while interleukin 6 production and kinase activity terms were enriched in the down regulated gene sets (Figure 4-7C). We confirmed the expression of known LPS induced genes using qRT-PCR in both subsets (Figure 4-7D). Pro-inflammatory genes *Il6, Il1b* and *Tnfa* were several fold elevated compared to the control. Furthermore genes involved in monocyte and neutrophil attraction – *Ccl2, Cxcl1, Cxcl2*- were also upregulated at this early time point.

Analysis of the translatome at 2 weeks compared to PBS control revealed that only 182 genes remained significantly upregulated in the liver subset at this time point, while another 139 were downregulated (Figure 4-8A). However the cardiac subset indicated 456 genes that remained upregulated by the end of 2 weeks with only 60 remaining downregulated (Figure 4-8B). The common response due to LPS induced acute inflammation was completely gone by this time point and only a handful of common genes still remained up or down regulated (Figure 4-8B). To demonstrate the global changes in the translatome of the embryo-derived long-lived macrophage subset in liver and heart due to LPS induced inflammation and its resolution we created a heat map of all genes for both tissues and performed principle component analysis (PCA) (Figure 4-9A). The heat map of the LPS time course and the PCA analysis clearly indicated that the embryo-derived subsets mounted a common response to LPS, while tissue specific responses were also detected. The common LPS induced response was gone by 2 weeks in the both subsets while only the liver subset showed almost identical gene expression to the control. At 2-weeks the heart subset still maintained differences but showed a trend towards becoming more like the subset prior to LPS stimulation.

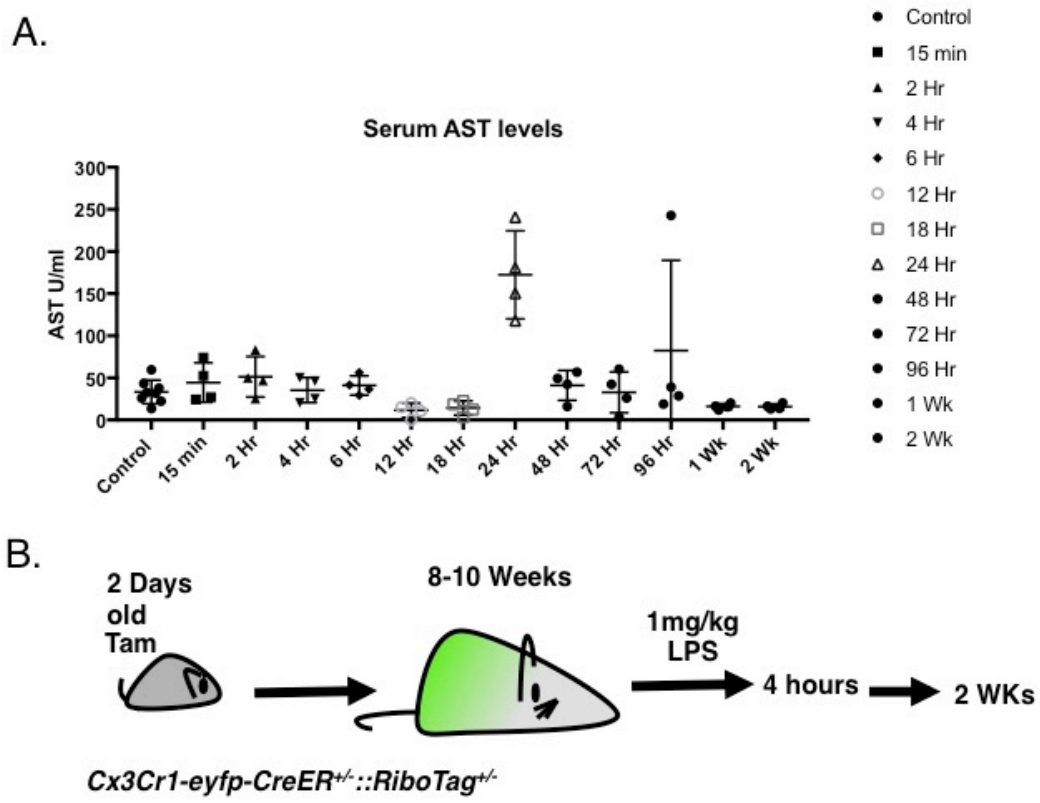

Figure 4-6: A model of Lipopolysaccharide (LPS) induced systemic inflammation. (A) Wild type mice were intra-peritoneally administered a dose LPS and harvested at the indicated time point. Serum was isolated and the AST levels were measured. At each time point symbols indicate the number of individual animals. (B) A diagram illustrating the acute systemic inflammation induction in mice harboring the HA-labeled embryo-derived macrophages.

A.

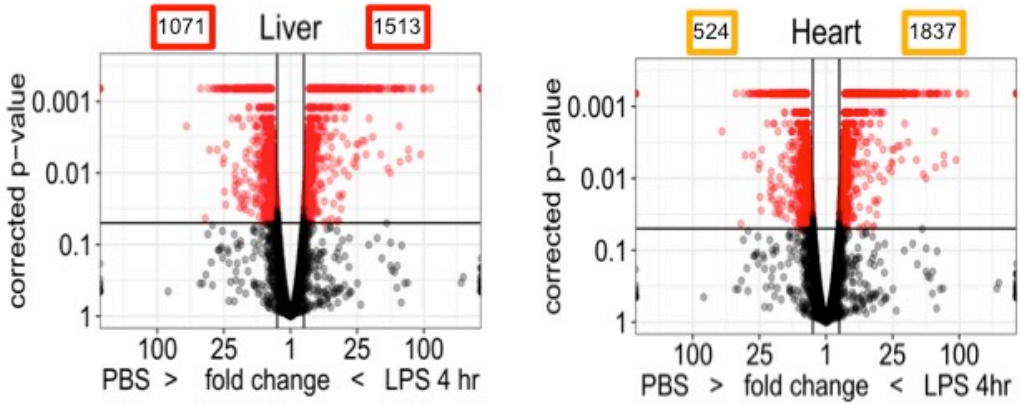
1071
Liver
1513
corrected p−value
0.001
0.01
0.1
1
100 25 1 25 100
PBS > fold change < LPS 4 hr
524
Heart
1837
corrected p−value
0.001
0.01
0.1
1
100 25 1 25 100
PBS > fold change < LPS 4hr

B.

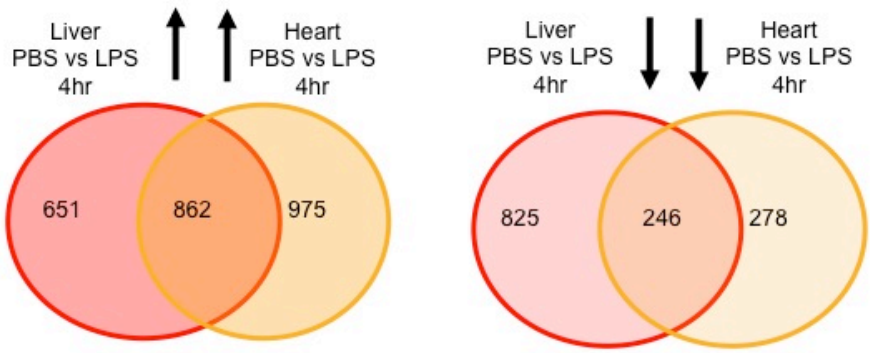
Liver
PBS vs LPS
4hr
Heart
PBS vs LPS
4hr
651
862
975
Liver
PBS vs LPS
4hr
Heart
PBS vs LPS
4hr
825
246
278

C.

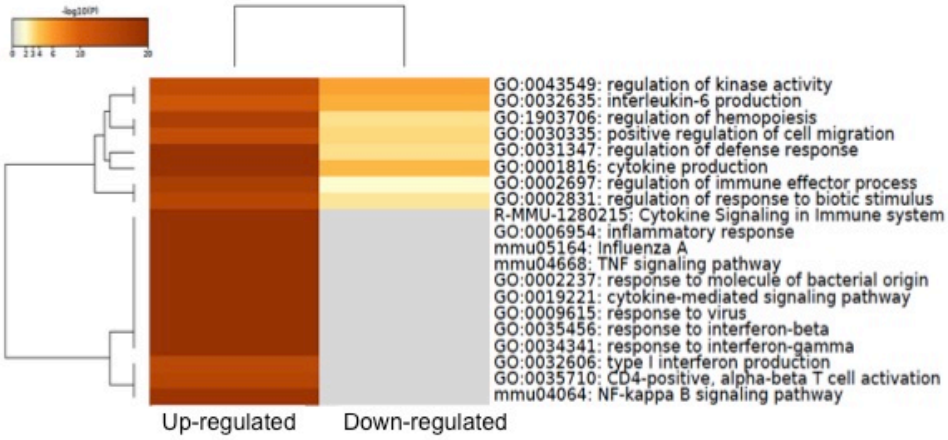
GO:0043549: regulation of kinase activity
GO:0032635: interleukin-6 production
GO:1903706: regulation of hemopoiesis
GO:0030335: positive regulation of cell migration
GO:0031347: regulation of defense response
GO:0001816: cytokine production
GO:0002697: regulation of immune effector process
GO:0002831: regulation of response to biotic stimulus
R-MMU-1280215: Cytokine Signaling in Immune system
GO:0006954: inflammatory response
mmu05164: Influenza A
mmu04668: TNF signaling pathway
GO:0002237: response to molecule of bacterial origin
GO:0019221: cytokine-mediated signaling pathway
GO:0009615: response to virus
GO:0035456: response to interferon-beta
GO:0034341: response to interferon-gamma
GO:0032606: type I interferon production
GO:0035710: CD4-positive, alpha-beta T cell activation
mmu04064: NF-kappa B signaling pathway
Up-regulated
Down-regulated

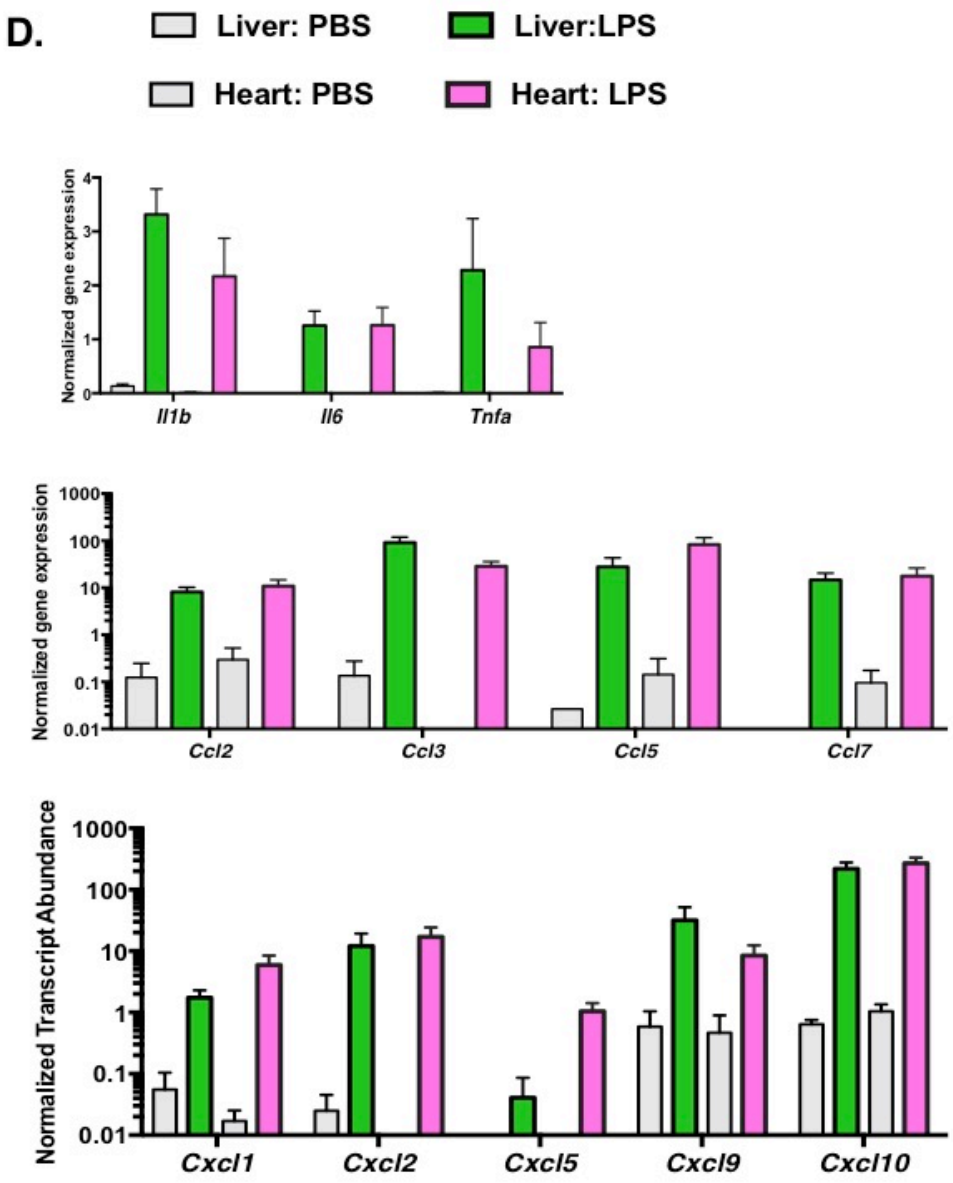

Figure 4-7:Gene expression analysis of embryo-derived hepatic and cardiac macrophages to LPS induced acute inflammation. (A) Volcano plots indicating the statistical significance (Y axis: P value) and magnitude of change (X-axis: fold change) in the RNAseq data set between the PBS control and 4 hour time point post LPS for embryo derived subset in liver and heart. Red dots indicate genes that show >2 fold with a P<0.05. (B) Venn diagrams indicate a comparison of the number of genes that are either upregulated or down regulated in response to LPS at 4 hours in the two tissues. (C) Pathway analysis of the LPS responsive common genes in the embryo-derived subset of liver and heart generated using www.metascape.org (D) qRT-PCR analysis of canonical LPS induced genes at 4 hours. A-C: n=2 mice D: n=6 mice. Gene expression is normalized to the mean of *Gapdh* and *Hprt.* Bar graphs indicate mean± S

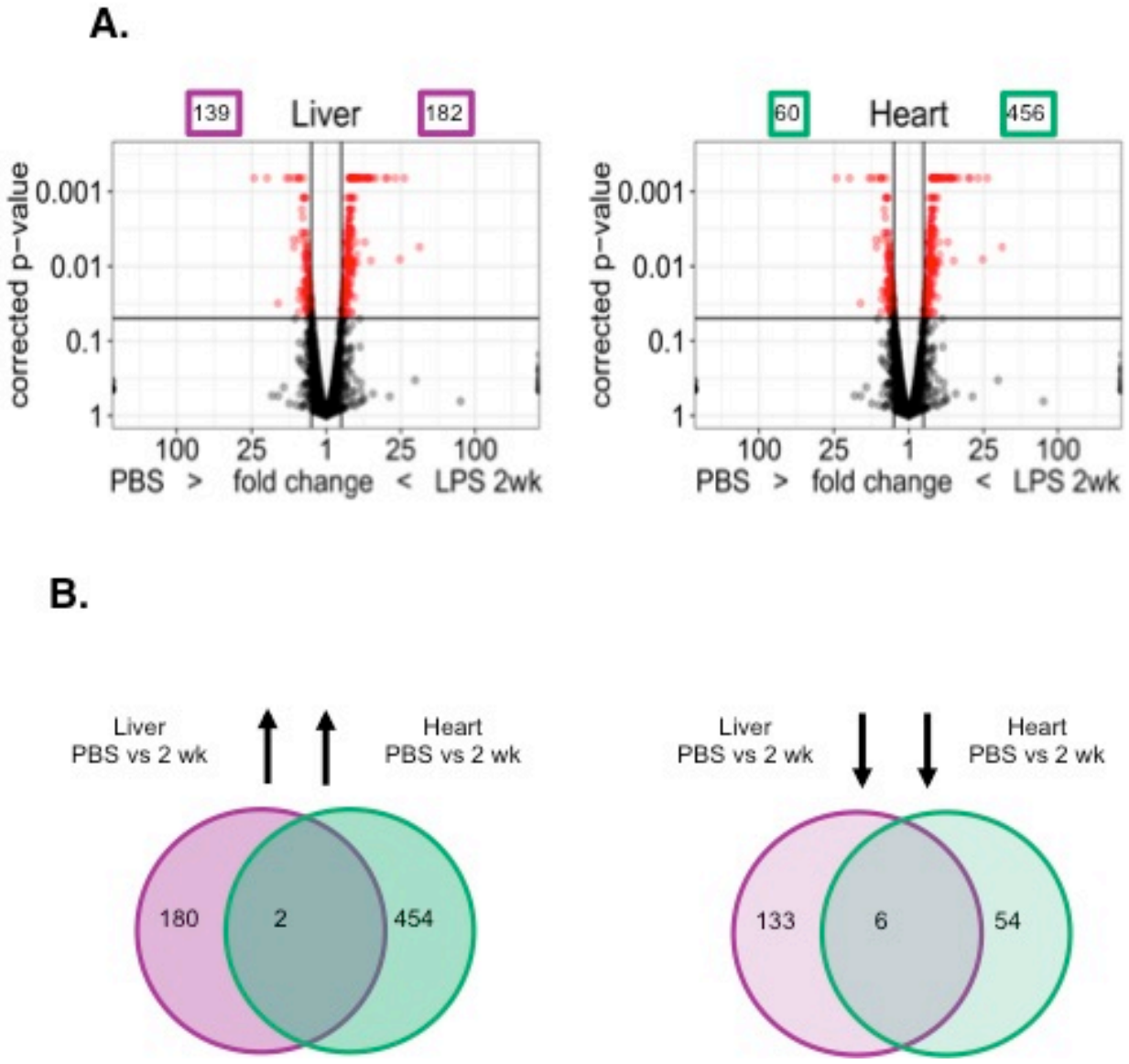

Figure 4-8: Gene expression analysis of embryo-derived hepatic and cardiac macrophages post LPS induced inflammation resolution. (A) Volcano plots indicating the statistical significance (Y axis: P-value) and magnitude of change (X-axis: fold change) in the RNAseq data set between the PBS control and 2 weeks time point post LPS treatment for embryo-derived subset in liver and heart. Red dots indicate genes that show >2 fold with a P<0.05. (B) Venn diagrams indicate a comparison of the number of genes that are either upregulated or down regulated from 4 hours to 2 weeks in liver and heart embryo-derived subsets.

A.

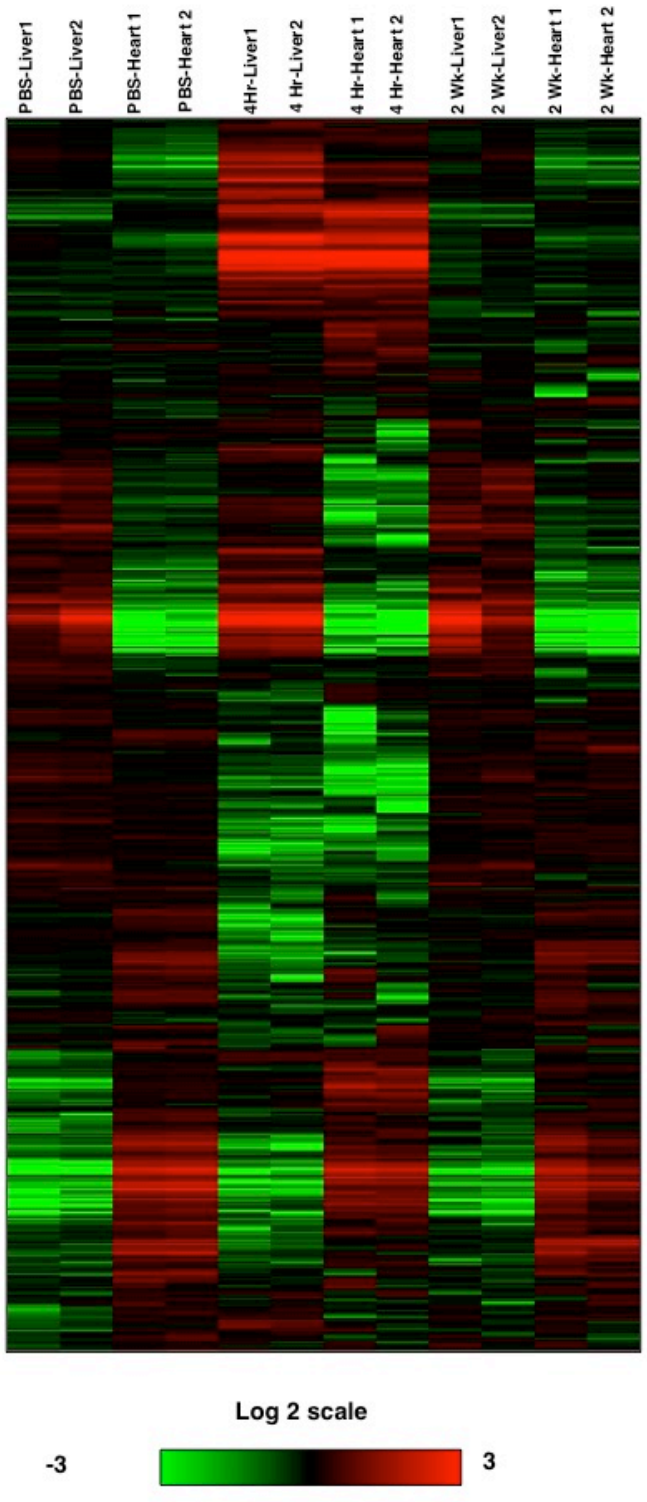
PBS-Liver1
PBS-Liver2
PBS-Heart 1
PBS-Heart 2
4Hr-Liver1
4 Hr-Liver2
4 Hr-Heart 1
4 Hr-Heart 2
2 Wk-Liver1
2 Wk-Liver2
2 Wk-Heart 1
2 Wk-Heart 2
Log 2 scale
-3
3

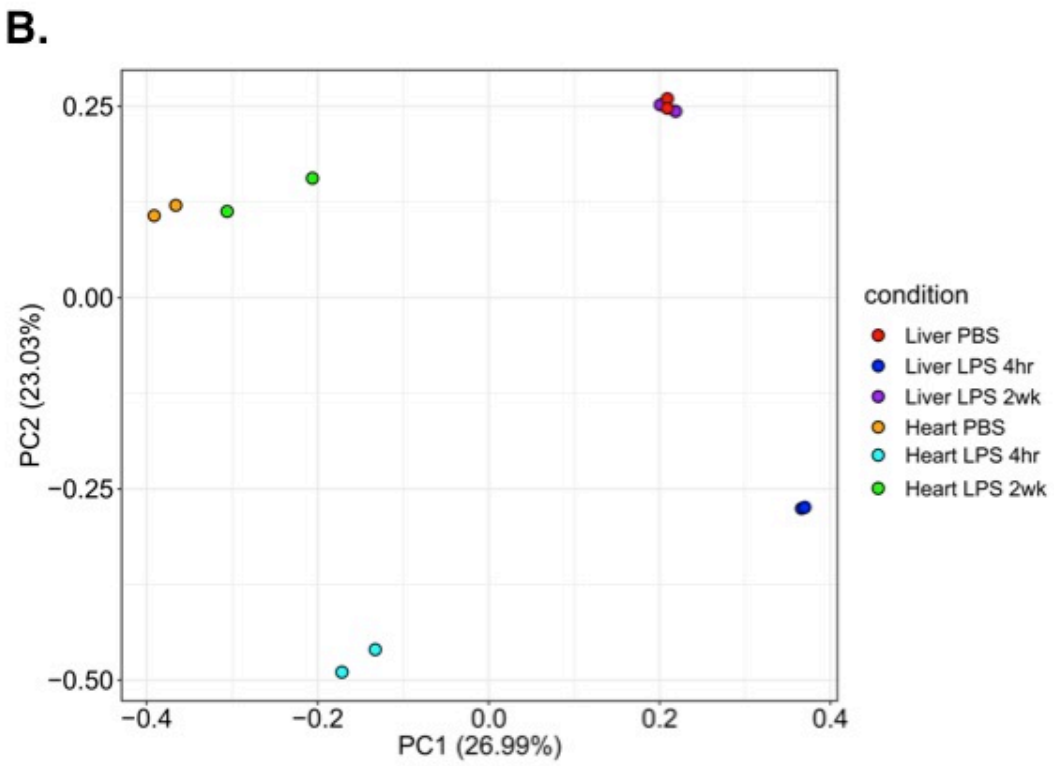

Figure 4-9: Global trends in the transcriptome changes from steady state, acute inflammation to post resolution state in embryo-derived macrophages. (A) Heat map (B) Principal component analysis showing all gene expressions across the tissues and time points. n=2 mice for all 3 time points. Short titles:

Discussion

The liver and heart both harbor a subset of embryo-derived macrophages that are long-lived into adult hood (112, 113). While the function of those macrophages in tissue specific injuries such as cardiac infarct(107) and radiation injury(66) in the liver are documented, the response to common inflammatory stimuli of these long-lived macrophages with similar origins in distinct tissue environments were not assessed. Here, we report that despite their common origin, embryonic subsets assume gene expression that is unique to the tissue of residence. This indicates that the tissue environment imprints their steady state functions. The embryo-derived subsets respond similarly to systemic acute inflammation and then resolve back to steady state gene expression post resolution. This indicates their intrinsic ability to reverse polarization in the context of acute inflammation demonstrating plasticity.

To specifically label the embryo-derived macrophages in tissues we used an inducible Cx3cr1CreER system combined with the RiboTag approach. We administered tamoxifen to neonates at day two, to label the long-lived embryo-derived subset. Since ~90% of the neonatal cardiac macrophages expressed CX3CR1, day 2 labeling should mark most of the macrophages. However in the adult, only a subset was HA-labeled indicating that not all day two Cx3cr1-marked macrophages survived into the adulthood. This observation parallels the previous report from Molawi et. al. that the embryo-derived macrophage subset in the heart is progressively lost with age(51). These observations contrast with the Cx3cr1-marked long-lived embryo-derived liver macrophages, since in the liver the embryo-derived subset maintains the ~37% ratio and long-live up to 1 year(66). Together, these observations indicate the organ specific dynamics of embryo-derived macrophages. In the adult mice, ~80% of the cardiac macrophages expressed CX3CR1, thus CX3CR1 expression on cardiac macrophages is heart specific and does not indicate the YS-origin. Our analysis showed that 80% of the Cx3Cr1-marked embryo-derived cardiac macrophages expressed MHC class II, indicating that they are a key subset involved in antigen presentation. Previous reports indicated that TIMD4 and CCR2 are markers of long-lived resident versus monocyte-derived cardiac macrophages, respectively (52). In contrast to this, our data showed that ~20% and ~8% of the long-lived embryo-derived cardiac macrophages expressed TIMD4 and CCR2, respectively. This indicates that neither of these markers exclusively identify cardiac macrophages with

distinct origins. Future studies are required to find phenotypic markers that will exclusively identify macrophage subsets with a specific origin.

Because more than a third of macrophages indicate embryonic origin in both tissues, it is possible that they perform specific roles compared to the rest of the macrophages within a tissue. Comparison of the embryo-derived subset to total macrophages in the liver did not show differences at gene expression levels in qRT-PCR analysis of small panel of genes. However, the embryo-derived subset in the heart showed differences in gene expression compared to the total cardiac macrophages. This may indicate that in the heart, the embryonic subset performs specific roles at steady state. A total translatome analysis to compare the embryonic subset with the total macrophages in each tissue is needed to gain an understanding of any functional differences.

A translatome comparison of the embryo-derived macrophage subsets in the liver and heart revealed unique gene expression patterns despite their common origin. This observation is in line with the previous observations that the tissue specific signals imprint resident macrophage functions (74, 75, 77, 114). However, our translatome analysis did not reveal any epigenetic imprinting that is specific to origin that may play a role in immune functions. In response to LPS induced systemic inflammation, both subsets showed notable changes in their global gene expression patterns that included a common response through NF-KB and IRF transcription factor activation. This LPS specific response was eliminated within two weeks. These results indicate that despite distinct tissue specific gene expression patterns, these embryo-derived subsets are able to switch to a pro-inflammatory gene expression in response to the inflammatory environment. Furthermore, this pro-inflammatory gene expression was reversed back to a steady state expression pattern; this indicates their response to the reestablished steady state environment and the functional plasticity of these embryo-derived macrophages. However, it is important to note that at two weeks, the embryo-derived subset in the liver closely resembled the steady state gene expression pattern, while the embryo-derived cardiac subset was not fully reversed, indicating a slower recovery. It will be interesting to study if over time, the cardiac subset resembles the steady state pattern. It may also indicate that embryo-derived subsets in the liver and the heart show distinct kinetics in plasticity. Interestingly, the tissue specific gene expression signature observed in the steady state remained unchanged throughout the time course. While our time course does not confirm

that this tissue specific gene expression pattern remains unchanged throughout the course of the inflammation and resolution, it does suggest the possibility that this tissue specific identity is maintained despite the inflammatory environment.

Taken together, our data provides insight into how embryo-derived macrophages with specialized tissue functions respond to acute inflammation and reestablished steady state. Generally speaking, these embryo-derived subsets show plasticity and assume functional states dictated by the tissue environment. These findings have implications in targeting resident macrophages as therapeutic agents.

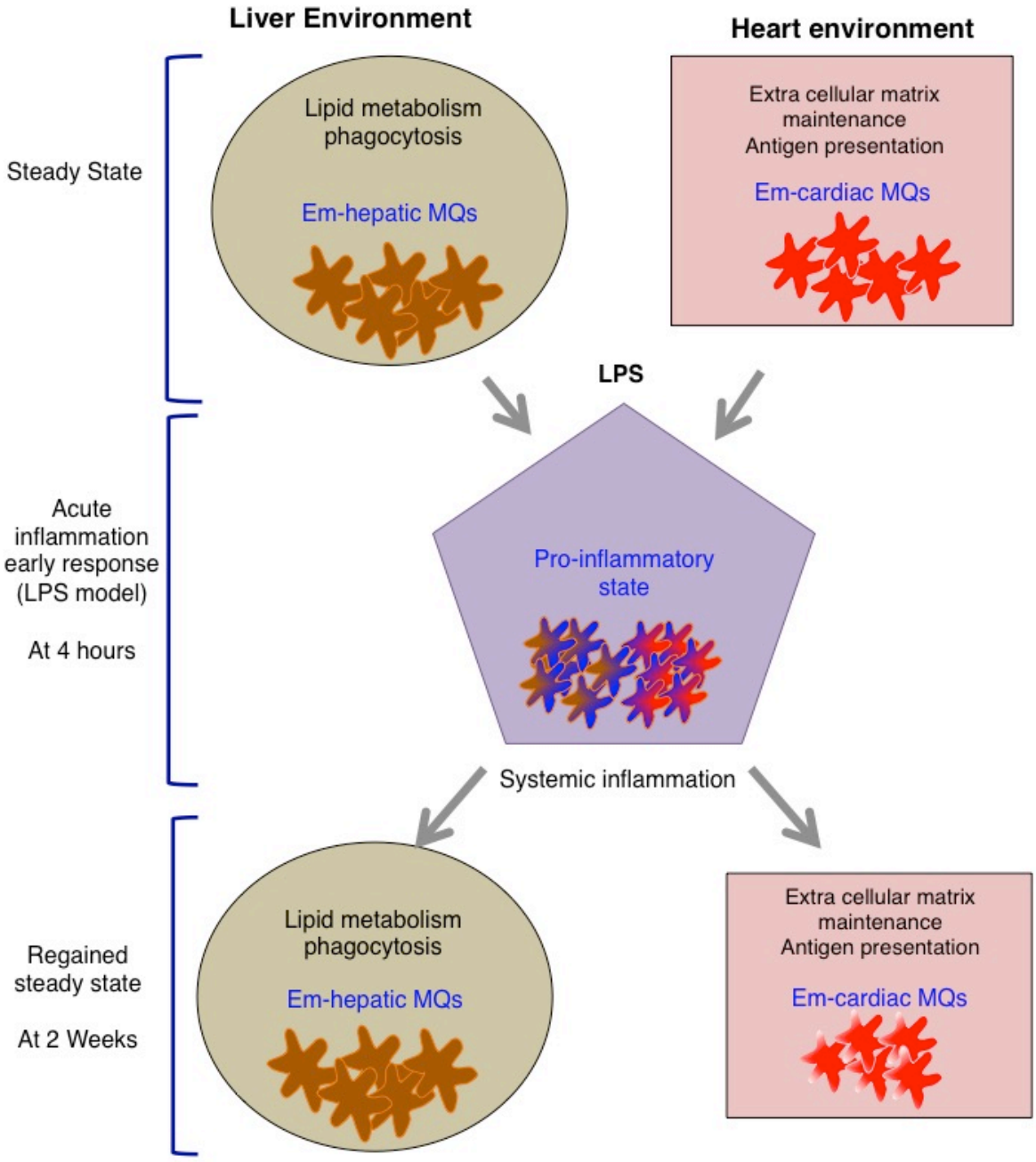

Figure 4-10: Graphical abstract

Table 1: List of antibodies used

Name	Supplier	Cat no.	Clone no.
Anti-Tie2	Biolegend	124007	TEK4
anti-Ly6C	BioLegend	128011	HK1.4
Anti-F4/80	BioLegend	123113	BM8
anti-CD11b	BD bioscience	563015	M1/70
Anti-1A/1E	BioLegend	107627	M5/114.15.2
Anti-Ly6G	BioLegend	127611	1A8
Anti-Cx3cr1	BioLegend	149003	SA011F11
Anti-CD45.1	BioLegend	110739	A20
Anti-CD45.2	BioLegend	109819	104
Anti-CD11c	BioLegend	117323	N418
Anti-HA	BioLegend	682404	16B12
Anti-CD31	BioLegend	102421	390
Anti-Tim4	Biolegend	129907	F31-5G3
Anti-IA/IE	Biolegend	107618	M5/114.15.2
Anti-SiglecF	BD Bioscience	562068	E50-2440
Live/Dead	ThermoFisher	L10120	

CHAPTER 5: CONCLUSIONS AND FUTURE DIRECTIONS

Overview

The studies described in this dissertation explore the functions of long-lived embryo-derived Kupffer cells. We used an inducible fate-mapping model to label the embryo-derived resident macrophage subset in the liver, and studied their dynamics during irradiation stress and acute inflammation. In chapter 3, we explored the embryo-derived subset's response to radiation-induced stress. Specifically, we asked the question "does the embryonic origin provide an advantage in surviving the radiation-induced damage?". We found that compared to bone marrow monocyte-derived Kupffer cell subset, the embryo-derived subset has higher survival potential to lethal irradiation. Furthermore, this enhanced survival is mediated through $p21^{-cip1/WAF1}$ protein expressed by the *Cdkn1a* gene. In Chapter 4, we sought to understand whether the embryo-derived subset has the capacity to respond to acute inflammatory stimuli. We used an LPS mediated acute inflammation model, analyzed gene expression during early phase of response and during the regained steady state. We found that the embryonic subset responds readily to the inflammatory environment with an elevated pro-inflammatory gene expression (*Tnf, Il6, Il18*), and this response was gone by post resolution indicating their ability to respond to a changing environment. We compared the embryo-derived cardiac macrophage subset's response in the same mice, and found that they respond similarly, and reversibly, to acute inflammation. Our results provide insights into the less known biology of embryo-derived Kupffer cells and tissue resident macrophages in general.

Discussion

The liver is the central energy-processing unit in the body. Apart from this, liver induces peripheral tolerance to harmless antigens and acts as a barrier to filter out any gut derived pathogens and their products. An important resident immune cell type in the liver that plays a major role in peripheral tolerance induction and scavenging are the resident macrophages. The liver constitutes the largest source of resident macrophages in mice. Apart from their contribution to maintain steady state in the liver, these resident macrophages, the Kupffer cells (KCs), provide immunity during stress conditions. Kupffer cells are heterogeneous in terms of their phenotype, ontogeny, and function(25, 63). While this multi

faceted heterogeneity is documented in post injury settings, it is understudied in the steady state KC compartment. Furthermore, whether or how phenotype, ontogeny, and function relate to each other is currently not understood.

In mice, a subset of KCs is originated during the embryonic stage and lives long into the adult stage (112, 113, 115, 116). While the embryonic origin of at least a subset of KCs is well established through a number of fate mapping models, the type of precursor, the time of tissue seeding, and the exact proportion in the adult, remain to be resolved. Given that only a subset of KCs can be traced for their embryonic origin using current fate mapping models, the ontogeny of the non-labeled subset remains to be identified. While some evidence from neonatal stage adoptive transfers indicates that circulating monocytes differentiate and integrate into the KC compartment, further fate mapping studies are needed to confirm monocytic origin of KCs. Thus, the exact ontogenetic nature of the KC compartment still remains a mystery.

Kupffer cells identified in pathogenic and non-pathogenic injury models, and in pathological settings indicate that they can be pro-inflammatory, anti-inflammatory, reparative, or immunosuppressive (117). How one type of cell performs all these functions has been a great interest in the field. Combining these distinct immune functions with the distinct ontogenies, one can question whether a certain ontogeny imprints a certain functional state on the KCs resulting functionally distinct subsets. The current challenge to explore this question is that there are no phenotypic markers to distinguish the embryo or the monocyte-derived KC subset. Thus it is critical to use fate-mapping tools to exclusively identify the ontogenetically distinct subsets.

In this dissertation, we developed an inducible Cx3cr1 fate-mapping model to label at least a subset of the embryo derived KCs in adult mice. We activated a reporter gene at day two, thus our model labeled any Cx3cr1 expressing KC at day two and retained the label on long-lived KCs into the adult stage. While this model may not distinguish between the KCs derived from distinct embryonic precursors (EPMs, fetal monocytes), it does label KCs that were embryonically originated and continue to express Cx3cr1 into early neonatal stages. This model consistently labeled at least 37% of the KCs and allowed us to explore their response to irradiation and acute inflammation.

It is long known that a subset of KCs resists lethal irradiation and continue to perform immune functions in the radiation chimeric mice(56, 83). What makes only a subset resist irradiation, and how this subset overcomes radiation induced stress, however, was unknown. Our studies indicated that the embryo-derived KC subset was predominately radioresistant while the bone marrow monocyte-derived subset was sensitive to radiation-induced depletion. The radioresistance of the embryo-derived subset was mediated through the cell cycle inhibitor protein p21-$^{cip1/WAF1}$. These findings indicate that in the liver, embryo origin promotes the survival to radiation-induced stress. Interestingly in mice, the other tissue resident macrophages that resisted irradiation included brain microglia and skin Langerhans cells (80, 82). Microglia have a near complete YS origin, while Langerhans cells are shown to derive mainly from fetal monocytes (80, 118). Furthermore in Langerhans cells, p21-$^{cip1/WAF1}$ mediated the survival to radiation-induced stress(92). These observations broadly indicate that despite the precursor type, the embryonic origin imprints a greater survival to radiation injury. While the gene *Cdkn1a* that encodes p21-$^{Cip1/WAF1}$protein is commonly upregulated in response to radiation stress in most of the cell types, our work and others show that the embryo-derived macrophage subset upregulate it to a greater extent(92). This may indicate that *Cdkn1a* has distinct regulatory mechanisms in embryo-derived cells, thus it will be interesting to study the mechanisms of *Cdkn1a* regulation, it's enhancer landscape in embryo- versus bone marrow-derived macrophages before, and after radiation. This ability to survive in the face of heavy ionization induced damage may be evolutionarily ingrained into these embryo-derived macrophages. This embryo-derived subset stems from a limited amount of precursors generated in unique waves during the embryonic stage, and thus maintenance depends solely on self-renewal, or longevity, but not on replenishment. Since these macrophages are indispensable for proper organ development before birth, they may be ingrained with unique mechanisms for survival. In contrast, once established post birth, bone marrow hematopoiesis provides a replenishable source of monocytes that are available as precursors for resident macrophage renewal. Thus the need for enhanced survival may not be an ingrained feature of these monocytic-derived resident macrophages.

Our studies and others have shown that the survival to radiation-induced stress is determined by the ontogeny of the tissue resident macrophages. This raises the question whether there is a relationship between the origin and response to other stresses such as acute, or chronic, inflammation. To explore

these questions, fate-mapping models that allow labeling of embryo- or the monocyte-derived subsets are needed. While several fate-mapping models allow at least a subset of embryo-derived KC labeling, no tools exist to label the monocyte-derived subset in the liver without using invasive strategies such as Clodronate or diphtheria toxin mediated depletion. Thus exploring ontogeny versus functional relationships of the KCs are still limited due to lack of tools.

Tissue resident macrophages show tissue specific transcriptomes(116, 119). This may suggest that despite of the origin all macrophage subsets within a tissue may result in a similar transcriptome assigned by their tissue environment. Our analysis of embryo-derived macrophage subset in liver and heart supported this idea in that they were very distinct in their steady state gene expression. These observations are further in line with the idea that once embryo-derived macrophages seed a tissue, they undergo profound epigenetic changes, and activate tissue specific transcription factors in response to the tissue specific cues (45). Translatome-based pathway analysis further suggests that these subsets are involved in tissue specific functions such as extra cellular matrix maintenance in the heart, and lipid metabolism in the liver. This raises the question to which extent that these embryo-derived macrophage subsets respond to a changing environment. In other words “do they retain plasticity to reversibly polarize in response to changing environment?”

A large body of literature exists on *in vitro* studies performed on bone marrow-derived macrophages showing that they can be polarized to distinct functional states by changing their environment (108). Specifically, LPS or IFNγ polarize macrophages to a pro-inflammatory state to produce pro-inflammatory cytokines (TNF, IL1b) while IL4 and IL13 polarize them to an anti-inflammatory state(68). These studies broadly indicate plasticity in *in vitro* experimental settings, especially for the bone marrow-derived macrophages. Some *in vivo* liver fibrosis models support the idea of monocyte-derived macrophage plasticity in that they convert from pro-inflammatory to a reparative phenotype over the course of inflammation and resolution(109, 120). Our translatome analysis of both embryo-derived liver and heart macrophage subsets in an acute inflammation model and at regained steady state indicated that they retain plasticity and respond to the changing environment readily. These results broadly suggest that despite their tissue specialized functions, the embryo-derived subsets remains plastic. Further studies using different acute inflammation models and chronic inflammation models are needed to solidify

these observations. If this plasticity is an inherent quality of these embryo-derived macrophages, one can envisage both benefits and drawbacks to it. A benefit will be to mount the right immune response to a pathogen and eliminate it, and resolve back to the steady state levels. This might be the case in some liver diseases that do not cause chronic illness, like hepatitis A. However, it could be quite different in the case of liver carcinomas, where the pro-tumor environment may alter the resident macrophage response to benefit the tumor rather than to mount an anti-tumor response.

Collectively, the research work detailed in this dissertation suggests that the survival to ionization-induced damage is ingrained by ontogeny of the macrophages, and that the embryo-derived subset maintains plasticity and responds to the changing environment. Thus, the nurture versus nature response of these embryonic macrophages may depend on the type of stress they encounter.

Conclusions

Liver diseases remain a major cause of morbidity and mortality globally. The role of immune system in these pathological settings and development of cell-based therapy to intervene has been a major focus in liver research. Kupffer cells, the abundant resident innate sensors in the liver, have shown to play a role in mounting immunity or exacerbating liver pathologies. Thus they provide an attractive target for cell-based therapy. The studies detailed in this dissertation advance understanding of the biology of a recently identified embryo-derived Kupffer cell subset. Our findings provide insights into developing macrophage-targeted therapy for liver diseases.

REFERENCES

1. Arlin B. Rogers RZD. 2012 Liver and Gallblader, Comparative Anatomy and Histology a Mouse and Human Atlas. Elsevier/Acedemic press.
2. WW L. 2009. Hepatic Circulation: Physiology and Pathophysiology. Morgan & Claypool Life Sciences, San Rafael(CA).
3. Halpern KB, Shenhav R, Matcovitch-Natan O, Toth B, Lemze D, Golan M, et al. 2017. Single-cell spatial reconstruction reveals global division of labour in the mammalian liver. Nature 542:352-356.
4. Crispe IN. 2009. The liver as a lymphoid organ. Annu Rev Immunol 27:147-63.
5. Lumsden AB, Henderson JM, Kutner MH. 1988. Endotoxin levels measured by a chromogenic assay in portal, hepatic and peripheral venous blood in patients with cirrhosis. Hepatology 8:232-6.
6. Balmer ML, Slack E, de Gottardi A, Lawson MA, Hapfelmeier S, Miele L, et al. 2014. The liver may act as a firewall mediating mutualism between the host and its gut commensal microbiota. Sci Transl Med 6:237ra66.
7. Mafra K, Nakagaki BN, Castro Oliveira HM, Rezende RM, Antunes MM, Menezes GB. 2019. The liver as a nursery for leukocytes. J Leukoc Biol doi:10.1002/JLB.MR1118-455R.
8. Soysa R, Wu X, Crispe IN. 2017. Dendritic cells in hepatitis and liver transplantation. Liver Transpl 23:1433-1439.
9. Knolle PA, Gerken G. 2000. Local control of the immune response in the liver. Immunol Rev 174:21-34.
10. Crispe IN. 2011. Liver antigen-presenting cells. J Hepatol 54:357-65.
11. Kawai T, Akira S. 2010. The role of pattern-recognition receptors in innate immunity: update on Toll-like receptors. Nat Immunol 11:373-84.
12. Shuai Z, Leung MW, He X, Zhang W, Yang G, Leung PS, et al. 2016. Adaptive immunity in the liver. Cell Mol Immunol 13:354-68.
13. Male V. 2017. Liver-Resident NK Cells: The Human Factor. Trends Immunol 38:307-309.
14. Norris S, Collins C, Doherty DG, Smith F, McEntee G, Traynor O, et al. 1998. Resident human hepatic lymphocytes are phenotypically different from circulating lymphocytes. J Hepatol 28:84-90.
15. Doherty DG. 2016. Immunity, tolerance and autoimmunity in the liver: A comprehensive review. J Autoimmun 66:60-75.
16. Tiegs G, Lohse AW. 2010. Immune tolerance: what is unique about the liver. J Autoimmun 34:1-6.
17. Bilzer M, Roggel F, Gerbes AL. 2006. Role of Kupffer cells in host defense and liver disease. Liver Int 26:1175-86.
18. Haubrich WS. 2004. Kupffer of Kupffer cells. Gastroenterology 127:16.
19. Wake K. 1989. Cell biology and kinetics of teh Kupffer cells in the liver, p 173-229, International review of Cytology, vol 118.
20. van Furth R, Cohn ZA, Hirsch JG, Humphrey JH, Spector WG, Langevoort HL. 1972. The mononuclear phagocyte system: a new classification of macrophages, monocytes, and their precursor cells. Bull World Health Organ 46:845-52.
21. Naito M, Hasegawa G, Takahashi K. 1997. Development, differentiation, and maturation of Kupffer cells. Microsc Res Tech 39:350-64.
22. Wisse E. 1974. Observations on the fine structure and peroxidase cytochemistry of normal rat liver Kupffer cells. J Ultrastruct Res 46:393-426.
23. van Furth R, Cohn ZA. 1968. The origin and kinetics of mononuclear phagocytes. J Exp Med 128:415-35.
24. Terpstra V, van Berkel TJ. 2000. Scavenger receptors on liver Kupffer cells mediate the in vivo uptake of oxidatively damaged red blood cells in mice. Blood 95:2157-63.
25. Tacke F, Zimmermann HW. 2014. Macrophage heterogeneity in liver injury and fibrosis. J Hepatol 60:1090-6.

26. Li P, He K, Li J, Liu Z, Gong J. 2017. The role of Kupffer cells in hepatic diseases. Mol Immunol 85:222-229.
27. Sieweke MH, Allen JE. 2013. Beyond stem cells: self-renewal of differentiated macrophages. Science 342:1242974.
28. Hashimoto D, Chow A, Noizat C, Teo P, Beasley MB, Leboeuf M, et al. 2013. Tissue-resident macrophages self-maintain locally throughout adult life with minimal contribution from circulating monocytes. Immunity 38:792-804.
29. Bouwens L, Baekeland M, Wisse E. 1984. Importance of local proliferation in the expanding Kupffer cell population of rat liver after zymosan stimulation and partial hepatectomy. Hepatology 4:213-9.
30. Laskin DL, Weinberger B, Laskin JD. 2001. Functional heterogeneity in liver and lung macrophages. J Leukoc Biol 70:163-70.
31. Gordon S, Pluddemann A. 2017. Tissue macrophages: heterogeneity and functions. BMC Biol 15:53.
32. Gordon S, Pluddemann A, Martinez Estrada F. 2014. Macrophage heterogeneity in tissues: phenotypic diversity and functions. Immunol Rev 262:36-55.
33. Austyn JM, Gordon S. 1981. F4/80, a monoclonal antibody directed specifically against the mouse macrophage. Eur J Immunol 11:805-15.
34. Hagemeyer N, Kierdorf K, Frenzel K, Xue J, Ringelhan M, Abdullah Z, et al. 2016. Transcriptome-based profiling of yolk sac-derived macrophages reveals a role for Irf8 in macrophage maturation. EMBO J 35:1730-44.
35. Schulz C, Gomez Perdiguero E, Chorro L, Szabo-Rogers H, Cagnard N, Kierdorf K, et al. 2012. A lineage of myeloid cells independent of Myb and hematopoietic stem cells. Science 336:86-90.
36. Brempelis KJ, Crispe IN. 2016. Infiltrating monocytes in liver injury and repair. Clin Transl Immunology 5:e113.
37. David BA, Rezende RM, Antunes MM, Santos MM, Freitas Lopes MA, Diniz AB, et al. 2016. Combination of Mass Cytometry and Imaging Analysis Reveals Origin, Location, and Functional Repopulation of Liver Myeloid Cells in Mice. Gastroenterology 151:1176-1191.
38. Sierro F, Evrard M, Rizzetto S, Melino M, Mitchell AJ, Florido M, et al. 2017. A Liver Capsular Network of Monocyte-Derived Macrophages Restricts Hepatic Dissemination of Intraperitoneal Bacteria by Neutrophil Recruitment. Immunity 47:374-388 e6.
39. Gautier EL, Shay T, Miller J, Greter M, Jakubzick C, Ivanov S, et al. 2012. Gene-expression profiles and transcriptional regulatory pathways that underlie the identity and diversity of mouse tissue macrophages. Nat Immunol 13:1118-28.
40. Han X, Wang R, Zhou Y, Fei L, Sun H, Lai S, et al. 2018. Mapping the Mouse Cell Atlas by Microwell-Seq. Cell 172:1091-1107 e17.
41. Lynch RW, Hawley CA, Pellicoro A, Bain CC, Iredale JP, Jenkins SJ. 2018. An efficient method to isolate Kupffer cells eliminating endothelial cell contamination and selective bias. J Leukoc Biol 104:579-586.
42. Crofton RW, Diesselhoff-den Dulk MM, van Furth R. 1978. The origin, kinetics, and characteristics of the Kupffer cells in the normal steady state. J Exp Med 148:1-17.
43. Wacker HH, Radzun HJ, Parwaresch MR. 1986. Kinetics of Kupffer cells as shown by parabiosis and combined autoradiographic/immunohistochemical analysis. Virchows Arch B Cell Pathol Incl Mol Pathol 51:71-8.
44. Stremmel C, Schuchert R, Wagner F, Thaler R, Weinberger T, Pick R, et al. 2018. Author Correction: Yolk sac macrophage progenitors traffic to the embryo during defined stages of development. Nat Commun 9:3699.
45. Mass E, Ballesteros I, Farlik M, Halbritter F, Gunther P, Crozet L, et al. 2016. Specification of tissue-resident macrophages during organogenesis. Science 353.
46. Gomez Perdiguero E, Klapproth K, Schulz C, Busch K, Azzoni E, Crozet L, et al. 2015. Tissue-resident macrophages originate from yolk-sac-derived erythro-myeloid progenitors. Nature 518:547-51.
47. Hoeffel G, Chen J, Lavin Y, Low D, Almeida FF, See P, et al. 2015. C-Myb(+) erythro-myeloid progenitor-derived fetal monocytes give rise to adult tissue-resident macrophages. Immunity 42:665-78.

48. Sheng J, Ruedl C, Karjalainen K. 2015. Most Tissue-Resident Macrophages Except Microglia Are Derived from Fetal Hematopoietic Stem Cells. Immunity 43:382-93.
49. Scott CL, Zheng F, De Baetselier P, Martens L, Saeys Y, De Prijck S, et al. 2016. Bone marrow-derived monocytes give rise to self-renewing and fully differentiated Kupffer cells. Nat Commun 7:10321.
50. Yona S, Kim KW, Wolf Y, Mildner A, Varol D, Breker M, et al. 2013. Fate mapping reveals origins and dynamics of monocytes and tissue macrophages under homeostasis. Immunity 38:79-91.
51. Molawi K, Wolf Y, Kandalla PK, Favret J, Hagemeyer N, Frenzel K, et al. 2014. Progressive replacement of embryo-derived cardiac macrophages with age. J Exp Med 211:2151-8.
52. Epelman S, Lavine KJ, Beaudin AE, Sojka DK, Carrero JA, Calderon B, et al. 2014. Embryonic and adult-derived resident cardiac macrophages are maintained through distinct mechanisms at steady state and during inflammation. Immunity 40:91-104.
53. Sleyster EC, Knook DL. 1982. Relation between localization and function of rat liver Kupffer cells. Lab Invest 47:484-90.
54. N AG, Quintana JA, Garcia-Silva S, Mazariegos M, Gonzalez de la Aleja A, Nicolas-Avila JA, et al. 2017. Phagocytosis imprints heterogeneity in tissue-resident macrophages. J Exp Med 214:1281-1296.
55. Wang J, Kubes P. 2016. A Reservoir of Mature Cavity Macrophages that Can Rapidly Invade Visceral Organs to Affect Tissue Repair. Cell 165:668-78.
56. Klein I, Cornejo JC, Polakos NK, John B, Wuensch SA, Topham DJ, et al. 2007. Kupffer cell heterogeneity: functional properties of bone marrow derived and sessile hepatic macrophages. Blood 110:4077-85.
57. Zigmond E, Samia-Grinberg S, Pasmanik-Chor M, Brazowski E, Shibolet O, Halpern Z, et al. 2014. Infiltrating monocyte-derived macrophages and resident kupffer cells display different ontogeny and functions in acute liver injury. J Immunol 193:344-53.
58. Mossanen JC, Krenkel O, Ergen C, Govaere O, Liepelt A, Puengel T, et al. 2016. Chemokine (C-C motif) receptor 2-positive monocytes aggravate the early phase of acetaminophen-induced acute liver injury. Hepatology 64:1667-1682.
59. Bleriot C, Dupuis T, Jouvion G, Eberl G, Disson O, Lecuit M. 2015. Liver-resident macrophage necroptosis orchestrates type 1 microbicidal inflammation and type-2-mediated tissue repair during bacterial infection. Immunity 42:145-58.
60. Jenkins SJ, Ruckerl D, Cook PC, Jones LH, Finkelman FD, van Rooijen N, et al. 2011. Local macrophage proliferation, rather than recruitment from the blood, is a signature of TH2 inflammation. Science 332:1284-8.
61. Lai SM, Sheng J, Gupta P, Renia L, Duan K, Zolezzi F, et al. 2018. Organ-Specific Fate, Recruitment, and Refilling Dynamics of Tissue-Resident Macrophages during Blood-Stage Malaria. Cell Rep 25:3099-3109 e3.
62. Marra F, Tacke F. 2014. Roles for chemokines in liver disease. Gastroenterology 147:577-594 e1.
63. Abdullah Z, Knolle PA. 2017. Liver macrophages in healthy and diseased liver. Pflugers Arch 469:553-560.
64. Sun Z, Wada T, Uchikura K, Ceppa E, Klein AS. 2001. Role of Fas/Fasl in Kupffer cell-dependent deletion of alloantigen activated T cells following liver transplantation. Transplant Proc 33:279-82.
65. Huang W, Metlakunta A, Dedousis N, Zhang P, Sipula I, Dube JJ, et al. 2010. Depletion of liver Kupffer cells prevents the development of diet-induced hepatic steatosis and insulin resistance. Diabetes 59:347-57.
66. Soysa R, Lampert S, Yuen S, Douglass AN, Li W, Pfeffer K, et al. 2019. Fetal origin confers radio-resistance on liver macrophages via p21(cip1/WAF1). J Hepatol doi:10.1016/j.jhep.2019.04.015.
67. Biswas SK, Mantovani A. 2010. Macrophage plasticity and interaction with lymphocyte subsets: cancer as a paradigm. Nat Immunol 11:889-96.
68. Sica A, Mantovani A. 2012. Macrophage plasticity and polarization: in vivo veritas. J Clin Invest 122:787-95.
69. Murray PJ. 2017. Macrophage Polarization. Annu Rev Physiol 79:541-566.
70. Wang N, Liang H, Zen K. 2014. Molecular mechanisms that influence the macrophage m1-m2 polarization balance. Front Immunol 5:614.

71. Xue J, Schmidt SV, Sander J, Draffehn A, Krebs W, Quester I, et al. 2014. Transcriptome-based network analysis reveals a spectrum model of human macrophage activation. Immunity 40:274-88.
72. Louvet A, Teixeira-Clerc F, Chobert MN, Deveaux V, Pavoine C, Zimmer A, et al. 2011. Cannabinoid CB2 receptors protect against alcoholic liver disease by regulating Kupffer cell polarization in mice. Hepatology 54:1217-26.
73. Barron L, Wynn TA. 2011. Macrophage activation governs schistosomiasis-induced inflammation and fibrosis. Eur J Immunol 41:2509-14.
74. Lavin Y, Winter D, Blecher-Gonen R, David E, Keren-Shaul H, Merad M, et al. 2014. Tissue-resident macrophage enhancer landscapes are shaped by the local microenvironment. Cell 159:1312-26.
75. Gosselin D, Link VM, Romanoski CE, Fonseca GJ, Eichenfield DZ, Spann NJ, et al. 2014. Environment drives selection and function of enhancers controlling tissue-specific macrophage identities. Cell 159:1327-40.
76. Scott CL, T'Jonck W, Martens L, Todorov H, Sichien D, Soen B, et al. 2018. The Transcription Factor ZEB2 Is Required to Maintain the Tissue-Specific Identities of Macrophages. Immunity 49:312-325 e5.
77. Okabe Y, Medzhitov R. 2014. Tissue-specific signals control reversible program of localization and functional polarization of macrophages. Cell 157:832-44.
78. Mohar I, Brempelis KJ, Murray SA, Ebrahimkhani MR, Crispe IN. 2015. Isolation of Non-parenchymal Cells from the Mouse Liver. Methods Mol Biol 1325:3-17.
79. Sanz E, Yang L, Su T, Morris DR, McKnight GS, Amieux PS. 2009. Cell-type-specific isolation of ribosome-associated mRNA from complex tissues. Proc Natl Acad Sci U S A 106:13939-44.
80. Ginhoux F, Lim S, Hoeffel G, Low D, Huber T. 2013. Origin and differentiation of microglia. Front Cell Neurosci 7:45.
81. Menzel F, Kaiser N, Haehnel S, Rapp F, Patties I, Schoneberg N, et al. 2018. Impact of X-irradiation on microglia. Glia 66:15-33.
82. Bogunovic M, Ginhoux F, Wagers A, Loubeau M, Isola LM, Lubrano L, et al. 2006. Identification of a radio-resistant and cycling dermal dendritic cell population in mice and men. J Exp Med 203:2627-38.
83. Beattie L, Sawtell A, Mann J, Frame TCM, Teal B, de Labastida Rivera F, et al. 2016. Bone marrow-derived and resident liver macrophages display unique transcriptomic signatures but similar biological functions. J Hepatol 65:758-768.
84. McDonald B, Kubes P. 2016. Innate Immune Cell Trafficking and Function During Sterile Inflammation of the Liver. Gastroenterology 151:1087-1095.
85. Hume DA, Perry VH, Gordon S. 1984. The mononuclear phagocyte system of the mouse defined by immunohistochemical localisation of antigen F4/80: macrophages associated with epithelia. Anat Rec 210:503-12.
86. Haimon Z, Volaski A, Orthgiess J, Boura-Halfon S, Varol D, Shemer A, et al. 2018. Re-evaluating microglia expression profiles using RiboTag and cell isolation strategies. Nat Immunol 19:636-644.
87. Schaller E, Macfarlane AJ, Rupec RA, Gordon S, McKnight AJ, Pfeffer K. 2002. Inactivation of the F4/80 glycoprotein in the mouse germ line. Mol Cell Biol 22:8035-43.
88. Abram CL, Roberge GL, Hu Y, Lowell CA. 2014. Comparative analysis of the efficiency and specificity of myeloid-Cre deleting strains using ROSA-EYFP reporter mice. J Immunol Methods 408:89-100.
89. Ginhoux F, Greter M, Leboeuf M, Nandi S, See P, Gokhan S, et al. 2010. Fate mapping analysis reveals that adult microglia derive from primitive macrophages. Science 330:841-5.
90. Mizutani M, Pino PA, Saederup N, Charo IF, Ransohoff RM, Cardona AE. 2012. The fractalkine receptor but not CCR2 is present on microglia from embryonic development throughout adulthood. J Immunol 188:29-36.
91. Van Rooijen N, Sanders A. 1994. Liposome mediated depletion of macrophages: mechanism of action, preparation of liposomes and applications. J Immunol Methods 174:83-93.
92. Price JG, Idoyaga J, Salmon H, Hogstad B, Bigarella CL, Ghaffari S, et al. 2015. CDKN1A regulates Langerhans cell survival and promotes Treg cell generation upon exposure to ionizing irradiation. Nat Immunol 16:1060-8.

93. Kuo LJ, Yang LX. 2008. Gamma-H2AX - a novel biomarker for DNA double-strand breaks. In Vivo 22:305-9.
94. Purbey PK, Scumpia PO, Kim PJ, Tong AJ, Iwamoto KS, McBride WH, et al. 2017. Defined Sensing Mechanisms and Signaling Pathways Contribute to the Global Inflammatory Gene Expression Output Elicited by Ionizing Radiation. Immunity 47:421-434 e3.
95. Teresa Pinto A, Laranjeiro Pinto M, Patricia Cardoso A, Monteiro C, Teixeira Pinto M, Filipe Maia A, et al. 2016. Ionizing radiation modulates human macrophages towards a pro-inflammatory phenotype preserving their pro-invasive and pro-angiogenic capacities. Sci Rep 6:18765.
96. Wu Q, Allouch A, Martins I, Modjtahedi N, Deutsch E, Perfettini JL. 2017. Macrophage biology plays a central role during ionizing radiation-elicited tumor response. Biomed J 40:200-211.
97. Georgakilas AG, Martin OA, Bonner WM. 2017. p21: A Two-Faced Genome Guardian. Trends Mol Med 23:310-319.
98. Brugarolas J, Chandrasekaran C, Gordon JI, Beach D, Jacks T, Hannon GJ. 1995. Radiation-induced cell cycle arrest compromised by p21 deficiency. Nature 377:552-7.
99. Abbas T, Dutta A. 2009. p21 in cancer: intricate networks and multiple activities. Nat Rev Cancer 9:400-14.
100. Koike M, Yutoku Y, Koike A. 2011. Accumulation of p21 proteins at DNA damage sites independent of p53 and core NHEJ factors following irradiation. Biochem Biophys Res Commun 412:39-43.
101. Chen W, Sun Z, Wang XJ, Jiang T, Huang Z, Fang D, et al. 2009. Direct interaction between Nrf2 and p21(Cip1/WAF1) upregulates the Nrf2-mediated antioxidant response. Mol Cell 34:663-73.
102. Suzuki A, Tsutomi Y, Akahane K, Araki T, Miura M. 1998. Resistance to Fas-mediated apoptosis: activation of caspase 3 is regulated by cell cycle regulator p21WAF1 and IAP gene family ILP. Oncogene 17:931-9.
103. Gorospe M, Wang X, Guyton KZ, Holbrook NJ. 1996. Protective role of p21(Waf1/Cip1) against prostaglandin A2-mediated apoptosis of human colorectal carcinoma cells. Mol Cell Biol 16:6654-60.
104. Baer K, Roosevelt M, Clarkson AB, Jr., van Rooijen N, Schnieder T, Frevert U. 2007. Kupffer cells are obligatory for Plasmodium yoelii sporozoite infection of the liver. Cell Microbiol 9:397-412.
105. Ensan S, Li A, Besla R, Degousee N, Cosme J, Roufaiel M, et al. 2016. Self-renewing resident arterial macrophages arise from embryonic CX3CR1(+) precursors and circulating monocytes immediately after birth. Nat Immunol 17:159-68.
106. Lavine KJ, Epelman S, Uchida K, Weber KJ, Nichols CG, Schilling JD, et al. 2014. Distinct macrophage lineages contribute to disparate patterns of cardiac recovery and remodeling in the neonatal and adult heart. Proc Natl Acad Sci U S A 111:16029-34.
107. Dick SA, Macklin JA, Nejat S, Momen A, Clemente-Casares X, Althagafi MG, et al. 2019. Self-renewing resident cardiac macrophages limit adverse remodeling following myocardial infarction. Nat Immunol 20:29-39.
108. Das A, Yang CS, Arifuzzaman S, Kim S, Kim SY, Jung KH, et al. 2018. High-Resolution Mapping and Dynamics of the Transcriptome, Transcription Factors, and Transcription Co-Factor Networks in Classically and Alternatively Activated Macrophages. Front Immunol 9:22.
109. Ramachandran P, Pellicoro A, Vernon MA, Boulter L, Aucott RL, Ali A, et al. 2012. Differential Ly-6C expression identifies the recruited macrophage phenotype, which orchestrates the regression of murine liver fibrosis. Proc Natl Acad Sci U S A 109:E3186-95.
110. Swirski FK, Nahrendorf M. 2018. Cardioimmunology: the immune system in cardiac homeostasis and disease. Nat Rev Immunol 18:733-744.
111. Walter W, Alonso-Herranz L, Trappetti V, Crespo I, Ibberson M, Cedenilla M, et al. 2018. Deciphering the Dynamic Transcriptional and Post-transcriptional Networks of Macrophages in the Healthy Heart and after Myocardial Injury. Cell Rep 23:622-636.
112. Epelman S, Lavine KJ, Randolph GJ. 2014. Origin and functions of tissue macrophages. Immunity 41:21-35.
113. Ginhoux F, Guilliams M. 2016. Tissue-Resident Macrophage Ontogeny and Homeostasis. Immunity 44:439-449.

114. van de Laar L, Saelens W, De Prijck S, Martens L, Scott CL, Van Isterdael G, et al. 2016. Yolk Sac Macrophages, Fetal Liver, and Adult Monocytes Can Colonize an Empty Niche and Develop into Functional Tissue-Resident Macrophages. Immunity 44:755-68.
115. Perdiguero EG, Geissmann F. 2016. The development and maintenance of resident macrophages. Nat Immunol 17:2-8.
116. Lavin Y, Mortha A, Rahman A, Merad M. 2015. Regulation of macrophage development and function in peripheral tissues. Nat Rev Immunol 15:731-44.
117. Krenkel O, Tacke F. 2017. Liver macrophages in tissue homeostasis and disease. Nat Rev Immunol 17:306-321.
118. Hoeffel G, Wang Y, Greter M, See P, Teo P, Malleret B, et al. 2012. Adult Langerhans cells derive predominantly from embryonic fetal liver monocytes with a minor contribution of yolk sac-derived macrophages. J Exp Med 209:1167-81.
119. Varol C, Mildner A, Jung S. 2015. Macrophages: development and tissue specialization. Annu Rev Immunol 33:643-75.
120. Sica A, Invernizzi P, Mantovani A. 2014. Macrophage plasticity and polarization in liver homeostasis and pathology. Hepatology 59:2034-42.